


 Cite this: *RSC Adv.*, 2025, 15, 5597

Recent advances on anticancer activity of benzodiazine heterocycles through kinase inhibition

 Mohamed S. Nafie, ^{*ab} Sherif Ashraf Fahmy, ^c Shaima H. Kahwash, ^b
 Mohamed K. Diab, ^d Kamal M. Dawood ^e and Ashraf A. Abbas ^e

The benzodiazines (phthalazine, quinazoline, quinoxaline, and cinnoline) have emerged as attractive scaffolds for creating novel anticancer drugs. These nitrogen-containing heterocycles are intriguing because they have a variety of configurations and can change chemically, allowing us to tailor their pharmacokinetic and pharmacodynamic features. Numerous studies have found that derivatives of these compounds have potent anticancer properties *via* inhibiting topoisomerases, protein kinases, and receptor tyrosine kinases. These compounds impair critical processes that control cancer proliferation and survival. Most benzodiazine derivatives have achieved clinical success, demonstrating the heterocycles' therapeutic potential. The use of phthalazine, cinnoline, and quinazoline derivatives should open new avenues in developing better and more targeted cancer treatments. In this overview, we summarize recent advances in synthesizing these compounds and illustrate how they serve as promising chemotherapeutic agents. Therefore, current research organizes the latest information to provide a clearer picture of design strategies that boost efficacy and selectivity, allowing the identification of potential anticancer drug candidates down the line. This research study also highlights the need to establish heterocyclic derivatives as a promising source of new molecules for cancer treatment with improved efficacy and decreased effects.

 Received 16th November 2024
 Accepted 11th February 2025

DOI: 10.1039/d4ra08134j

rsc.li/rsc-advances

1. Introduction

Cancer is among the leading causes of morbidity and mortality globally and imposes major healthcare and economic burdens.¹ The high incidence of acquired resistance, in addition to serious side effects associated with contemporary therapeutic agents, sustains the search for new anticancer agents despite the fact that many chemotherapeutic agents were introduced and progress with targeted therapy was made.² Heterocyclic compounds have attracted considerable interest in this context owing to a structural diversity that can interact with diverse targets of biological significance.³ Different heterocyclic systems have been studied in this respect, and phthalazine, cinnoline, and quinazoline derivatives appear to be good candidates for building blocks for potent anticancer drugs.⁴

Organic compounds with a ring structure of at least two distinct elements are known as heterocyclic compounds. Nitrogen, oxygen, and sulfur are the most common

heteroatoms.⁵ These are used for many medicines, and their importance in medicinal chemistry is well established. These heteroatoms in the structures provide other interactions with proteins and nucleic acids (NAs), which make them candidates for drug design.⁶ In addition, the potential for chemical manipulation of these scaffolds facilitates the balancing of pharmacokinetic parameters, such as solubility, bioavailability, and metabolic stability, which are key determinants for therapeutic success.⁷ Nitrogen-containing heterocycles, such as phthalazine, cinnoline, quinazoline, and quinoxaline, all are isomeric forms of benzodiazine with the molecular formula C₈H₆N₂ (Fig. 1), each of them has unique structural features and can interact with cancer cells in distinct ways.⁴ Because these heterocyclic frameworks are adaptable, much research has been conducted on how to create them and how they work in living organisms.³ This has resulted in the discovery of several derivatives with potent anticancer activity. Recent studies have proven their ability to disrupt various oncogenic pathways,

^aDepartment of Chemistry, College of Sciences, University of Sharjah, Sharjah, 27272, United Arab Emirates. E-mail: mohamed.elsayed@sharjah.ac.ae

^bDepartment of Chemistry, Faculty of Science, Suez Canal University, Ismailia, 41522, Egypt. E-mail: mohamed_nafie@science.suez.edu.eg

^cDepartment of Pharmaceutics and Biopharmaceutics, University of Marburg, Robert-Koch-Str. 4, 35037, Marburg, Germany

^dPest Physiology Department, Plant Protection Research Institute, Agricultural Research Center, Giza, 12311, Egypt

^eChemistry Department, Faculty of Science, Cairo University, Giza, 12613, Egypt

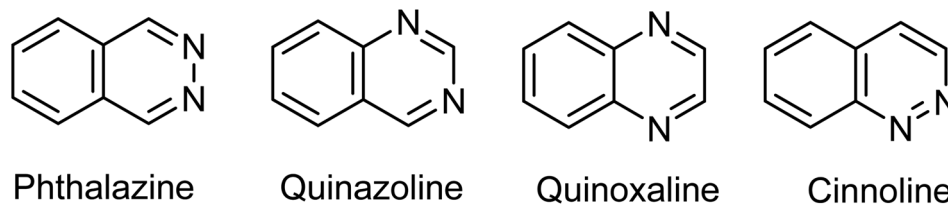



Fig. 1 Isomeric forms of benzodiazines with the molecular formula C₈H₆N₂.

making them potential templates for future drug development efforts.⁸

Phthalazine (2,3-benzodiazine) has a bicyclic structure featuring a benzene ring fused to a pyridazine ring.⁹ This rigid scaffold can hold multiple substituents, allowing for diverse biological functions.¹⁰ The derivatives of phthalazines have been extensively screened for their antibacterial, anticonvulsant, anti-inflammatory, and anticancer actions. Among them,

some of the FDA-approved phthalazine anticancer drugs are shown in Fig. 2, known for their capacity to alter critical biological targets implicated in cancer growth.¹¹ Phthalazine derivatives with anticancer properties frequently work through their interactions with enzymes, including topoisomerases and kinases. These were associated with DNA replication, transcription, and cell cycle regulation.¹² Topoisomerase II activity is inhibited by phthalazine-based inhibitors, for example.



Mohamed S. Nafie

Mohamed S. Nafie (Ph.D., MRSC). Assistant Prof. of Bioorganic Chemistry, College of Sciences, University of Sharjah, United Arab Emirates (UAE). In 2024, he is recognized as one of the top 2% World Scientists' List by Stanford University Published 16 September 2024, Version 7, DOI: <https://doi.org/10.17632/btchxktzyw.7>. In 2022, he was awarded with the best Scholar in Suez Canal University, Egypt. He is

a member of Member of the Royal Society of Chemistry (MRSC, since 2022), American Chemical Society member (ACS, since 2021) and the European Society for Medical Oncology (ESMO, since 2024). He got his Ph.D. in Bioorganic Chemistry (2018), M.Sc. in Biochemistry 2015, and B.Sc. in Chemistry from Suez Canal University (Egypt). In 2017 he was awarded the Erasmus+KA107 scholarship at the Faculty of Pharmacy, University of Pisa, Italy. In 2020, he was awarded the Daniel Turnberg Travel Fellowship at the Institute of Medical Sciences, University of Aberdeen, UK. His research interest is to design and synthesize novel target-oriented chemotherapeutic anticancer agents using the Computer-Aided Drug Design (CADD), medicinal chemistry, biochemical, and molecular biology assays. He established and led several research groups and international collaborations funded by prestigious grants and institutions. His research work was awarded as Top cited articles in WILEY for 2021–2022 and 2022–2023. He published more than 138 peer-reviewed articles in international journals with Scopus H-index 23. Additionally, he served as scientific editor in Frontiers in Chemistry, Metabolites (MDPI) and as reviewers in more than 225 papers in distinguished international journals (Clarivate analytics).



Sherif Ashraf Fahmy

Dr. Sherif Ashraf Fahmy is Visiting Assistant Professor at the Department of Pharmaceutics and Biopharmaceutics, Faculty of Pharmacy, Philipps-Universität Marburg, Germany. Furthermore, he is the Head of the Herbal Medicine and Nanotherapeutics Research Group. Dr Sherif Ashraf Fahmy obtained his B.Pharm. with Honors from the Faculty of Pharmacy, Cairo University, and his M.Sc. and Ph.D. from the American

University in Cairo, in collaboration with the Department of Pharmaceutics and Biopharmaceutics, Philipps-Universität Marburg, Germany. Dr Fahmy was selected as one of the first recipients of the prestigious fellowship offered by the Alfi Foundation for Ph.D. students. He has received several other awards and recognitions, most notably the Alexander von Humboldt Georg Forster Research Fellowship, the Royal Society of Chemistry Research Fund, and the Fulbright Scholarship at Ohio University. Also, he has been listed in the top 2% World Scientists' List by Stanford University published 16 September 2024, Version 7, DOI: <https://doi.org/10.17632/btchxktzyw.7>. His research interests revolve around natural products, inorganic complexes, nanomedicine, and drug delivery. Dr Fahmy has published several peer-reviewed articles in international journals and many abstracts at local and international conferences. Furthermore, he serves as a reviewer and editor for several international journals and serves as a member of the topical advisory panel for the Pharmaceutics journal, member of the Royal Society of Chemistry (MRSC), American Chemical Society member and the European Society for Medical Oncology (ESMO).



Normal cells need this enzyme to copy their DNA when they divide rapidly. Topoisomerase II inhibitors promote DNA damage and apoptosis, effectively treating various cancer types.¹³ Several phthalazine derivatives are also known to function as potent tyrosine kinase inhibitors, key regulators of cell growth, and survival-supporting signal transduction pathways.¹³ Such characteristics highlighted the possibility of phthalazine derivatives being chemotherapeutics.¹⁴

Quinazoline (1,3-benzodiazine) has been the subject of extensive research for therapeutic purposes.¹⁶ The adaptability of the quinazoline scaffold allowed for a wide range of functional alterations that increase activity and selectivity.¹⁷ Quinazoline derivatives showed many biological activities such as antibacterial, anti-inflammatory, and anticancer.¹⁸ Some FDA-approved quinazoline anticancer drugs are depicted in Fig. 3. Quinazoline compounds target essential cellular pathways cancer cells rely on for growth and survival.¹⁹ Gefitinib, a selective epidermal growth factor receptor (EGFR) inhibitor, established one of the most convincing examples of quinazoline derivatives for non-small cell lung cancer therapy.²⁰ It was, therefore, possible to identify small molecules that inhibit distinct receptor tyrosine kinases (RTKs) and pathways that drive tumorigenesis. Biomedicinally, it is found that the quinazoline derivatives inhibited the activity of EGFR, VEGFR, and

other kinases, in turn inhibiting critical processes such as cell division, migration, and angiogenesis.²¹ This inhibited critical processes such as cell division, migration, and angiogenesis.²² These results demonstrate the possibilities of quinazoline derivatives as a therapeutic target for generating new anticancer approaches.

Quinoxaline (1,4-benzodiazine) derivatives have received great attention as anticancer agents because of their unique structural properties and activity.²⁴ Their core structure surfaces a benzene ring, which forms the solid base for numerous modifications of pyrazine ring that withstands many chemical reactions.²⁵ As shown in Fig. 4, with some quinoxaline anticancer drugs. Various quinoxaline derivatives can interact with different molecular targets in cancer cells. These include kinases, topoisomerases, and other proteins that help control the cell cycle and kill cells.²⁶ According to studies, these compounds effectively block tyrosine kinases, interfere with DNA synthesis, and cause oxidative stress in tumor cells, ultimately leading to cell death.²⁷ They also control many signaling pathways, such as the PI3K/AKT/mTOR and MAPK pathways, which makes them more likely to work as multi-targeted cancer treatments.²⁸ Recent studies have highlighted the importance of quinoxaline derivatives in inhibiting cell proliferation, angiogenesis, and metastasis, making them promising for further



Kamal M. Dawood

Kamal M. Dawood graduated from Cairo University, Egypt in 1987, and received his Ph.D. in 1995 from Cairo University. In 1997 he was awarded the UNESCO Fellowship at TIT for one year and in 1999 he was awarded the JSPS Fellowship for two years and in both fellowships he worked with Professor T. Fuchigami at Tokyo Institute of Technology (TIT) in the field of "Anodic Selective Fluorination of Heterocycles". Further,

he was awarded the Alexander von Humboldt (AvH) Fellowship at Hanover University in 2004–2005 with Prof. A. Kirschning (in the area of polymer supported palladium catalyzed cross coupling reactions) and as AvH three short visits in 2007, 2008 and 2012 with Prof. P. Metz at TU-Dresden (in the field of Metathesis Reactions in Domino Processes). Since May 2007 – to date, he has been appointed as full Professor of Organic Chemistry, Faculty of Science, Cairo University. He worked as Professor of Organic Chemistry at Chemistry Department, Kuwait University from September 2013 till August 2017. He received a number of National Awards: Cairo University Award in Chemistry (2002), the State-Award in Chemistry (2007), Cairo University Award for Academic Excellence (2012) and Cairo University Merit Award (2017). He published about 160 scientific papers, reviews and book chapters in distinguished international journals. There are about 4000 citations of his work (Scopus h-index 33).



Ashraf A. Abbas

Ashraf A. Abbas was born in Egypt in September 1968 and he is presently Professor of Organic Chemistry, Department of Chemistry, Faculty of Science, Cairo University, Giza, Egypt since 2009. He graduated from Cairo University in 1990. He received his M.Sc. and Ph.D. degrees in 1994 and 1997, respectively, from Cairo University. He spent six months in the Fakultät für Chemie, Universität of Konstanz (Germany) on

a DAAD fellowship (1996) to finish his Ph.D. thesis and one year in Tokyo Institute of Technology (TIT, Japan) as UNESCO fellow (postdoctoral fellowship) from October 2001 to September 2002. He received several research prizes in chemistry; (1) he was awarded the prize of Prof. Dr Mohamed Abdel Salam in chemistry (2001) for young scientists provided by Academy of Scientific Research and Technology (Egypt). (2) He was awarded the Cairo University encouragement prize in chemistry in 2004. (3) He was awarded the Third World Academy of Science (TWAS) prize in chemistry for young scientists in 2004 provided by ICTP-Strada, Trieste-Italy, (4) he was awarded the State Award in Chemistry, Egypt 2005. He published many papers in the field of synthesis and applications of macrocycles and bis-heterocycles chemistry.



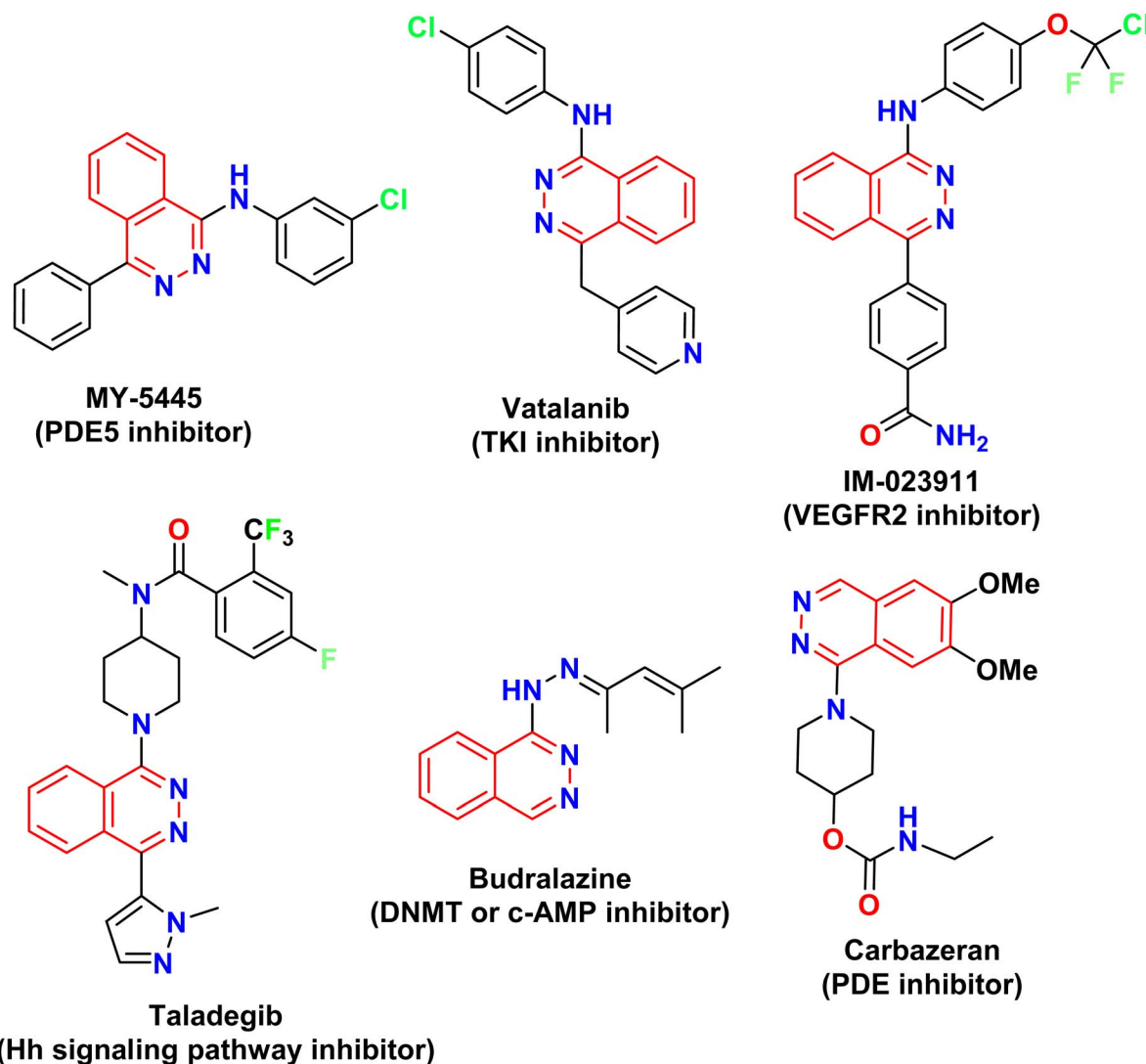


Fig. 2 Some FDA-approved phthalazine-based anticancer drugs.¹⁵ Molecular targets are; phosphodiesterase 5 (PDE5) inhibitor, tyrosine kinase inhibitor, vascular endothelial growth factor receptor 2, Hedgehog (Hh) signaling pathway, DNA methyltransferase (DNMT), cAMP-dependent protein kinase (PKA), and phosphodiesterase (PDE) inhibitor.

development as chemotherapeutic medicines.²⁹ The ability to synthesize these molecules using a variety of catalytic and microwave-assisted procedures increased their appeal, allowing the development of derivatives with greater efficacy and lower toxicity.³⁰ As a result, quinoxaline derivatives provided an essential framework for creating new anticancer drugs with broad therapeutic applications.

Cinnoline (1,2-benzodiazine) is a structural analog of phthalazine in which the nitrogen atoms are adjacent in the diazine ring.³² Such a relatively minor structural modification can lead to dramatic variances in biological activities that enable selective inhibition of distinct cancer pathways. Derivatives of 3H-cinnoline derivatives have gained immense interest in medicinal chemistry due to their diverse pharmacological applications, principally as anticancer agents, showcasing lucrative physicochemical properties and potential to be modified *via* various synthetic strategies.³³ The synthesis of

cinnoline derivatives was carried out through catalytic methods.³⁴ Such synthetic improvements have been beneficial in producing drugs based on the structure of cinnoline with improved potency against cancer cells.³⁵ Cinnoline derivatives have been shown to induce apoptosis, reduce cell proliferation, and inhibit angiogenesis *in vitro* and *in vivo*.³⁶ They typically do this by inhibiting the actions of enzymes like cyclin-dependent kinases (CDKs) and protein kinases.³⁷ These enzymes are necessary for cancer cells to cycle through the cell cycle and to transmit signals.³⁸ These characteristics suggested cinnoline derivatives as promising candidates for further exploration in oncology.^{39–41}

Advances in molecular biology and computational chemistry have helped us better grasp how these heterocyclic scaffolds interact with their biological targets.⁴² Researchers have used high-throughput screening, molecular docking studies, and structure–activity relationship analysis to find important



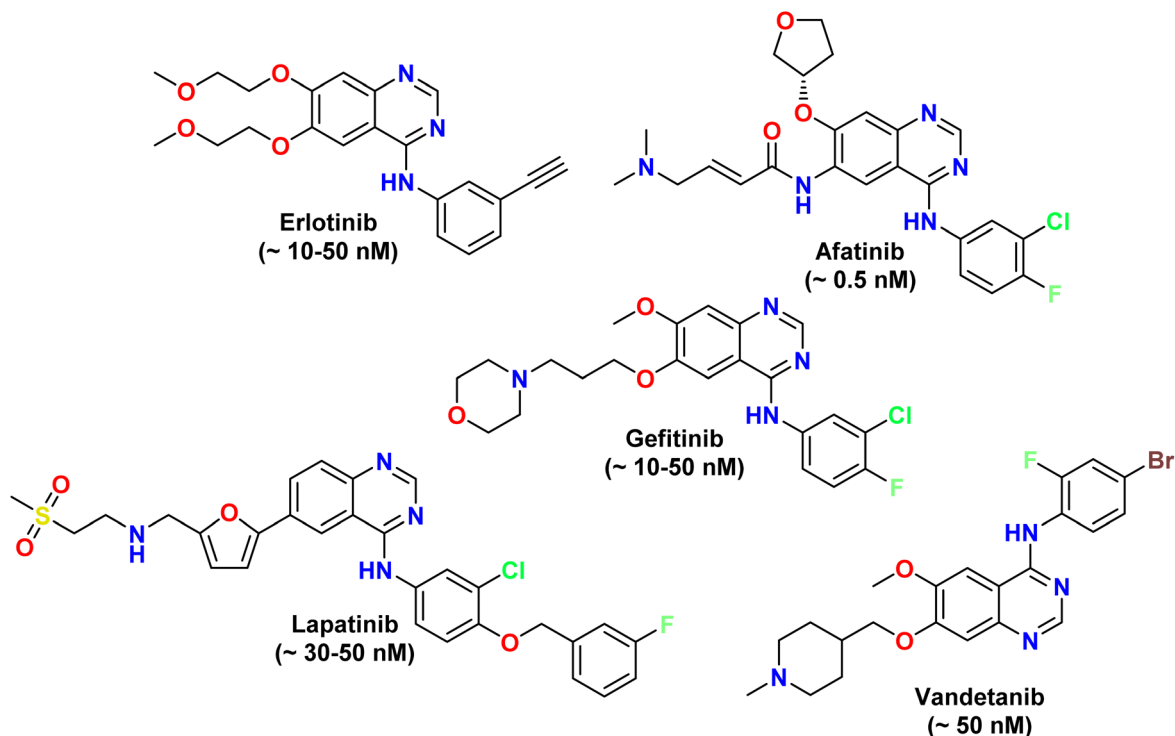


Fig. 3 Some FDA-approved quinazoline-based anticancer drugs.²³ Most of these drugs as mainly EGFR inhibitors, while Vandetanib is a multi-targeted tyrosine kinase inhibitor (TKI).

structural features needed to fight cancer. This knowledge has been helpful in guiding the design and synthesis of novel derivatives with increased effectiveness.⁴³ Additionally, recent research demonstrates that phthalazine, cinnoline, and

quinazoline derivatives can simultaneously alter multiple signaling pathways, enabling their multifaceted application in cancer treatment.⁸ This multi-targeted activity is beneficial in the case of heterogenous cancers, where a single-target

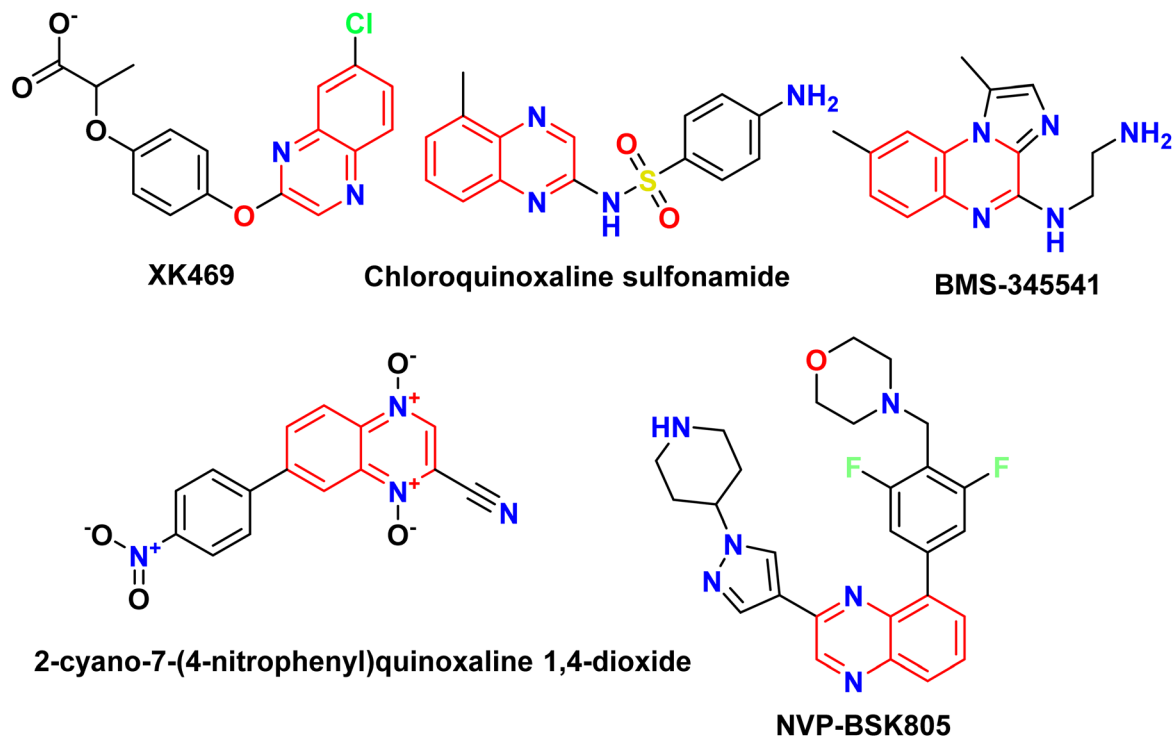


Fig. 4 Some quinoxaline-based anticancer drugs.³¹



medication may fail to deliver long-term therapeutic effects.⁴⁴ By targeting several elements of cancer cell survival, proliferation, and metastasis, these compounds have the potential to produce more effective and long-lasting responses in cancer patients.⁶

Recently, our research target has been to build up a wide array of simple- and bis-organic molecules incorporating various heterocyclic nuclei and different functionalities with promising anticancer inhibitory activities against many human cell lines.^{34,45–49} Encouraged by the facts and in continuation of our longstanding interest in the synthesis of biologically active heterocycles, we are engaged in a new, interesting protocol. The purpose of this work is to provide a comprehensive update on the synthetic pathways of fused 6-membered N-heterocyclic scaffolds with two N-atoms, particularly phthalazines, quinoxalines, cinnolines, and quinazolines, that have been documented in the most recent literature between 2020 and 2024 and emphasizing their potentials as promising anticancer agents.

2. Phthalazine derivatives

The reaction of 1-chloro-4-phenylphthalazine **1** with the methyl 4-aminobenzoate under reflux resulted in the production of methyl 4-[(4-phenylphthalazin-1-yl)amino]benzoate (**2**) in 81% yield. Heating of the ester **2** with hydrazine hydrate produced

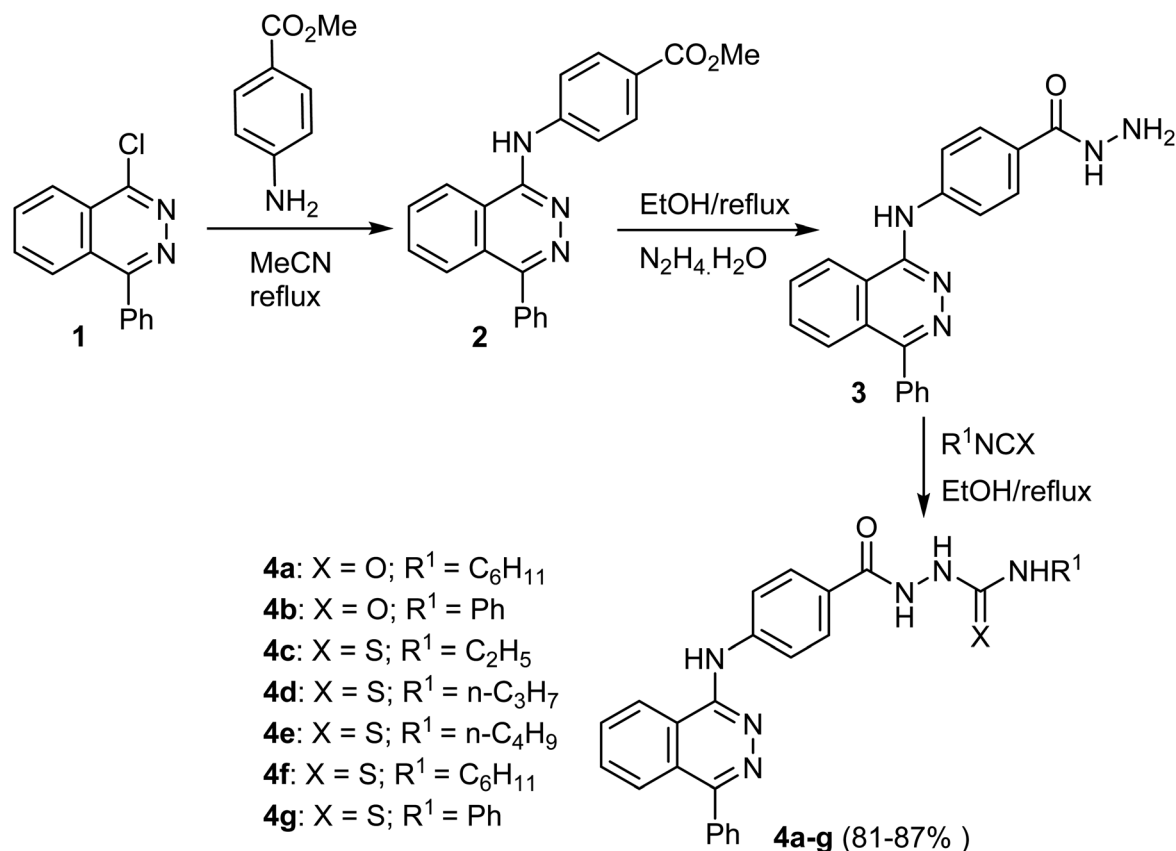
the hydrazide **3**, which upon heating with the appropriate isocyanate and/or isothiocyanate produced the corresponding semicarbazide **4a, b** and/or thiosemicarbazide **4c–g**, derivatives respectively in 81–87% yields (Scheme 1).⁵⁰

Khedr *et al.* reported the synthesis of novel phthalazine scaffolds **7a–g** as depicted in Scheme 2. Thus, heating of 1-chloro-4-phenylphthalazine **1** with the 4-aminoacetophenone gave the acetyl derivative **5**, which, upon condensation with the suitable aromatic benzaldehyde produced the chalcone derivatives **6a–g** in 81–88% yields. Cyclocondensation of **6a–g** with hydrazine hydrate yielded corresponding pyrazoline derivatives **7a–g** in 70–78% yields (Scheme 2).⁵¹

The acetyl derivative **9** was obtained by refluxing the chloro derivative **8** with 4-aminoacetophenone. The matching hydrazine derivatives **10a–g** were produced in 65–79% yields by condensation of **8** with the suitable acid hydrazides. Additionally, reaction of urea or thiourea derivatives with **8** yielded the corresponding phthalazine derivatives **11a, b** in 72–75% yields (Scheme 3).⁵²

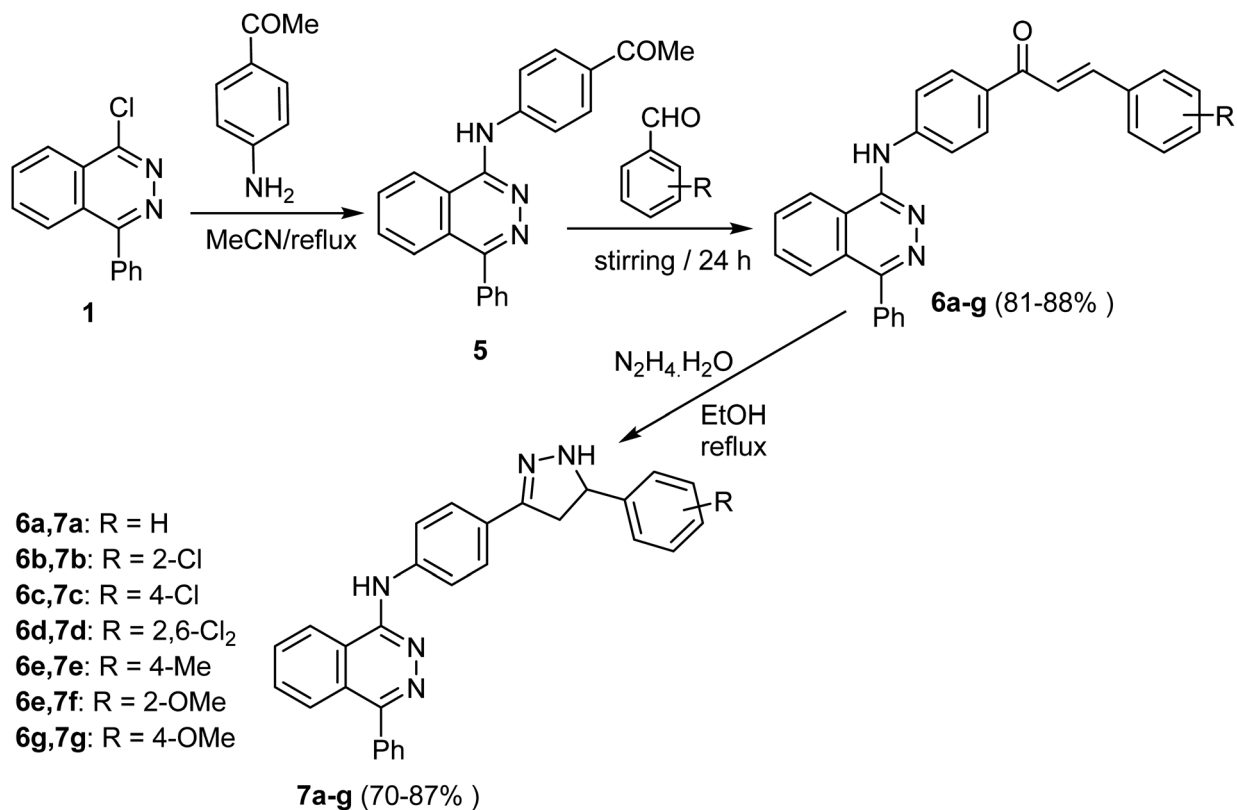
Hydrazinolysis of the methyl(2-(4-benzyl-1-oxophthalazin-2(1H)-yl)acetyl)glycinate ester (**12**) produced the corresponding hydrazide derivative **13**. Condensation of the hydrazide **13** with some active methylene compounds furnished the corresponding hydrazones **14a–c** in 84–91% yields, as shown in Scheme 4.⁵³

Scheme 5 describes the synthetic pathway to 2-phenyl-2,3-dihydrophthalazine-1,4-dione-1,2,3-triazole hybrids **20a–l**.

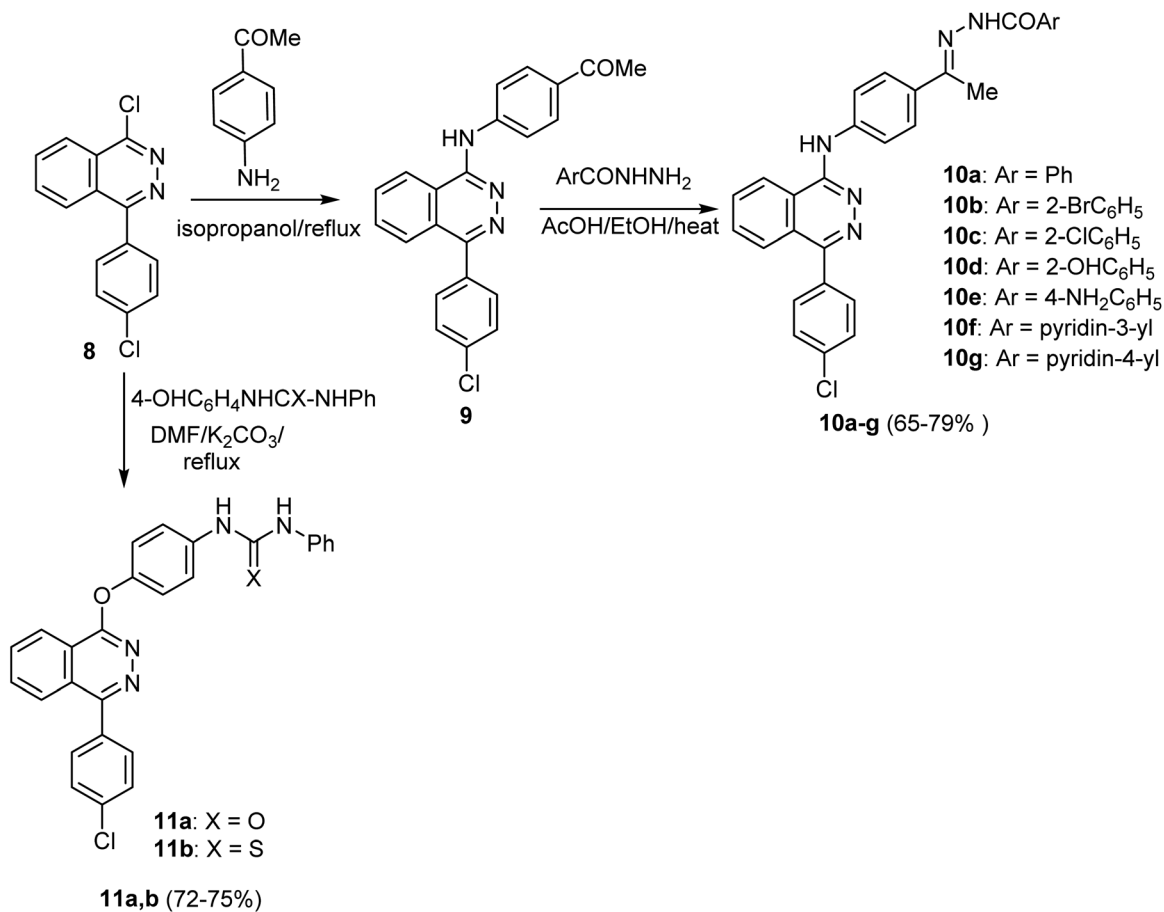


Scheme 1 Synthetic route for the preparation of phthalazine derivatives **4a–g**.



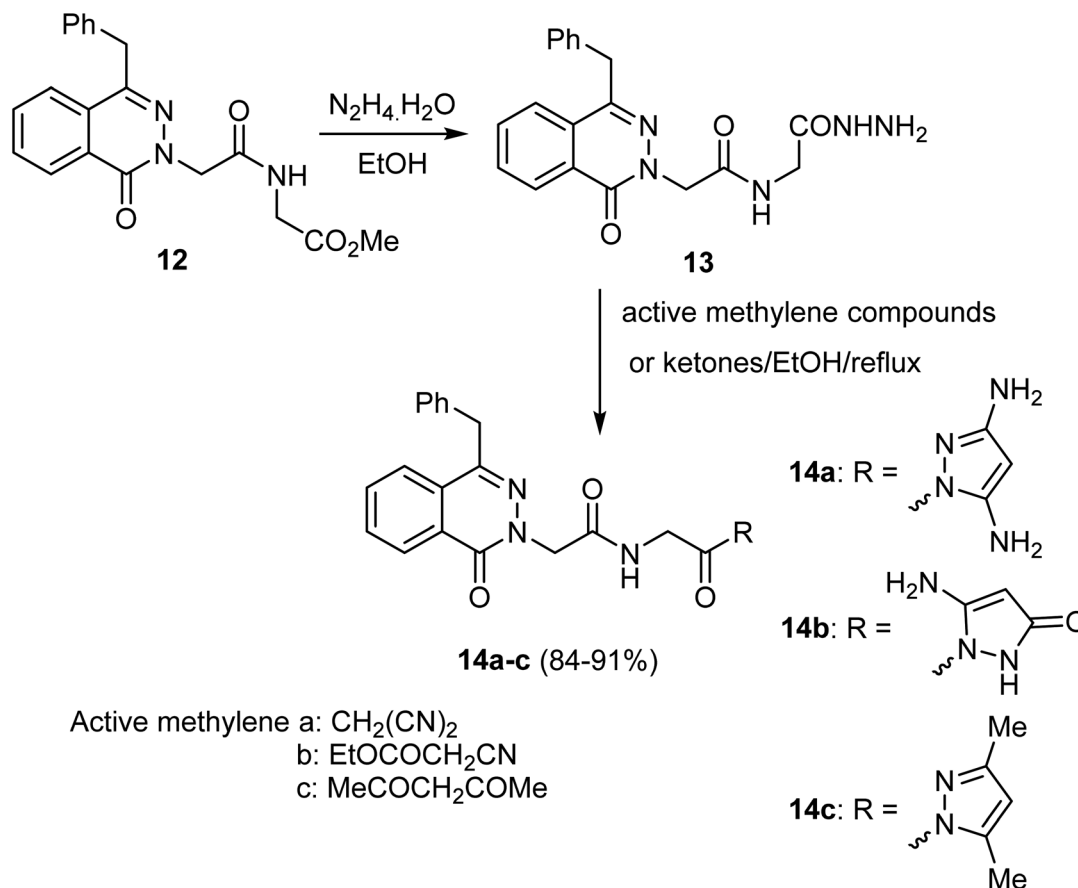


Scheme 2 Synthetic route for the preparation of target compounds 5–7.



Scheme 3 Synthetic route for the preparation of phthalazine derivatives 10 and 11.





Scheme 4 Preparation of phthalazine derivatives 14a–c.

Firstly, the reaction of phthalic anhydride (15) with phenylhydrazine (16) in acetic acid containing sodium acetate produced 2-phenyl-2,3-dihydrophthalazine-1,4-dione (17). Then, using potassium *tert*-butoxide as a base, compound 17 was alkylated with propargyl bromide in DMF to yield the 2,3-dihydrophthalazine derivative 18. Next, the 1,3-dipolar cycloaddition reaction between aryl azides 19a–I and terminal alkyne 18 in the presence of copper(i) iodide in THF produced the 2-phenyl-2,3-dihydrophthalazine-1,4-dione-1,2,3-triazole hybrids 20a–I in moderate to good yields, 76–88%. It's crucial to note that aryl azides 19 with electron-withdrawing groups produced higher yields than those with electron-donating groups.⁵⁴

Most compounds 20a–I exhibited promising physicochemical properties through ADME pharmacokinetics regarding obeying Lipinski's rule of drug-likeness.⁵⁵ Using Molsoft web-based software, compounds exhibited a good scale of obeyable parameters, particularly number of H-bond acceptors (HBA = 4 lower than 10), H-bond donor (HBD = 0, lower than 5), MW \leq 500, $\log p \leq$ 4.25, and in a summary a drug-likeness score is 0.40 (positive value as a drug-like). The incorporation of hydrogen bonding is critically important in the binding of drugs to their targets due to its ability to provide specificity, stability, and strength to the drug–target complex.⁵⁶

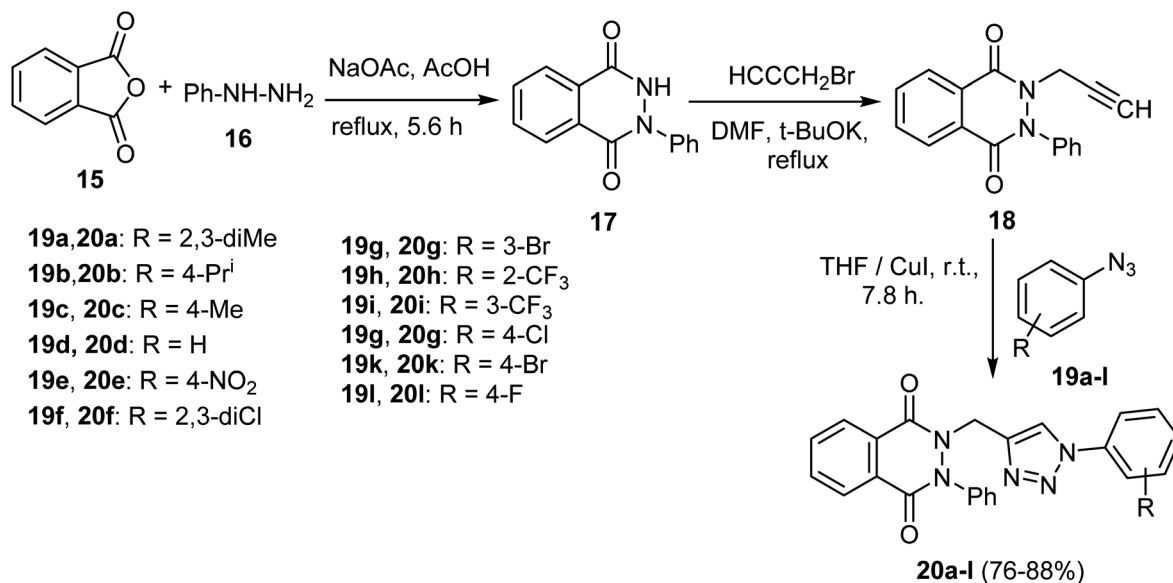
2.1 Anticancer activity of phthalazine-based derivatives

Synthesis of 4f and evaluation of its cytotoxic activity against three human cancer cell lines (HepG2, HCT-116, and MCF-7) was reported. Compound 4f exhibited notable cytotoxicity against tested cell lines “HepG2, HCT-116, and MCF-7” with IC_{50} values of 3.97 μM , 4.83 μM , and 4.58 μM , respectively. The inhibitory effects of 4f against VEGFR-2 were also significant with IC_{50} 0.08 μM , compared to the reference drug Sorafenib (IC_{50} = 0.10 μM). The ability of 4f to interact with VEGFR-2 was also confirmed by docking studies.⁵⁰

The antiproliferative activity of compound 6e was evaluated *in vitro* against three human cancer cell lines: HepG2, HCT-116, and MCF-7. Compound 6e showed significant anticancer activity against all the tested cell lines HepG2, HCT-116, and MCF-7 with IC_{50} values of 11.23 μM , 10.12 μM , and 13.92 μM , respectively, compared with Sorafenib (IC_{50} = 9.18 μM , 5.47 μM , and 7.26 μM , respectively) and Doxorubicin (IC_{50} = 7.94 μM , 8.07 μM , and 6.75 μM , respectively). The inhibitory effects of 6e against VEGFR-2 were also significant with IC_{50} 0.11 μM , compared to the reference drug Sorafenib (IC_{50} = 0.10 μM). The ability of 6e to interact with VEGFR-2 was also confirmed by docking studies.⁵¹

The antiproliferative activity of another series of phthalazine derivatives 10g and 11a was evaluated against two human





Scheme 5 Preparation of phthalazine derivatives 20a–l.

cancer cell lines, MCF-7 (breast cancer) and HepG-2 (hepatocellular carcinoma), compared with Sorafenib as a reference drug. The two derivatives, **10g** and **11a** demonstrated, exhibited notable activity against MCF-7 and HepG-2, with IC₅₀ values (0.15 μM and 0.12 μM for **10g**) and IC₅₀ values (0.18 μM and 0.09 μM for **11a**), respectively. They showed significant anticancer activities against the tested cancer cell lines compared to the reference drug. The ability of **10g** and **11a** to inhibit VEGFR-2 was evaluated *in vitro*, and these two compounds showed significant activity with IC₅₀ values 0.148 μM and 0.196 μM, respectively, compared to Sorafenib (IC₅₀ = 0.059 μM). Docking studies supported the obtained results and demonstrated the ability of these derivatives to interact with VEGFR-2 active sites.⁵²

Compound **14b** was screened for anticancer activity *in vitro* against two human cancer cell lines, MCF-7 and MDA-MB-231, using Erlotinib as a reference drug and tested against a normal cell line (MCF-10A) to determine their specificity. Compound **14b** showed significant cytotoxic activity against the cell lines MCF-7 and MDA-MB-231 with IC₅₀ values of 1.9 μM and 0.57 μM, respectively, compared to Erlotinib with IC₅₀ 1.32 μM and 1.02 μM, respectively. In addition, the IC₅₀ value of **14b** against MCF-10A was 41.6 μM. The inhibition activity of this **14b** against EGFR was evaluated; the inhibitory effects of **14b** against EGFR were also significant with IC₅₀ 21.4 nM, compared to reference drug Erlotinib (IC₅₀ = 80.1 nM) and the percentage of inhibition of EGFR with 10 μM of **14b** was 97.6%, compared to the Erlotinib 93.9%. The ability of **14b** to interact with EGFR was also confirmed by docking studies.⁵³

The antiproliferative activity of compound **20e** was evaluated *in vitro* against three human cancer cell lines, A-375, A-549, and MCF-7, and Doxorubicin was used as a reference drug. **20e** displayed significant cytotoxicity against the three cell lines, A-375, A-549, and MCF-7, with IC₅₀ values of 2.33 μM, 7.21 μM, and 3.96 μM, respectively. The ability of these novel derivatives

to interact with EGFR active sites and to inhibit its activity was also confirmed by docking studies (Table 1).⁵⁴

3. Quinazoline derivatives

Synthesis of the quinazoline-based molecular hybrids **24a–g** was reported by Xu *et al.* by applying the Buchwald–Hartwig coupling of **22** with aminoindazole derivative **23** to afford the targeted *N*-(1*H*-indazol-3-yl)quinazolin-4-amine products **24a–g** in 65–96% yields (Scheme 6).⁵⁷

Liu *et al.* described a synthetic route for the quinazoline compounds **31a–g** starting with 7-methoxyquinazolin-4(3*H*)-one (**25**). Thus, chlorination of **25** with thionyl chloride followed by subsequent nucleophilic displacement with aniline derivatives **27** gave products **28a–e**. Reduction of **28a–e** with stannous chloride dihydrate afforded **29a–e**, which upon treatment with the isocyanates **30a–c** yielded the target compounds **31a–g** in 70–89% yields (Scheme 7).⁵⁸

The synthetic route to the 3-phenylquinazolin-2,4(1*H*,3*H*)-dione derivatives **33a–j** was described by Hassan *et al.* These compounds were synthesized, in 65–82% yields, *via* a single pot three-component reaction of 4-(2,4-dioxo-1,4-dihydro-2*H*-quinazolin-3-yl)-benzoyl chloride **32** with ammonium thiocyanate followed by aryl(hetaryl)amines at reflux condition (Scheme 8).⁵⁹

Mortazavi *et al.* designed and synthesized a series of quinazoline-triazole molecular hybrids **38a–i** as targeted anti-cancer agents. The reaction of 4-(prop-2-ynyloxy)benzaldehyde (**35**) with quinazolin-4-yl-hydrazine (**34**) in ethanol afforded 4-(2-(4-(prop-2-ynyloxy)benzylidene)-hydrazinyl)quinazoline **36**. The reaction of **36** with the intermediate benzyl azide **37a–i** at room temperature afforded the targeted compounds **38a–i** (Scheme 9).⁶⁰

El-Hamaky *et al.* designed and synthesized a series of quinazoline-1,2,3-triazole hybrids **45a–r** (in 74–92% yields) *via*





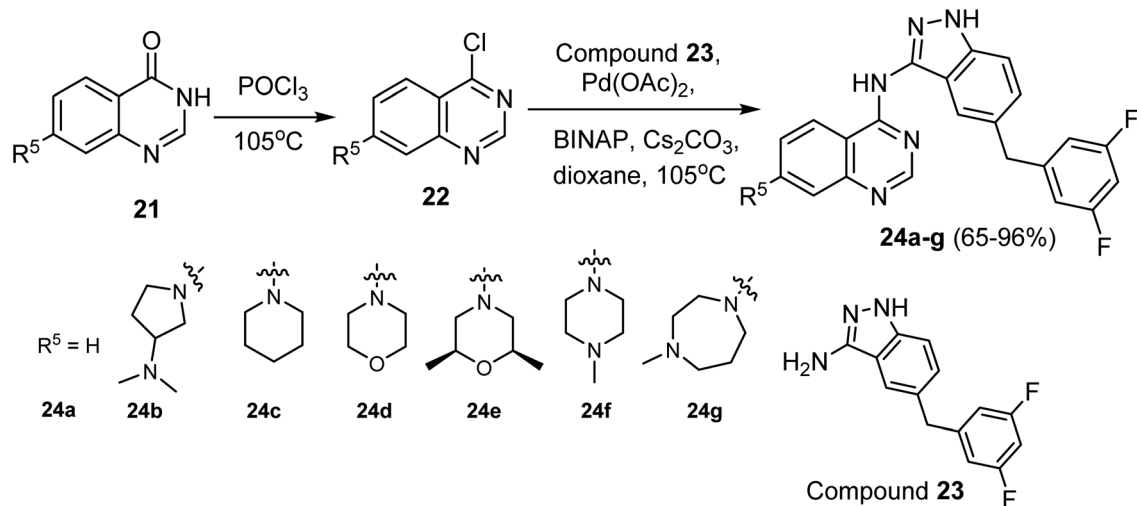
Table 1 Cytotoxicity of phthalazine-based derivatives with kinase inhibition

Entry	Structure	Kinase inhibition activity		Anticancer activity		Ref.			
1		Enzymes VEGFR-2	IC ₅₀ [μM] (4f) 0.08 ± 0.01	Sorafenib 0.10 ± 0.02	Cell lines HepG2 HCT116 MCF-7	IC ₅₀ [μM] (4f) 3.97 ± 0.2 4.83 ± 0.2 4.58 ± 0.3	Sorafenib 9.18 ± 0.6 5.47 ± 0.3 7.26 ± 0.3	Doxorubicin 7.94 ± 0.6 8.07 ± 0.8 6.75 ± 0.4	50
2		Enzymes VEGFR-2	IC ₅₀ [μM] (6e) 0.11 ± 0.02	Sorafenib 0.10 ± 0.02	Cell lines HepG2 HCT116 MCF-7	IC ₅₀ [μM] (6e) 11.23 ± 1.1 10.12 ± 1.0 13.92 ± 1.2	Sorafenib 9.18 ± 0.6 5.47 ± 0.3 7.26 ± 0.3	Doxorubicin 7.94 ± 0.6 8.07 ± 0.8 6.75 ± 0.4	51
3		Enzymes VEGFR-2	IC ₅₀ [μM] (10g) 0.148 ± 0.01	Sorafenib 0.059 ± 0.01	Cell lines MCF-7 Hep G2	IC ₅₀ [μM] (10g) 0.15 ± 0.1 0.12 ± 0.01	Sorafenib 0.05 ± 0.01 0.03 ± 0.01		52
4		Enzymes VEGFR-2	IC ₅₀ [μM] (11a) 0.196 ± 0.01	Sorafenib 0.059 ± 0.01	Cell lines MCF-7 Hep G2	IC ₅₀ [μM] (11a) 0.18 ± 0.1 0.09 ± 0.01	Sorafenib 0.05 ± 0.01 0.03 ± 0.01		52

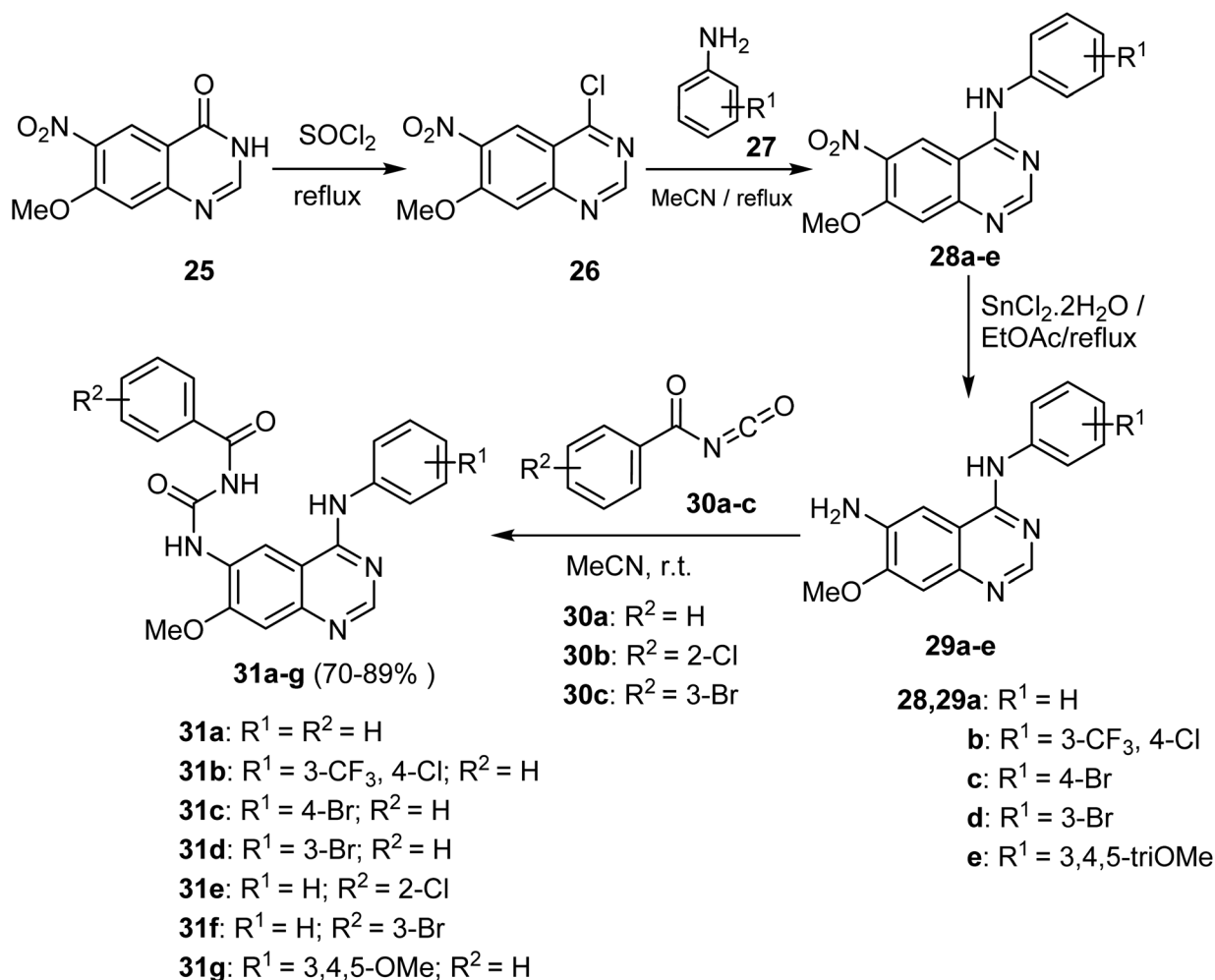


Table 1 (Contd.)

Entry	Structure	Kinase inhibition activity	Anticancer activity	Ref.
5		Enzymes EGFR IC ₅₀ [μM] (14b) 21.4 ± 0.67 Kinase inhibition (%) at 10 μM (21) 97.6 ± 2.49	Cell lines MCF-7 MDA-MB-231 MCF-10A Erlotinib 80.1 ± 1.21 Erlotinib 93.9 ± 2.68 IC ₅₀ [μM] (14b) 1.9 ± 0.01 0.57 ± 0.09 41.6 ± 1.8	Erlotinib 1.32 ± 0.04 1.02 ± 0.1 30.9 ± 1.8 53
6		Enzymes EGFR Docking study (20e) Compound 20e displayed the best docking score of -11.16	Cell lines A-375 A-549 MCF-7 IC ₅₀ [μM] (20e) 2.33 ± 0.43 7.21 ± 0.61 3.96 ± 0.41	Doxorubicin 2.18 ± 0.18 5.51 ± 0.039 2.02 ± 0.17 54



Scheme 6 Synthetic routes of quinazolin-4-amine derivatives 24a–g.



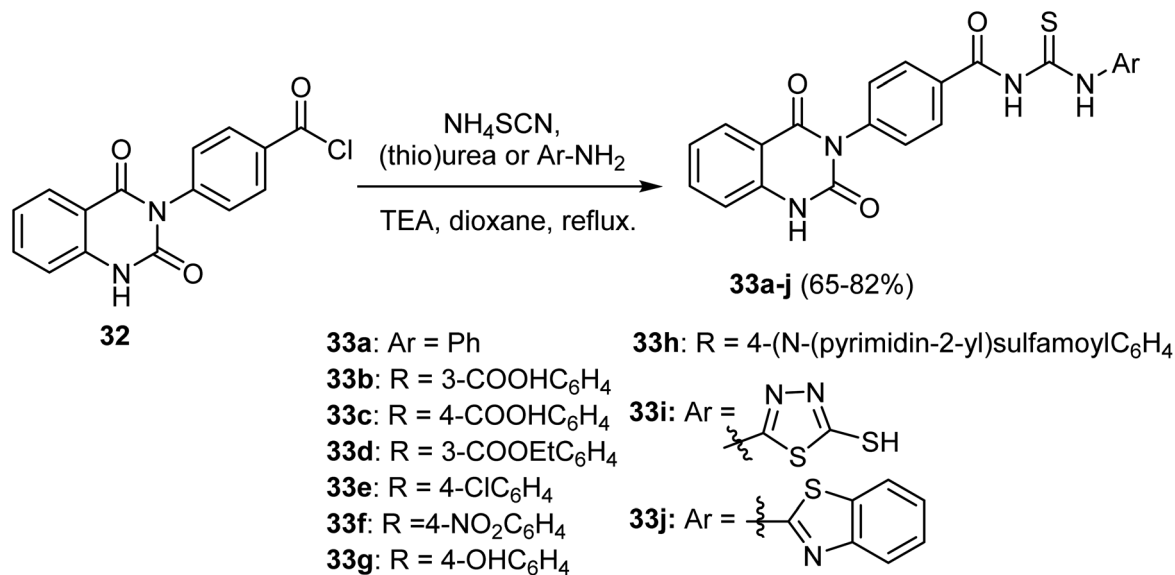
Scheme 7 Synthetic routes of quinazoline derivatives 31a–g.

a step-wise protocol starting with anthranilic acid (39) according to the described procedure in Scheme 10.⁶¹

A series of 4-(3-1*H*-indazolyl)aminoquinazoline derivatives were described by Han *et al.* as shown in Scheme 11. Thus,

protecting the NH group of indazole ring in 4-((1*H*-indazol-3-yl)amino)-quinazoline (46) with Boc moiety followed by hydrolysis of the ester function produced the quinazoline-2-carboxylic acid derivative 48. Acylchlorination of compound 48 with oxalyl





Scheme 8 Synthetic pathway of 3-phenylquinazolin-2,4-dione derivatives 33a–j.

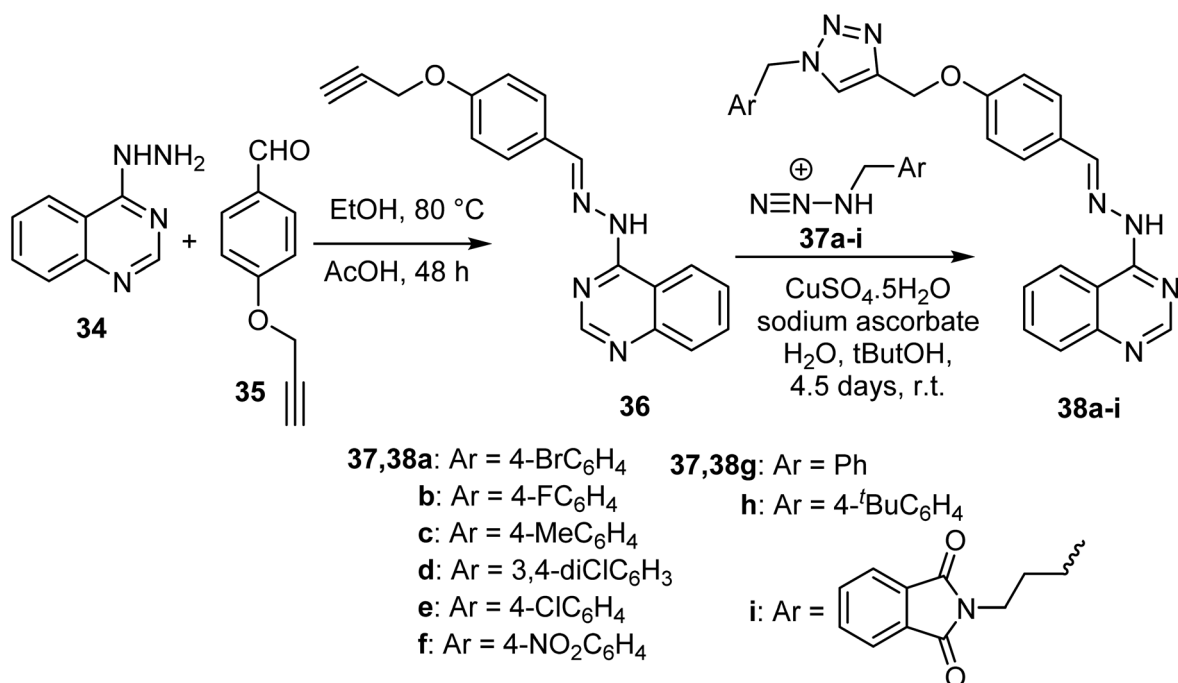
chloride, then amidation with various amines, resulted in the formation of compounds **49a–51j** in 27–43% yields.⁶²

The reaction of 4-(6-iodo-2-mercapto-4-oxoquinazolin-3(4*H*)-yl)benzenesulfonamide **52** with 2-chloro-*N*-substituted acetamides **53a–o** in the presence of K₂CO₃ at room temperature, afforded a series of alkyl quinazolyl sulfides hybrids **54a–o** in 60–91% yield (Scheme 12).²⁰

Suzuki cross-coupling reaction of the boronic acid pinacol ester **55** with the bromoquinazoline derivative **56** afforded the corresponding cross-coupled product **57**. The latter compound

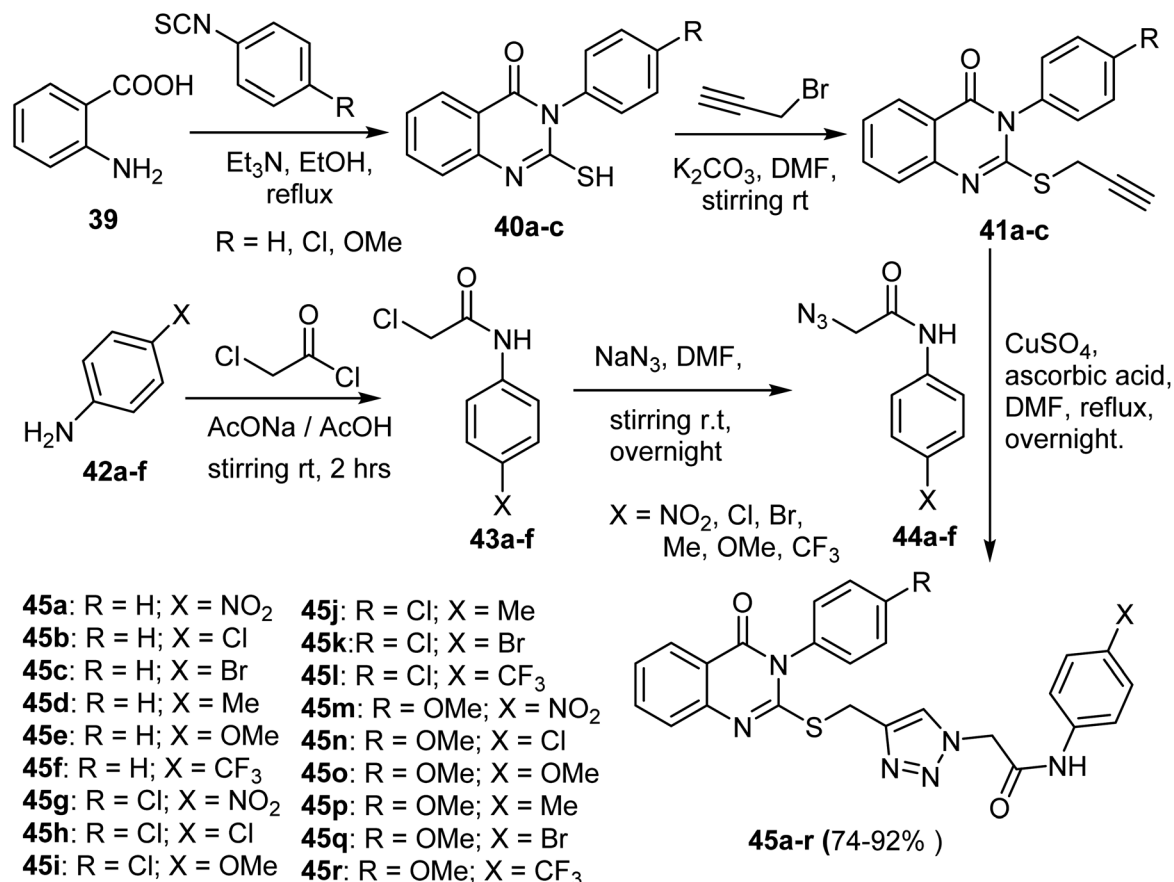
57 underwent Buchwald coupling reaction with aryl(heteroaryl) halides to afford compounds **58a–k**. Deprotections of the protecting groups of **58** resulted in the formation of the pyrido[2,3-*b*][1,4]oxazin-7-ylquinazoline derivatives **59** and **60** in 42–93% yields (Scheme 13).⁶³

Ahmed *et al.* designed and synthesized some quinazoline compounds aiming to discover new anticancer agents. Thus, the reaction of 6-bromo-2-mercapto-3-phenylquinazolin-4(3*H*)-one (**61a**) with ethyl 2-chloroacetate in DMF afforded **62a**, which was then heated with hydrazine hydrate in ethanol to



Scheme 9 Synthesis of quinazoline triazole derivatives 38a–i.





Scheme 10 Quinazoline-1,2,3-triazole hybrids 45a-r.

afford the hydrazide derivative **63a**. The condensation reaction of **63a** and appropriate aromatic aldehydes gave the corresponding hydrazones **64a-d** in 66–80% yields (Scheme 14).⁶⁴

Treatment of 6-chloro-2-mercapto-3-phenylquinazolin-4(3*H*)-one (**61b**) with ethyl 2-chloroacetate in DMF afforded compound **62b**, which was then refluxed with hydrazine hydrate in ethanol to give hydrazide derivative **63b**. Condensation of **63b** with the appropriate aromatic aldehyde afforded the corresponding target hydrazones **64e-h** in 74–82% yields (Scheme 15).⁶⁵

Wang *et al.* described a synthetic route for the 4-aminoquinazoline derivatives **68a-o** via Buchwald coupling of aryl amines with 4-chloro-6-iodoquinazoline (**65**) to give the intermediates **66a-o**. Suzuki-Miyaura cross-coupling reaction with 2-aminopyridine-5-boronic pinacol acid ester **67** with **67** gave the corresponding products **68a-o** as depicted in Scheme 16.⁶⁶

Heating the quinazoline derivatives **68a-o** with the bromopyruvate esters **69** gave the target products **70a-s** in 37–63% yields, as shown in (Scheme 17). Treatment of the intermediate **67** with alpha-bromoketones **71** afforded compounds **72**, which upon coupling with intermediates **66** yielded the target products 6-(2-phenylimidazo[1,2-*a*]pyridin-6-yl)quinazolin-4-amine derivatives **73a-i** in 55–73% yields.⁶⁶

Allam *et al.* described the synthesis of 6-bromo-2-(pyridin-3-yl)-4-substituted quinazolines **76a-c** (in 55–63% yields) from the

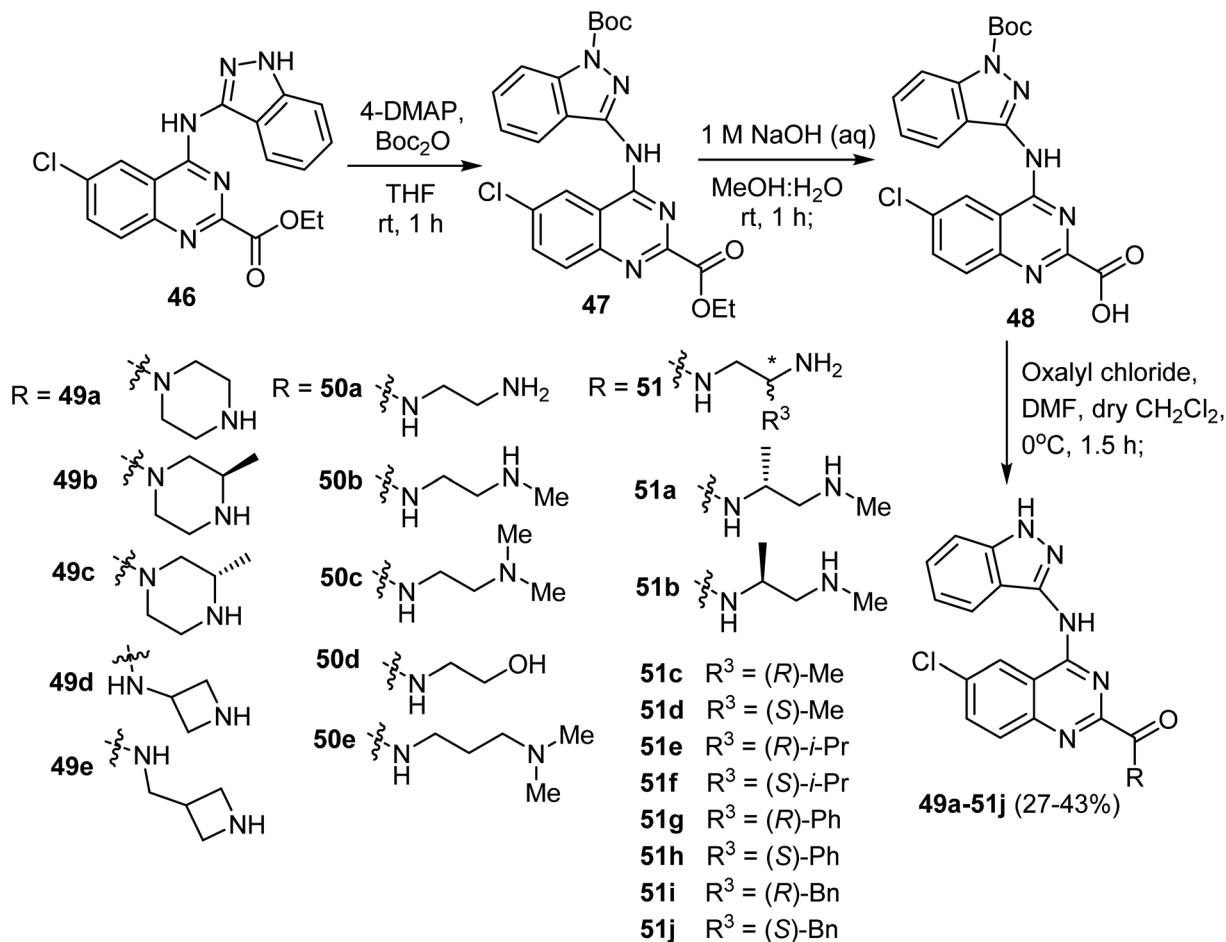
reaction of 4-chloro derivative **74** with 2-aminobenzothiazoles **75** in refluxing DMF as depicted in Scheme 18.⁶⁷

A series of quinazoline-thioacetamide derivatives **79a-j** and quinazoline-thioacetamides constituting sulfonamide tail **79k-q**, were designed and synthesized by Ghorab *et al.* according to Scheme 19. Thus, 2-mercapto-3-phenylquinazolinone **77** reacted with 2-chloro-*N*-substituted acetamide **78** in dry acetone and K₂CO₃, afforded the 2-((4-oxo-3-phenyl-3,4-dihydroquinazolin-2-yl)thio)acetamide derivatives **79a-q** in 61–89% yields.¹⁹

A series of 8-methoxy-2-trimethoxyphenyl-3-substituted quinazoline-4(3)-one derivative **81-84** were reported by Altamimi *et al.* and screened for antitumor activity. Thus, synthesis of the target compounds started with hydrazinolysis of 8-methoxy-2-trimethoxyphenyl-4*H*-benzo[*d*][1,3]oxazin-4-one (**80**) with hydrazine to afford 3-amino-quinazoline-4(3*H*)-one derivative (**81**) in 81% yield. Treatment of compound **81** with benzene sulphonyl chloride yielded the benzenesulfonylaminoquinazoline derivative **82** in 80% yield. Treatment of compound **80** with ammonia produced the benzamide derivative **83** in 92% yield. When compound **80** was refluxed with 3,4,5-trimethoxy aniline, it afforded the quinazoline-4(3*H*)-one **84** derivatives in 83% yields (Scheme 20).⁶⁸

The synthesis of the target quinazoline heterocycles **88** and **89** was achieved by the route depicted in Scheme 21. Thus, the reaction of 3-(4-hydroxyphenyl)propanoic acid (**85**) and ethyl 2-





Scheme 11 Preparation of 4-(3-1H-indazolyl)amino quinazoline derivatives 49a–51j.

amino-5-chlorobenzoate (**86**) in xylene, in the presence of phosphorus trichloride under reflux condition furnished the corresponding ester **87** in 73% yield. Cyclocondensation of the benzoate ester **87** with hydrazine hydrate in *n*-butanol afforded the quinazolin-4-one scaffold **88** in 65% yield. Finally, condensation of *N*-amino derivative **88** with 4-hydroxy-3-methoxybenzaldehyde in refluxing *n*-butanol afforded the corresponding Schiff base **89** in 84% yield.⁶⁹

3.1 Anticancer activity of quinazoline-based derivatives

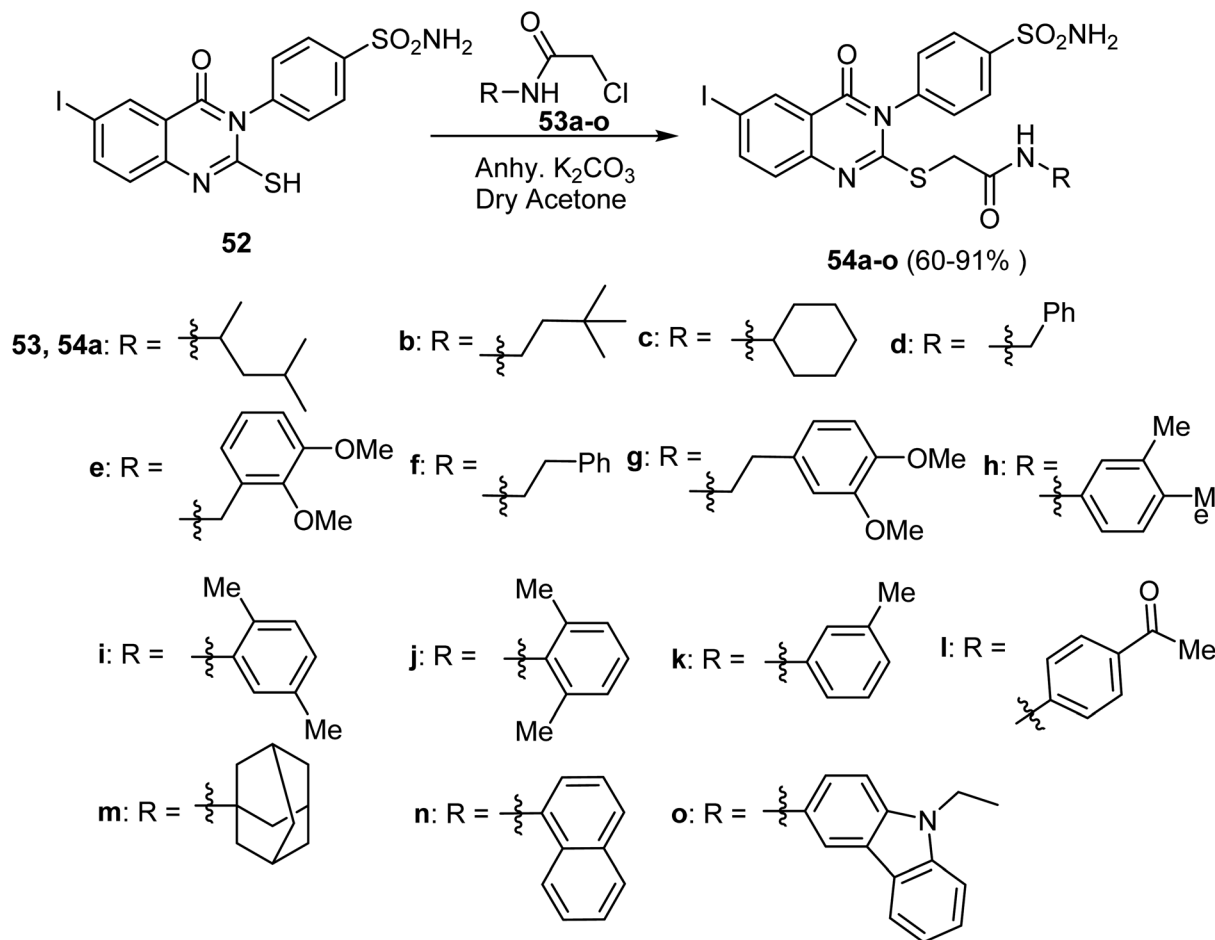
Compound **24f** was designed, synthesized, and tested against tropomyosin receptor kinases (TRKs); the compound showed good inhibitory activity against TRK^{WT} (IC₅₀ = 0.55 nM), TRK^{G595R} (IC₅₀ = 25.1 nM) and TRK^{G667C} (IC₅₀ = 5.1 nM), compared to Larotrectinib with IC₅₀ values 1.1 nM, 81.7 nM, and 51.1 nM respectively. The compound also demonstrated potent superior to Larotrectinib antiproliferative activity against a panel of Ba/F3 cell lines transformed with NTRK wild type and mutant fusions (IC₅₀ = 10–200 nM).⁵⁷

The antiproliferative activity of another series of quinazoline derivatives was evaluated against ten human cancer cell lines A375, HeLa, Eca-109, H1975, MDA-MB-453, SW1353, Sgc7901, A549, HT-29, and MCF-7 compared with Gefitinib as reference drugs. Compound **31c** demonstrated exhibited

notable activity against A375, HeLa, Eca-109, H1975, MDA-MB-453, SW1353, Sgc7901, A549, HT-29, and MCF-7, with IC₅₀ values (3.36, 2.48, 6.27, 7.66, 2.77, 2.01, 3.78, 1.04, 2.57 and 2.26 μM) respectively. It showed significant anticancer activities against the tested cancer cell lines compared to the reference drug Gefitinib. The ability of **31c** to inhibit EGFR was evaluated *in vitro*, and this compound showed significant activity with IC₅₀ values of 10.66 nM, compared to Gefitinib (IC₅₀ = 25.42 nM). Docking studies supported the obtained results and demonstrated the ability of these derivatives to interact with EGFR active sites.⁵⁸

The antiproliferative activity of a novel series of 3-phenylquinazolin-2,4(1*H*,3*H*)-diones was evaluated against HCT-116 (colorectal carcinoma) compared with Cabozantinib as a reference drug. Compound **33e** demonstrated exhibited notable activity against HCT-116, with IC₅₀ value 3.403 μM. It showed significant anticancer activities against the tested cancer cell line compared to the reference drug. The ability of **33e** to inhibit both VEGFR-2/*c*-MetTKs was evaluated *in vitro*, and the compound showed significant activity with IC₅₀ values 83 nM and 48 nM, respectively, compared to Cabozantinib with IC₅₀ values 59 nM, 30 nM, respectively. Docking studies supported the obtained results and demonstrated the ability of this compound to interact with VEGFR-2/*c*-MetTKs active sites.⁵⁹





Scheme 12 Synthesis of the quinazolinone derivatives 54a–o.

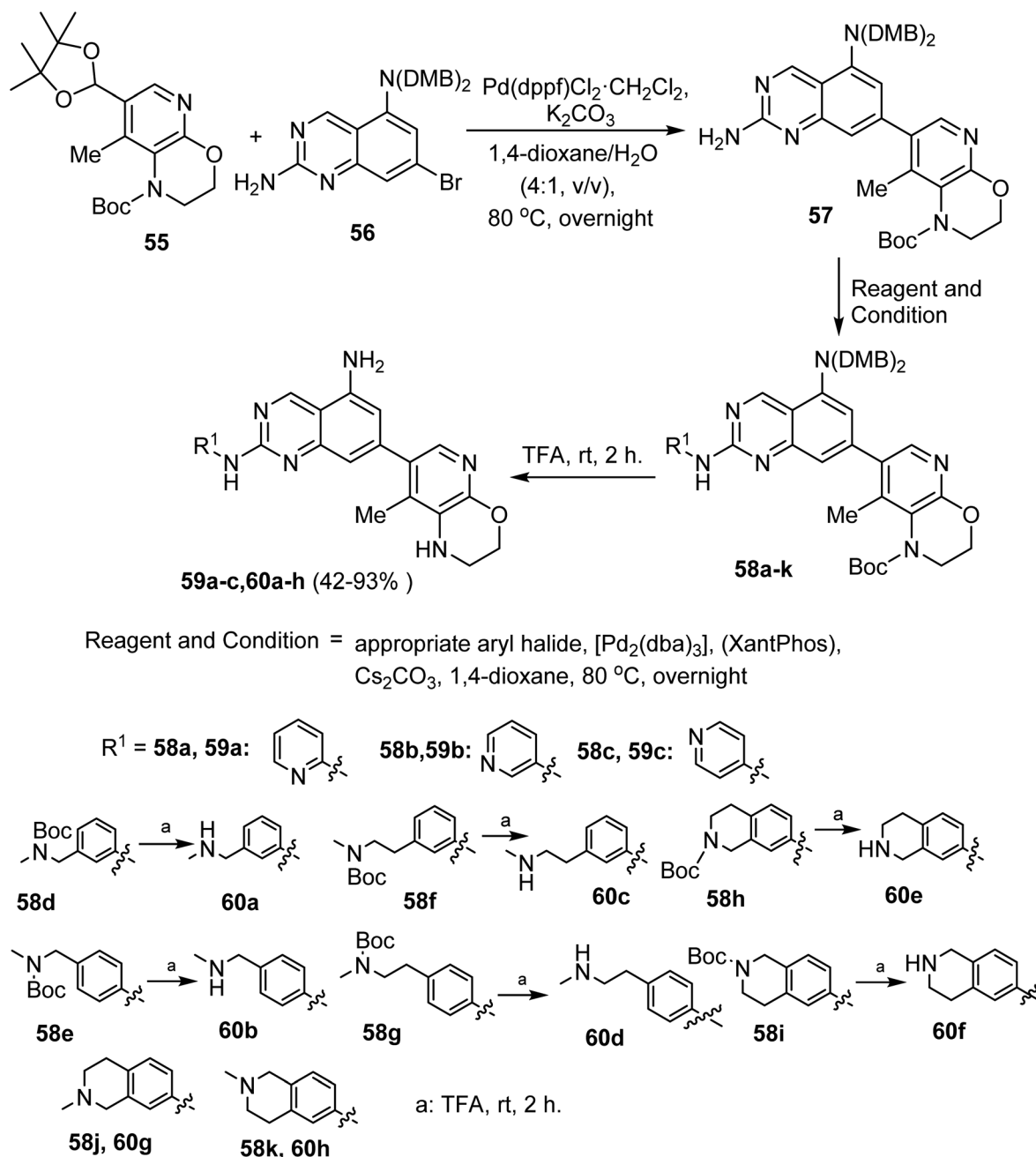
A novel series of quinazoline derivatives with 1,2,3-triazole moiety was synthesized and then evaluated against the following cancer cell lines: AsPC-1 and Mia-Paca-2 (pancreatic cancer), HT-29 (colorectal cancer cells), MKN-45 (gastric cancer), EBC-1 (lung cancer) and K562 (leukemia). Compound **38c** demonstrated exhibited notable activity against AsPc-1, EBC-1, MKN-45, Mia-Paca-2, HT-29, and K562, with IC_{50} values (15.3, 19.0, 22.0, 25.6, 21.0 and 31.5 μM) respectively. Compound **38c** showed the highest inhibition activity against MET among the tested derivatives, which was also confirmed by the results of the western blot test. Compound **38c** also inhibited PDGFRA activity by 58% at 10 μM concentration.⁶⁰

The antiproliferative activity of another series of 4-(3-*H*-indazolyl)amino quinazoline derivatives were evaluated against a human cancer cell line A549 compared with PF-3758309 as a reference drug. The structural–activity relationship (SAR) studies showed that a hydrophobic group at the 1' or 2'-position of the ethylenediamine side chain of **51a–j** (Scheme 11) enhanced their binding affinity. PAK4 inhibition test demonstrated that both **51c** and **51d** with 2'-methyl group displayed higher activity than that of **51a–b** with 1'-methyl group. Larger hydrophobic substituents; *i*-propyl group at 2'-position of the ethylenediamine side chain of **51e–f** resulted in a significant

improvement of enzymatic activities. Compounds with 2'-large substituents *e.g.* phenyl (**51g–h**) or benzyl (**51i–j**) showed similar inhibitory potency to **51e–f**. Thus, the IC_{50} values of **51e–j** were determined against PAK4. The derivative **51e** demonstrated notable activity against A549, with IC_{50} value (0.61 μM). It showed significant anticancer activities against the tested cancer cell line compared to reference drugs. The ability of **51e** to inhibit PAK4 was evaluated *in vitro*, and this compound showed significant activity with an IC_{50} value 10 nM, compared to PF-3758309 ($IC_{50} = 9$ nM). Docking studies supported the results obtained and demonstrated the ability of these derivatives to interact with PAK4 active sites.⁷⁰

The antiproliferative activity of compound **54n** was evaluated *in vitro* against four human cancer cell lines HepG2, MCF-7, HCT-116, and A549, and Sorafenib and Erlotinib were used as reference drugs. Compound **54n** displayed significant cytotoxicity against the four cell lines, HepG2, MCF-7, HCT-116, and A549, with IC_{50} values of 0.3425 μM , 0.0977 μM , 0.2000 μM , and 0.5134 μM , respectively. Compound **54n** also showed good *in vitro* inhibition potency of EGFR and VEGFR-2 with IC_{50} values 0.0728 μM and 0.0523 μM , respectively. With almost similar potency as the reference drugs Sorafenib ($IC_{50} = 0.1400$ μM against VEGFR) and Erlotinib ($IC_{50} = 0.2420$ μM against EGFR).





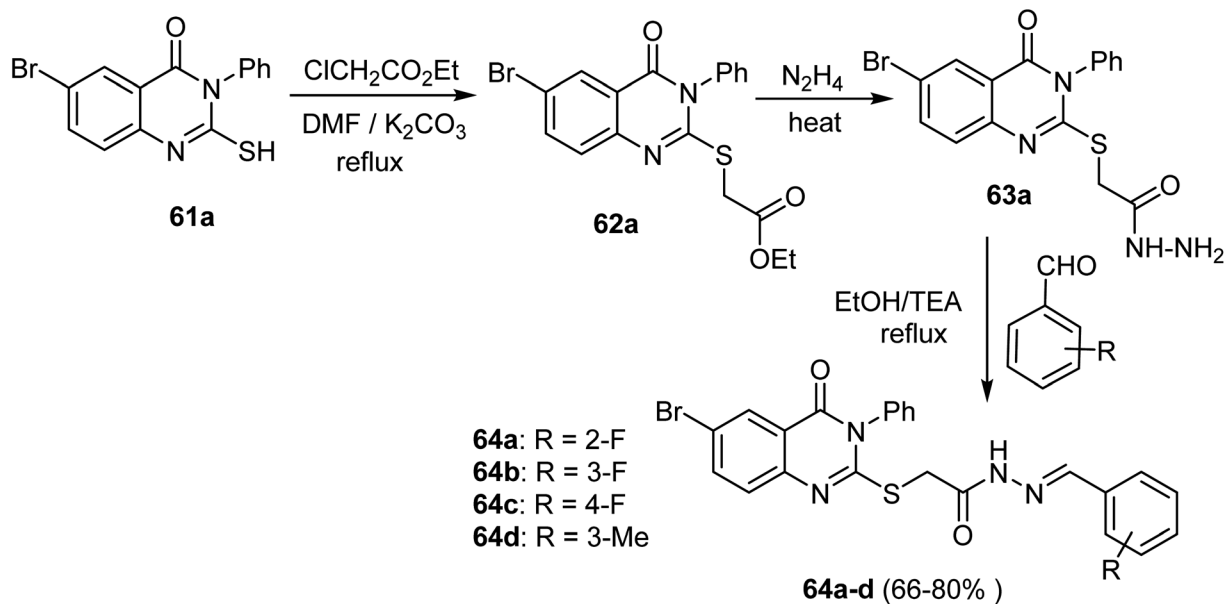
Scheme 13 Synthesis of compounds 59a–c and 60a–h.

The ability of these novel derivatives to interact with EGFR and VEGFR-2 active sites and to inhibit their activities was also confirmed by docking studies.²⁰ The SAR study showed that the impact of substituting the pyridine and two methoxy moieties, the urea, and amino linkers of **54** derivatives (Scheme 12) played a significant influence in the anticancer action. The impact of substituents of varied electronic and lipophilic natures on anticancer activity was also examined. It was found that compounds **54g**, **n** (having neoheptyl and naphthyl groups) showed the most significant anticancer activity compared to the other derivatives against MCF-7, HepG2, A549, and HCT116 cell lines. Both derivatives **54g**, **n**, also displayed the highest

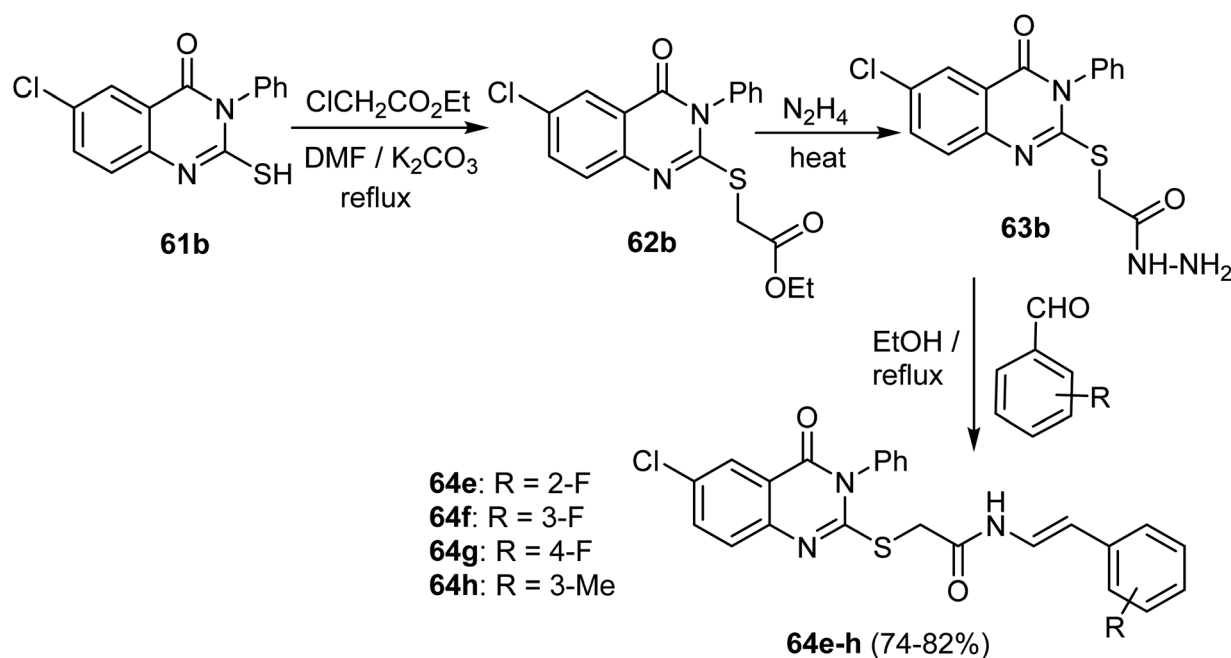
inhibition of EGFR T790M and VEGFR-2 enzymes. Compound **8** has the hydrophobic 3,4-dimethoxyphenethyl group, showed more significant activity against the MCF-7 and HCT-116 cell lines than compound **54d** (having benzyl group), **54e** (having 2,3-dimethoxybenzyl moiety), and **54f** (with phenethyl moiety). Furthermore, the naphthalene-containing compound **54n** was more active against MCF-7, HCT116, and A549 cell lines than those having a carbazole or an adamantyl group.

Compound **45d** was screened for anticancer activity *in vitro* against four human cancer cell lines, HeLa, HePG2, MCF7, and HCT116, using Doxorubicin as a reference drug, and also tested against a normal Caucasian fibroblast-like fetal lung cell line





Scheme 14 Synthetic route of compounds 64a-d.

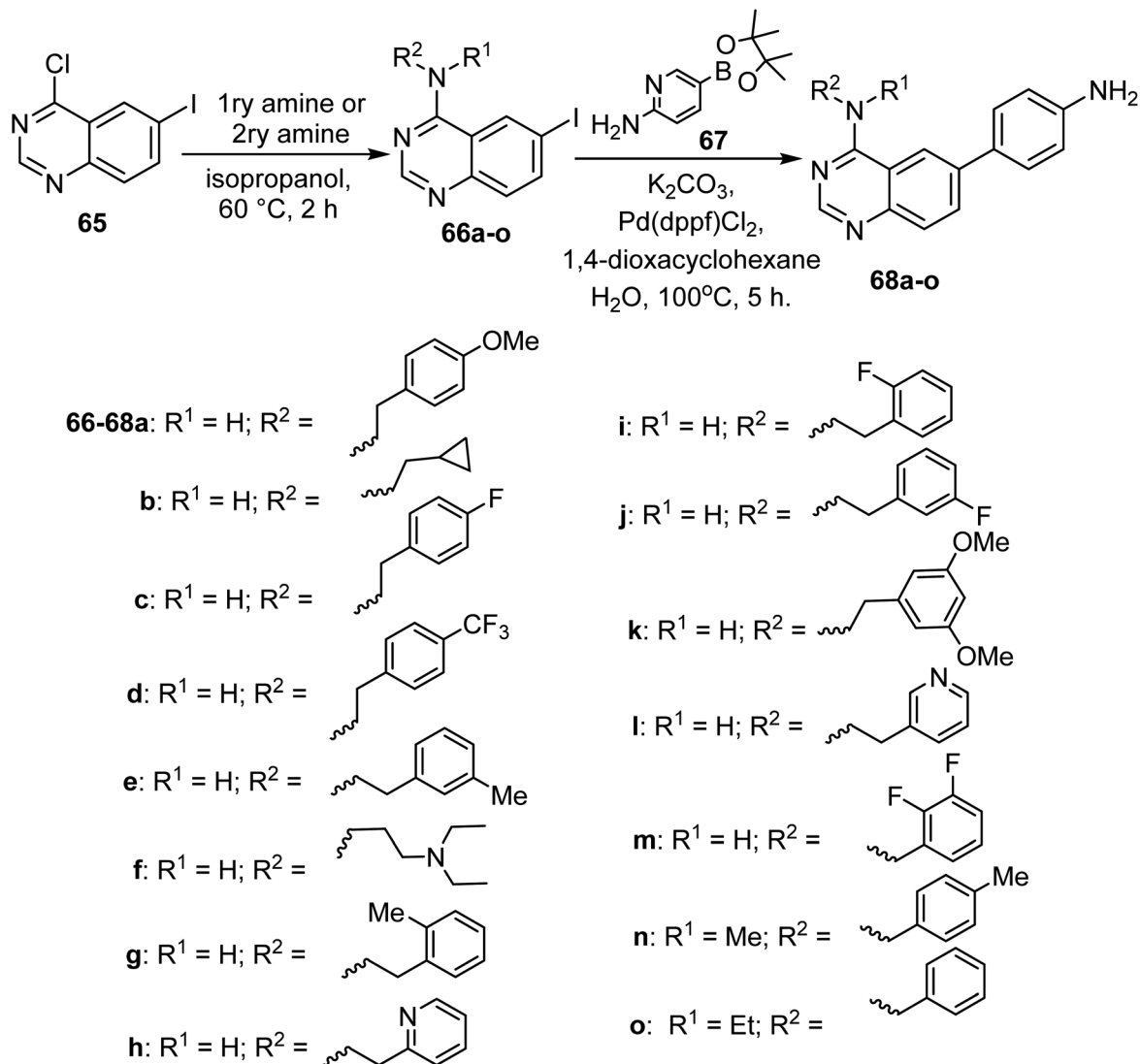


Scheme 15 Synthesis of the target quinazolines 64e-h.

(WI-38) to determine their specificity. Compound **45d** showed significant cytotoxic activity against the cell lines HeLa, HePG2, MCF7, and HCT116 with IC_{50} values of 2.57 μM , 5.96 μM , 6.41 μM , and 10.63 μM , respectively, compared to Doxorubicin with IC_{50} 5.57 μM , 4.50 μM , 4.17 μM , and 5.23 μM , respectively. In addition, the IC_{50} value of **45d** against WI-38 was 40.53 μM . The inhibition activity of this **45d** against EGFR and VEGFR-2 was evaluated, with IC_{50} values 0.103 μM and 0.069 μM , respectively, with almost similar potency as the reference drugs Sorafenib (IC_{50} = 0.031 μM against VEGFR) and Erlotinib (IC_{50} = 0.049 μM

against EGFR). The ability of these novel derivatives to interact with EGFR and VEGFR-2 active sites and to inhibit their activities was also confirmed by docking studies.⁶¹ The structure-activity correlation of the synthesized derivatives **45a-r** (Scheme 10) against HeLa, HePG-2, MCF-7, and HCT-116 cell lines showed that quinazolinone derivative **45d** having 4-methylphenyl moiety as an electron-donating group demonstrated the best inhibitory activity against the four cell lines. As shown in Scheme 10, for compounds **45** (R=H), replacing X=Me with bulky groups (X = MeO, CF₃, Br, or Cl) resulted in a decrease in





Scheme 16 Preparation of 4-amino-quinazoline derivatives 68a–o.

the inhibitory activity against all cell lines. However, for compounds **45** ($R=Cl$), the data exhibited that the best activity was obtained for $X=Br$ against all cell lines; however, replacing $X=Br$ with ($X = MeO, CF_3, NO_2, \text{ or } Cl$) resulted in moderate to weak activity against all cell lines.

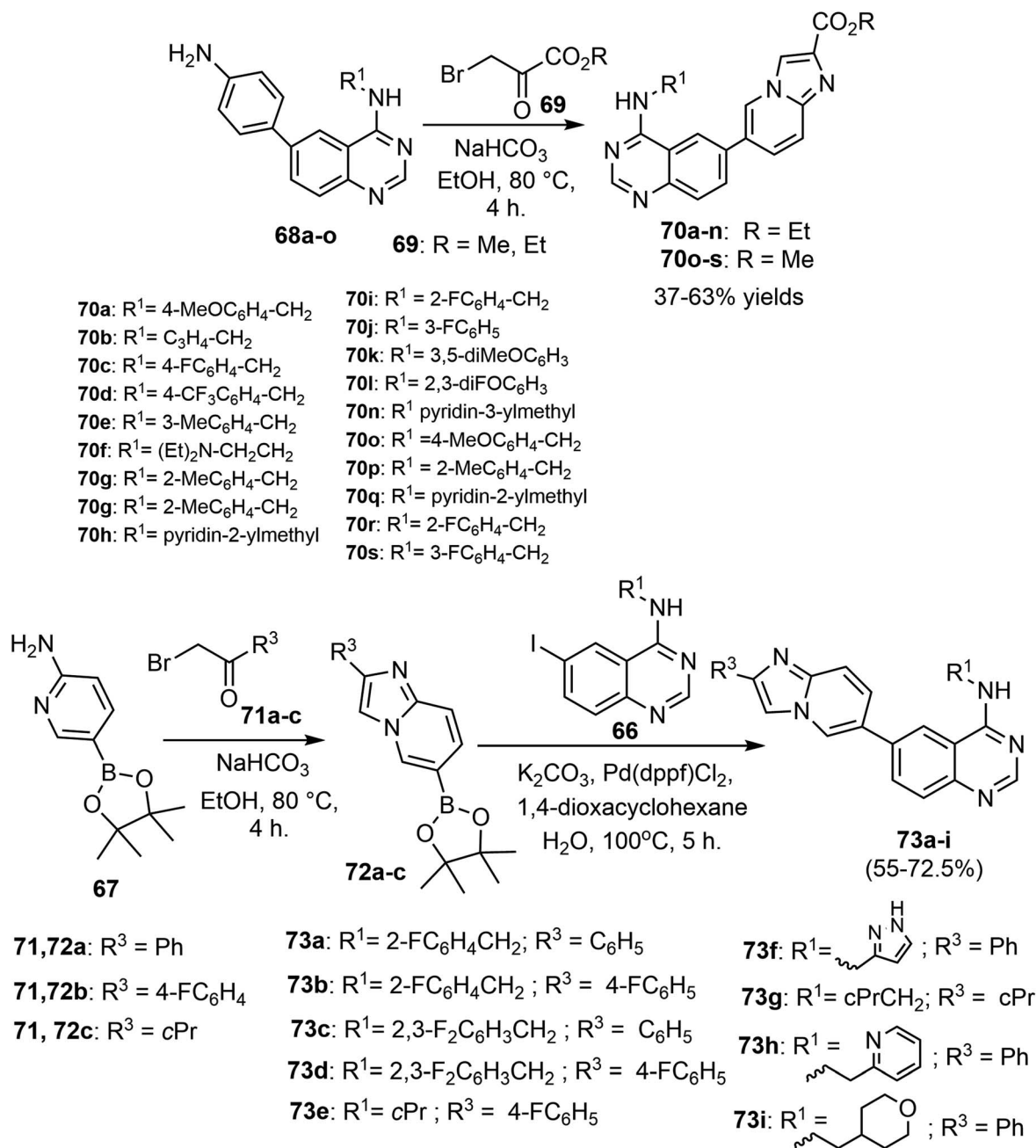
A novel series of quinazoline derivatives with 2,5-diamine moiety was synthesized. The inhibition activity of these compounds against HPK1 was tested. Compound **60h** showed good inhibition potency of HPK1 with IC_{50} value 2.7 nM.⁶³

The antiproliferative activity of **64b** was evaluated *in vitro* against two human cancer cell lines MCF-7 and HCT116, and Doxorubicin was used as a reference drug. Compound **64b** displayed significant cytotoxicity against the two cell lines, MCF-7 and HCT116, with IC_{50} values of 4.43 μM and 8.23 μM , respectively. Compound **64b** also showed good *in vitro* inhibition potency of VEGFR-2, and the percentage of inhibition of VEGFR-2 was 71.28%; Sorafenib was utilized as a positive control.⁶⁴

The antiproliferative activity of **64f** was evaluated *in vitro* against two human cancer cell lines MCF-7 and HCT116, and Doxorubicin was used as a reference drug. Compound **64f** displayed significant cytotoxicity against the two cell lines, MCF-7 and HCT116, with IC_{50} values of 9.63 μM and 1.58 μM , respectively, compared to Doxorubicin with IC_{50} 8.09 μM and 11.26 μM , respectively. Compound **64f** also showed good *in vitro* inhibition potency of VEGFR-2 with IC_{50} value 3.19 μM , with almost similar potency as the reference drug Sorafenib ($IC_{50} = 3.24 \mu M$).⁶⁵

Compound **73i** was screened for anticancer activity *in vitro* against five human cancer cell lines HCC827, A549, SH-SY5Y, HEL, and MCF-7, using HS-173 as a reference drug, and also tested against normal cell line (MRC-5) to determine their specificity. Compound **73i** showed significant cytotoxic activity against the cell lines HCC827, A549, SH-SY5Y, HEL and MCF-7 with IC_{50} values of 0.09 μM , 0.18 μM , 0.37 μM , 0.19 μM , and 0.43 μM , respectively, compared to HS-173 with IC_{50} 3.90 μM ,





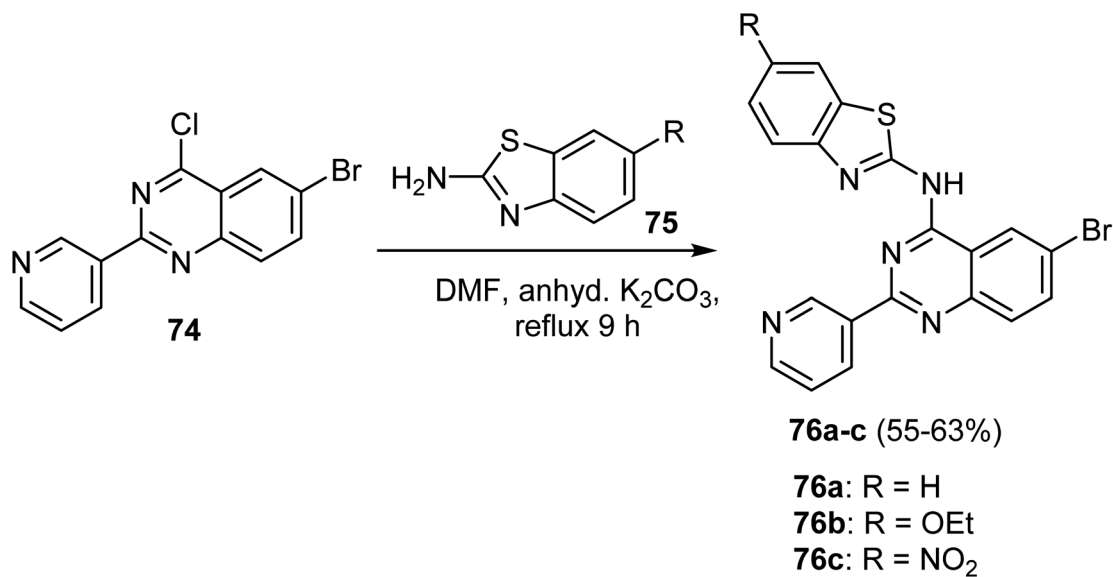
Scheme 17 Preparation of quinazoline derivatives 70a–s and 73a–i.

5.91 μM , 10.71 μM , 5.24 μM , and 4.36 μM , respectively. In addition, the IC_{50} value of 73i against MRC-5 was 1.98 μM . The inhibition activity of this derivative 73i against PI3K α was evaluated, with IC_{50} value 1.94 nM with higher potency than the reference drug HS-173 (IC_{50} = 3.72 nM). The ability of 73i to interact with PI3K α active sites and to inhibit their activity was also confirmed by docking studies.⁶⁶

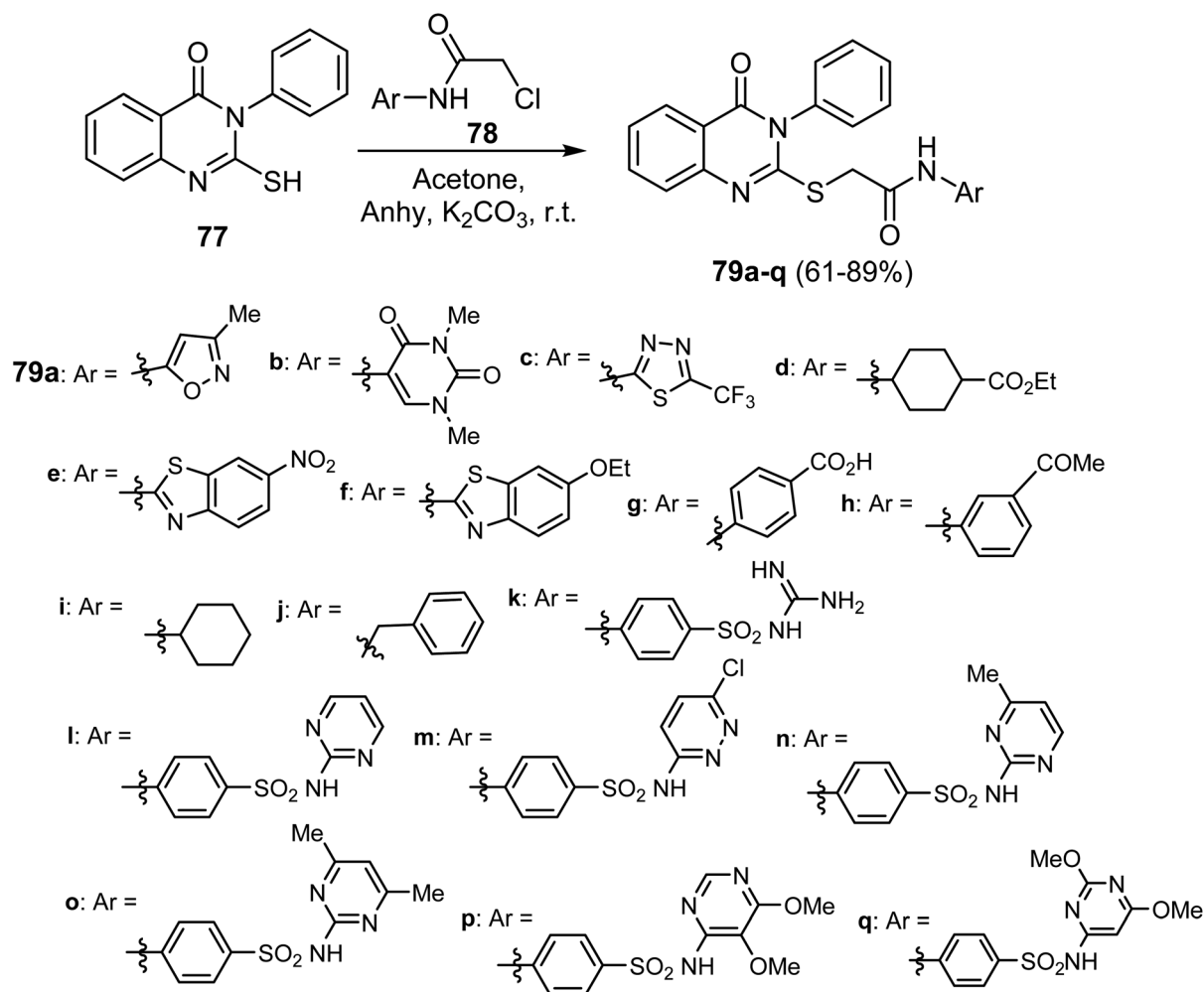
Compound 76a was screened for its antiproliferative activity *in vitro* against four human cancer cell lines A549, MCF-7, PC9, and HCC827, using Gefitinib as a reference drug, and also tested against normal cell line (WI38) to determine their specificity. The bioassay results disclosed that 76a had a promising cytotoxic activity with IC_{50} values of 178.34 μM , 2.49 μM , 1.05

μM , and 3.43 μM against A549, MCF-7, PC9 and HCC827, respectively, compared to Gefitinib with IC_{50} values of 34.389 μM , 4.972 μM , 1.36 μM , and 3.99 μM , respectively. In addition, the IC_{50} value of compound 76a against WI38 was 82.8 μM . The ability of 76a to inhibit EGFR was evaluated *in vitro* and showed a significant IC_{50} value of 0.096 μM , compared to Gefitinib (IC_{50} = 0.166 μM). Docking studies supported the obtained results and demonstrated the ability to interact with EGFR active sites.⁶⁷

Synthesis of compound 79g and evaluation of its cytotoxic activity against MCF-7 was reported, using Doxorubicin as a reference drug. 79g exhibited notable cytotoxicity against tested cell line “MCF-7” with IC_{50} value of 38.42 μM , compared

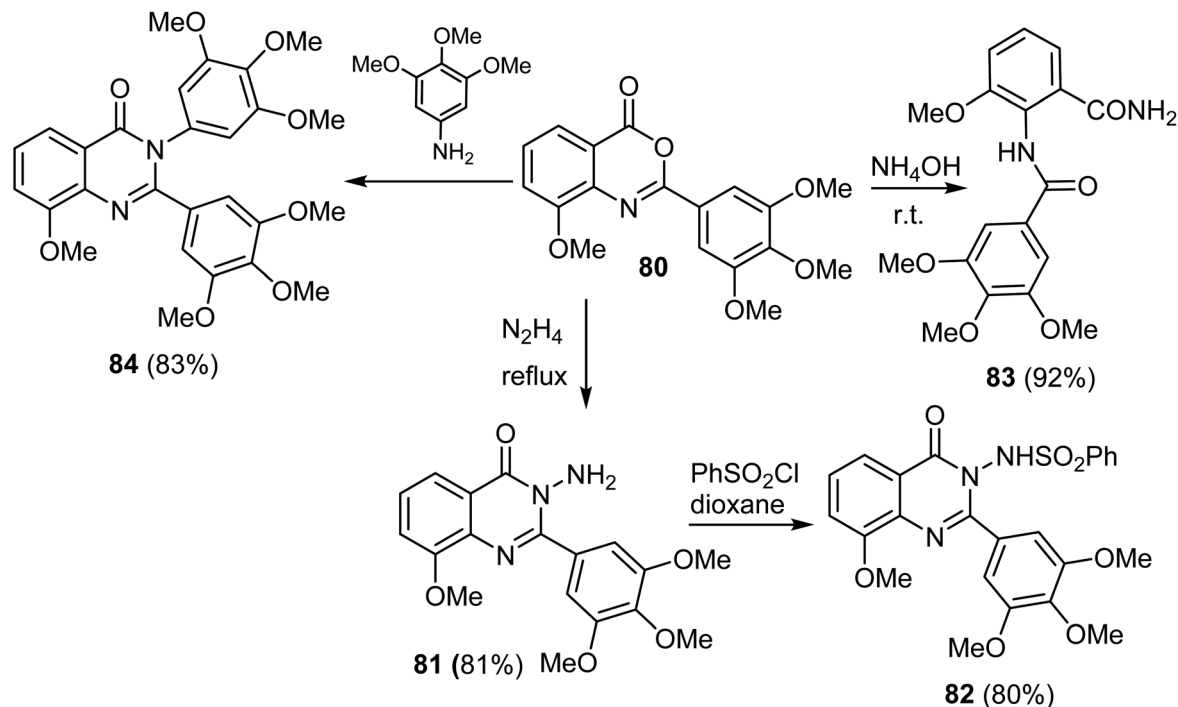
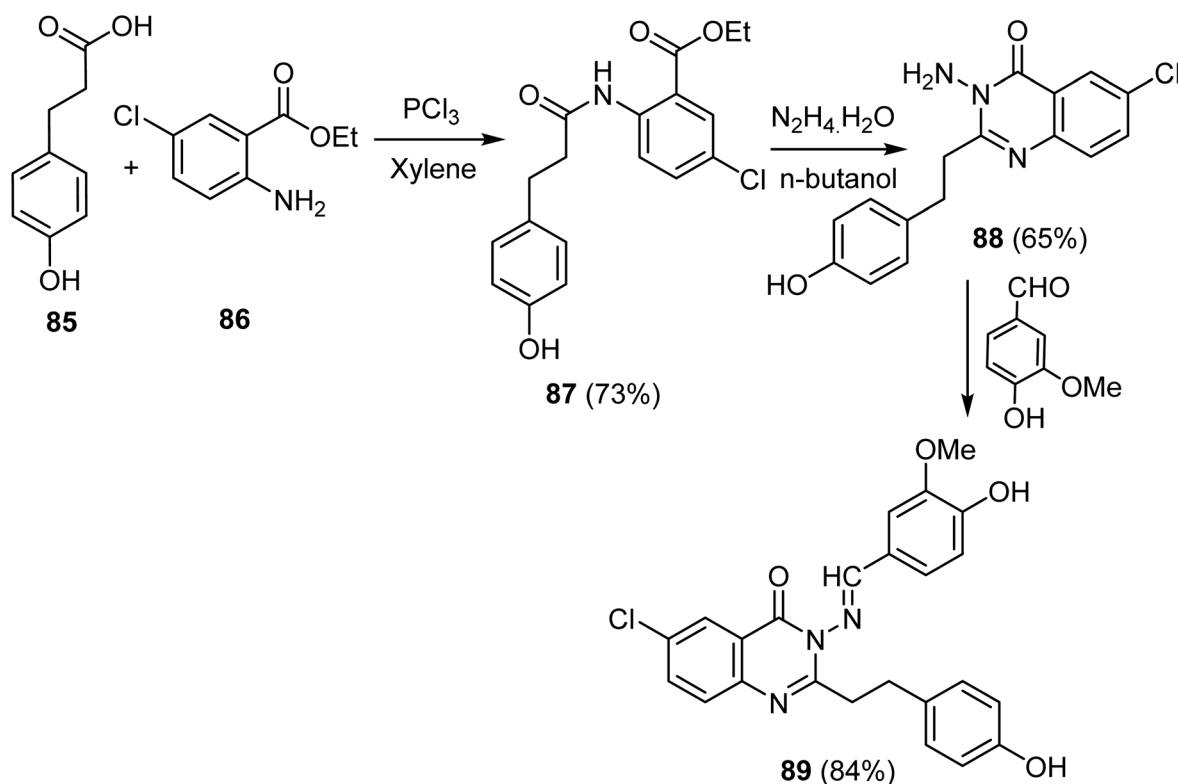


Scheme 18 Synthesis of quinazoline derivatives 76a–c.



Scheme 19 Synthesis of quinazoline-thioacetamide derivatives 79a–q.



Scheme 20 Synthesis of 8-methoxy-2-trimethoxyphenyl-3-substituted quinazoline-4(3)-one **81**–**84**.Scheme 21 Synthesis of quinazolin-4-one scaffold **89**.

to Doxorubicin with IC_{50} value of 32.02 μM . The inhibitory effects of **79g** against VEGFR were also significant with IC_{50} 0.176 μM , compared to reference drug Sorafenib (IC_{50} 0.042

μM). The ability of **79g** to interact with VEGFR was also confirmed by docking studies.¹⁹

A series of trimethoxy quinazolines derivatives were designed, synthesized, and evaluated for antiproliferative





Table 2 Cytotoxicity of quinazoline-based derivatives with kinase inhibition

Entry	Structure	Kinase inhibition activity	Anticancer activity	Ref.
7		Enzymes TRKA ^{WT} 0.55 TRK ^{G595R} 25.1 TRK ^{G667C} 5.4 IC ₅₀ [nM] (24f) Larotrectinib 1.1 81.7 51.1	Cell lines Ba/F3-ETV6-TRKAWT 14.6 Ba/F3-ETV6-TRKBWT 4.9 Ba/F3-LMNA-TRKAG595R 2886.4 Ba/F3-LMNA-TRKAG667C 755.0 IC ₅₀ [nM] (24f) Larotrectinib 9.5 3.7 205.0 48.3	57
8		Enzymes EGFR 10.66 IC ₅₀ [nM] (31c) Gefitinib 25.42	Cell lines A375 3.36 ± 0.24 HeLa 2.48 ± 0.22 Eca-109 6.27 ± 0.81 H1975 7.66 ± 0.87 MDA-MB-453 2.77 ± 0.16 SW1353 2.01 ± 0.34 Sgc7901 3.78 ± 0.92 L02 21.03 ± 1.16 A549 1.04 ± 0.32 HT-29 2.57 ± 0.18 MCF-7 2.26 ± 0.46 IC ₅₀ [μM] (31c) Gefitinib 8.46 ± 0.65 20.82 ± 1.43 43.82 ± 5.66 27.80 ± 2.09 21.55 ± 2.36 37.02 ± 4.21 22.30 ± 5.55 25.42 ± 1.65 12.08 ± 0.88 8.06 ± 0.53 13.87 ± 0.68	58
9		Enzymes VEGFR-2 83 ± 5 c-Met 48 ± 3 IC ₅₀ [nM] (33e) Cabozantinib 59 ± 3 30 ± 2	Cell lines HCT116 3.403 ± 0.18 W138 11.61 ± 0.69 IC ₅₀ [μM] (33e) Cabozantinib 16.350 ± 0.86 44.71 ± 2.65	59
10		Enzyme PDGFRA 58 Kinase inhib. (%) at 10 μM (38c)	Cell lines AsPc-1 15.3 ± 2.3 EBC-1 19.0 ± 0.7 MKN-45 22.0 ± 4.8 Mia-Paca-2 25.6 ± 2.4 HT-29 21.0 ± 4.7 K562 31.5 ± 6.4 IC ₅₀ [μM] (38c) Crizotinib 2.45 ± 1.3 Cabozantinib 1.4 ± 0.1 0.006 ± 0.001 0.05 ± 0.003 2.36 ± 1.2 ND ND 0.059 ± 0.014 1.04 ± 0.06 3.8 ± 0.6 3.7 ± 0.67 4.0 ± 1.0	60



Table 2 (Contd.)

Entry	Structure	Kinase inhibition activity	Anticancer activity	Ref.
11		Enzymes PAK4 Enzymes PAK4 IC ₅₀ [nM] (51e) 10 Kinase inhibition (%) at 100 nM (51e) 73	Cell lines A549 T293 IC ₅₀ [μM] (51e) 0.61 ± 0.03 >10	PF-3758309 0.67 ± 0.13 >10 70
12		Enzymes EGFR VEGFR IC ₅₀ [μM] (54n) 0.0728 ± 0.01 0.0523 ± 0.01	Cell lines HepG2 MCF-7 HCT-116 A549 IC ₅₀ [μM] (54n) 0.3425 ± 0.02 0.0977 ± 0.01 0.2000 ± 0.02 0.5134 ± 0.05	Sorafenib — 0.1400 ± 0.01 Erlotinib 0.2420 ± 0.02 — Sorafenib 0.400 ± 0.03 0.404 ± 0.03 0.558 ± 0.05 0.505 ± 0.05 Erlotinib 0.773 ± 0.07 0.549 ± 0.05 0.820 ± 0.06 0.1391 ± 0.01 20
13		Enzymes EGFR VEGFR IC ₅₀ [μM] (45d) 0.103 ± 0.005 0.069 ± 0.003	Cell lines Hela HepG2 MCF7 HCT116 WI38 IC ₅₀ [μM] (45d) 2.57 ± 0.1 5.96 ± 0.3 6.41 ± 0.4 10.63 ± 0.8 40.53 ± 2.2	DOX 5.57 ± 0.4 4.50 ± 0.2 4.17 ± 0.2 5.23 ± 0.3 6.72 ± 0.65 61
14		Enzymes HPK1 IC ₅₀ [nM] (60h) 2.7 ± 2.2	Cell lines — IC ₅₀ [μM] — —	— — 63
15		Enzymes VEGFR Kinase inhibition (%) (64b) 71.28	Cell lines MCF-7 HCT116 IC ₅₀ [μM] (64b) 4.43 ± 0.006 8.23 ± 0.009	DOX 8.09 ± 0.006 11.26 ± 0.007 64

Table 2 (Contd.)

Entry	Structure	Kinase inhibition activity	Anticancer activity	Ref.	
16		Enzymes VEGFR IC ₅₀ [μM] (64f) 3.19	Cell lines MCF-7 HCT116 IC ₅₀ [μM] (64f) 9.63 ± 0.016 11.26 ± 0.009	DOX 8.09 ± 0.007 11.26 ± 0.009	65
17		Enzymes PI3Kα IC ₅₀ [nM] (73f) 1.94 ± 0.66	Cell lines HCC827 A549 SH-SY5Y HEL MCF-7 MRC-5 IC ₅₀ [μM] (73f) 0.09 ± 0.01 0.18 ± 0.01 0.37 ± 0.08 0.19 ± 0.01 0.43 ± 0.04 1.98 ± 0.89	HS-173 3.90 ± 0.34 5.91 ± 0.19 10.71 ± 1.92 5.24 ± 1.28 4.36 ± 0.90 —	66
18		Enzymes EGFR IC ₅₀ [μM] (76a) 0.09 ± 0.00278	Cell lines A549 MCF-7 W138 PC9 HCC827 IC ₅₀ [μM] (76a) 178.34 ± 8.9 2.49 ± 0.12 82.8 ± 4.14 1.05 ± 0.02 3.43 ± 0.066	Gefitinib 4.389 ± 0.21 4.972 ± 0.24 34.95 ± 1.72 1.36 ± 0.02 3.99 ± 0.07	67
19		Enzymes VEGFR IC ₅₀ [μM] (79g) 0.176 ± 0.007	Cell lines MCF-7 IC ₅₀ [μM] (79g) 38.42 ± 1.45	Doxorubicin 32.02 ± 0.06	19
20		Enzymes VEGFR2 EGFR IC ₅₀ [nM] (83) 98.1 ± 2.93 106 ± 2.22	Cell lines Hela A549 MDA IC ₅₀ [μM] (83) 2.8 ± 0.07 81 ± 2.1 0.79 ± 0.04	Docetaxel 9.65 ± 0.2 10.8 ± 0.23 3.98 ± 0.08	68

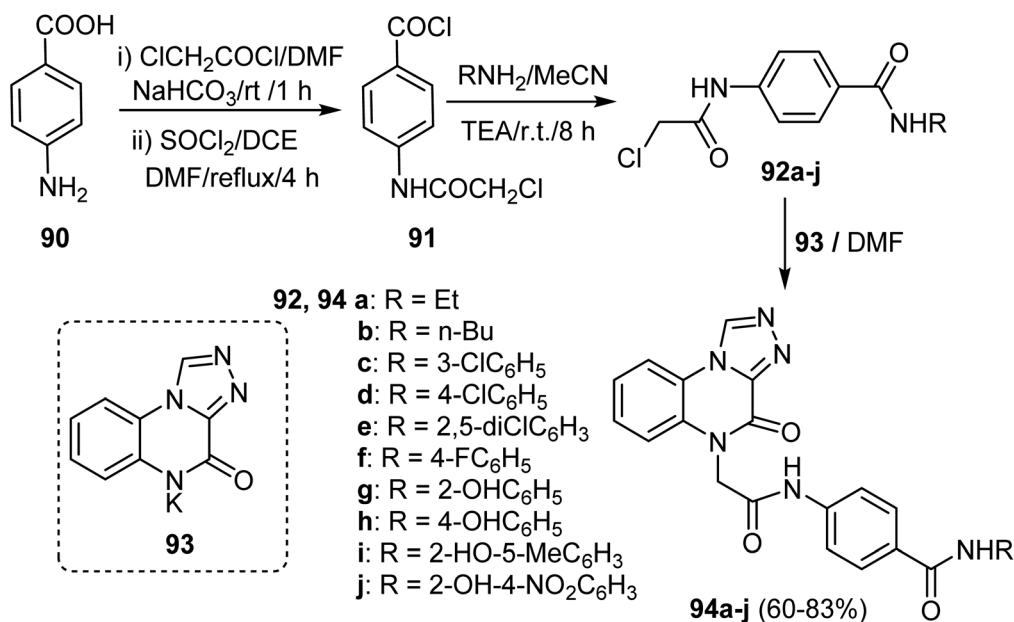


activity using MTT assay against three cancer cell lines: HeLa, A549 and MDA, and Docetaxel was employed as a reference drug. Particularly, compound **83** exhibited potent cytotoxicity with IC_{50} values of 2.8 μ M, 81 μ M, and 0.79 μ M against the tested cell lines HeLa, A549, and MDA, respectively, compared to the reference drugs Docetaxel with IC_{50} values of 9.65 μ M, 10.8 μ M, and 3.98 μ M, respectively. The inhibitory activity of **83** against VEGFR and EGFR was evaluated, and Docetaxel was used as a reference drug. Compound **83** showed the most potent VEGFR and EGFR inhibitory activity, with IC_{50} values 98.1 nM and 106 nM, respectively, compared to the reference drugs Docetaxel (IC_{50} = 89.3 nM and 56.1 nM against VEGFR and EGFR, respectively). The ability of these novel derivatives to interact with EGFR and VEGFR-2 active sites and to inhibit their activities was also confirmed by docking studies (Table 2).⁶⁸

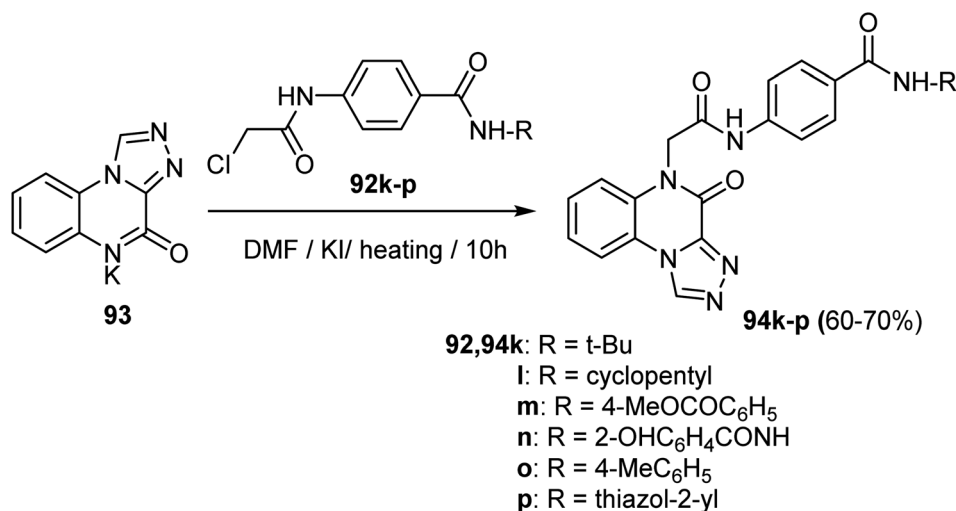
4. Quinoxaline derivatives

A series of [1,2,4]triazolo[4,3-*a*]quinoxaline derivatives **94a-j** were designed, synthesized, and biologically tested for their anti-proliferative activities against two selected tumor cell lines, MCF-7 and HepG2. Thus, acetylation of *p*-aminobenzoic acid **90** using chloroacetyl chloride in DMF followed by thionyl chloride provided 4-(2-chloroacetamido)benzoyl chloride **91**. Stirring of **91** with different amines in acetonitrile in the presence of TEA afforded the target intermediate **92a-j**. Finally, reaction of potassium salts **93** with the intermediates **92a-j** in dry DMF afforded the anticipated triazolo-quinoxalines **94a-j** in 60–83% yields (Scheme 22).⁷⁰

Similarly, Alsaif *et al.* reported the synthesis of a new series of triazolo-quinoxaline hybrids derivatives, **94k-p**, as VEGFR-2



Scheme 22 Preparation of triazolo quinoxalines **94a-j**.



Scheme 23 Synthesis of triazoloquinoxaline-based derivatives, **94k-p**.



inhibitors, as depicted in Scheme 23. Thus, heating the potassium salt **93** with the intermediates **92k-p** in dry DMF in the presence of KI as a catalyst afforded the triazolo-quinoxaline derivatives **94k-p** in 60–70% (Scheme 23).⁷¹

A series of quinoxaline-2(1*H*)-one derivatives were synthesized from the reaction of the potassium salt **96** with the appropriate 4-(2-chloroacetamido)-*N*-(substituted)benzamides **97** and **99a-c**. The reaction occurred in dry DMF at reflux, in the presence of a catalytic amount of KI to yield the target quinoxaline derivatives **98** in 70% yield and **100a, b** in 73–93% yield, respectively (Scheme 24).⁷²

Synthesis of a series of condensed bis([1,2,4]triazolo)[4,3-*a*:3',4'-*c*]quinoxaline derivatives **102a-n** were reported and investigated for their cytotoxic activities against HepG2 and MCF-7 and examined *in vitro* for their VEGFR-2 inhibitory activity. Thus, the synthetic pathway of the target structures **102a-n** started with heating the potassium salt **101** with the intermediates **92**. The was carried out in dry DMF using KI as a catalyst to furnish the triazolo-quinoxaline scaffolds **102a-n** in 63–80% yields (Scheme 25).⁷³

Alanazi *et al.* described a synthetic route to the bis([1,2,4]triazolo)[4,3-*a*:3',4'-*c*]quinoxaline derivatives and examined them as VEGFR-2 inhibitors. Therefore, the bis([1,2,4]triazolo)[4,3-*a*:3',4'-*c*]quinoxalin-3-ylthio)acetamido)-*N*-phenylbenzamide derivatives **102o-aa** were obtained in 68–80% yield by refluxing the potassium

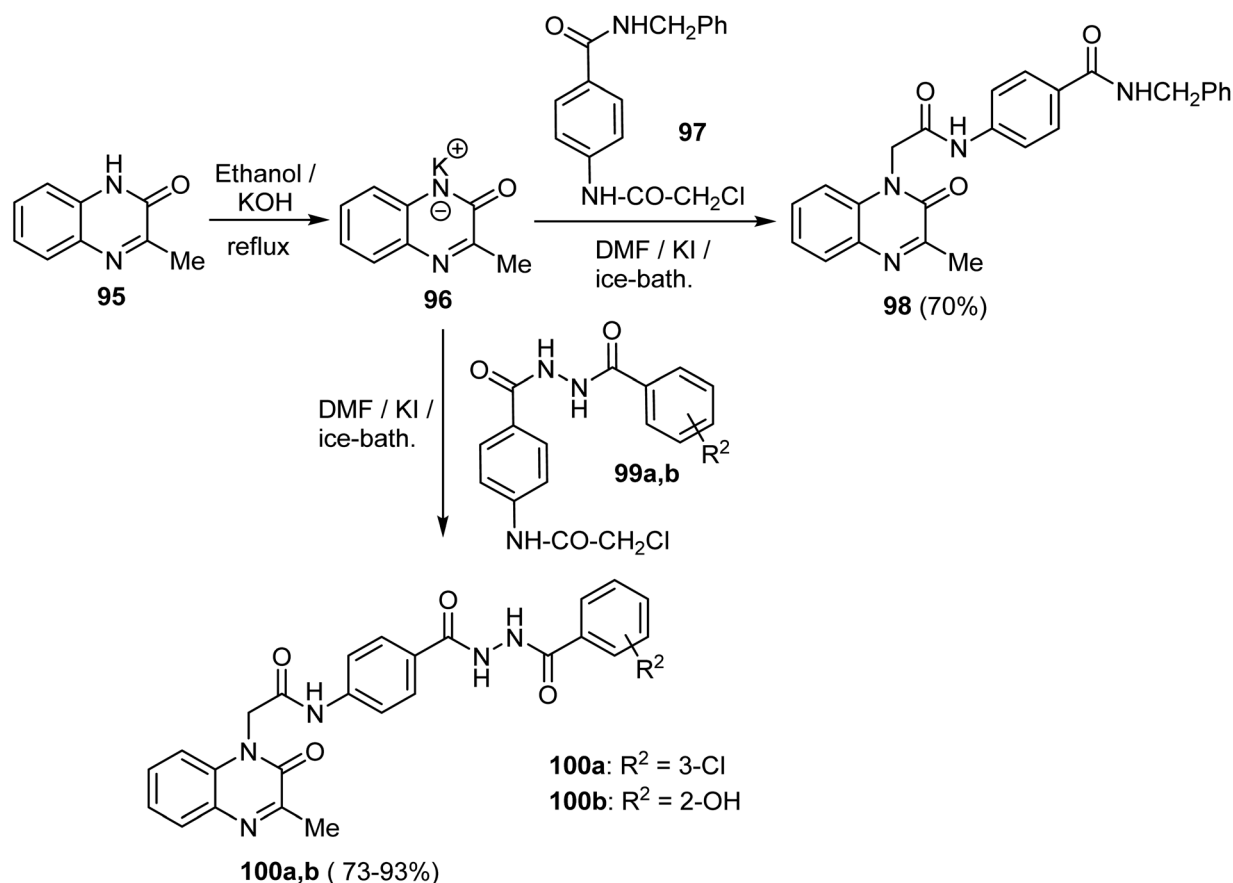
salt **101** with the intermediates **92** in dry DMF in the presence of KI catalyst (Scheme 26).⁷⁴

Synthesis of a series of [1,2,4]triazolo[4,3-*a*]quinoxaline derivatives **104a-i** was achieved by treatment of the potassium salt **103** with the intermediates **92** under typical reaction conditions as above to produce the derivatives **104a-i** in 75–85% yields (Scheme 27).⁷⁵

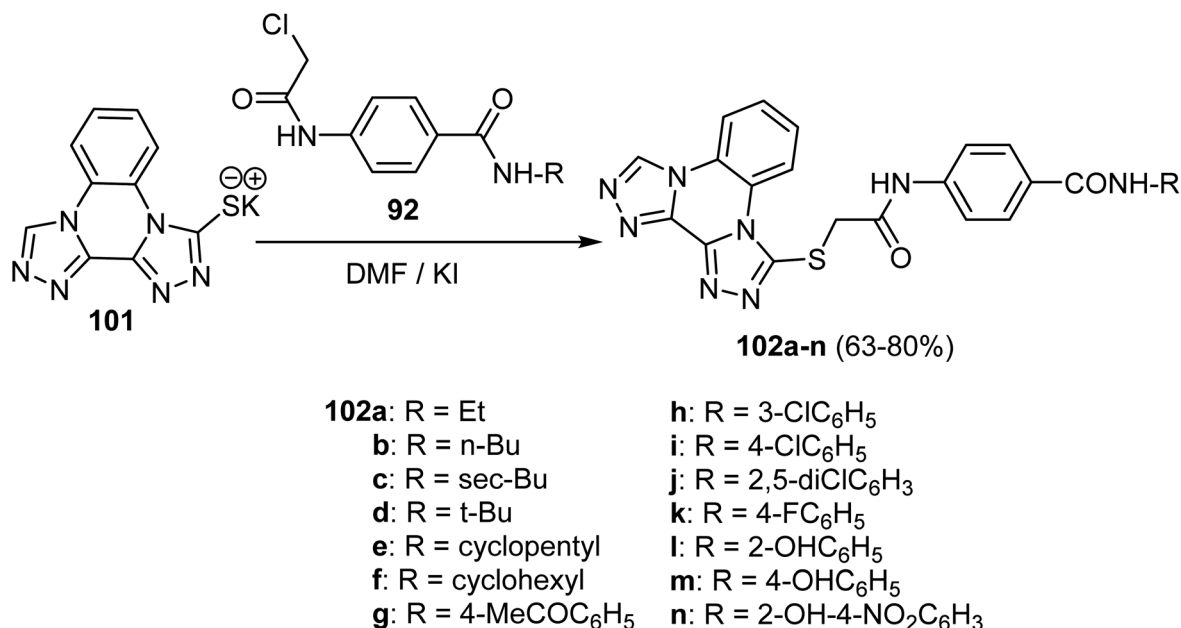
The [1,2,4]triazolo[4,3-*a*]quinoxaline molecular hybrids **94q-v** and **104k-p** were reported as anticancer agents with potential effects against VEGFR-2, the synthesis of compounds **94q-v** took place smoothly upon treatment of the potassium salt **93** with the chloroacetyl derivatives **92** under similar conditions as above to produce the products **94q-v** in 55–70% yields. Analogously, the target triazolo[4,3-*a*]quinoxalin compounds **104k-p** were produced in 55–70% yields by heating the potassium salt **103** with **92** in DMF in the presence of KI in a water-bath for 10 hours (Scheme 28).⁷⁶

As illustrated in Scheme 29 the quinoxaline products **106a-d** and **107a-c** were obtained in satisfactory yields 50–60% by reacting the starting compound quinoxalin-2(1*H*)-one (**105**) with 4,4-(2-chloroacetamido)-*N*-substituted arylamide derivatives **92** and **99** in the presence of K₂CO₃ and catalytic quantity of KI (Scheme 29).⁷⁷

In a similar protocol, a new series of 3-methylquinoxalin-2(1*H*)-one derivative **108a-j** was constructed employing 3-methylquinoxalin-2(1*H*)-one **95**. Thus, heating **95** with alcoholic



Scheme 24 Synthesis of quinoxaline-2(1*H*)-one derivatives, **98**, **100**.



Scheme 25 Synthesis of quinoxaline scaffolds 102a–n.

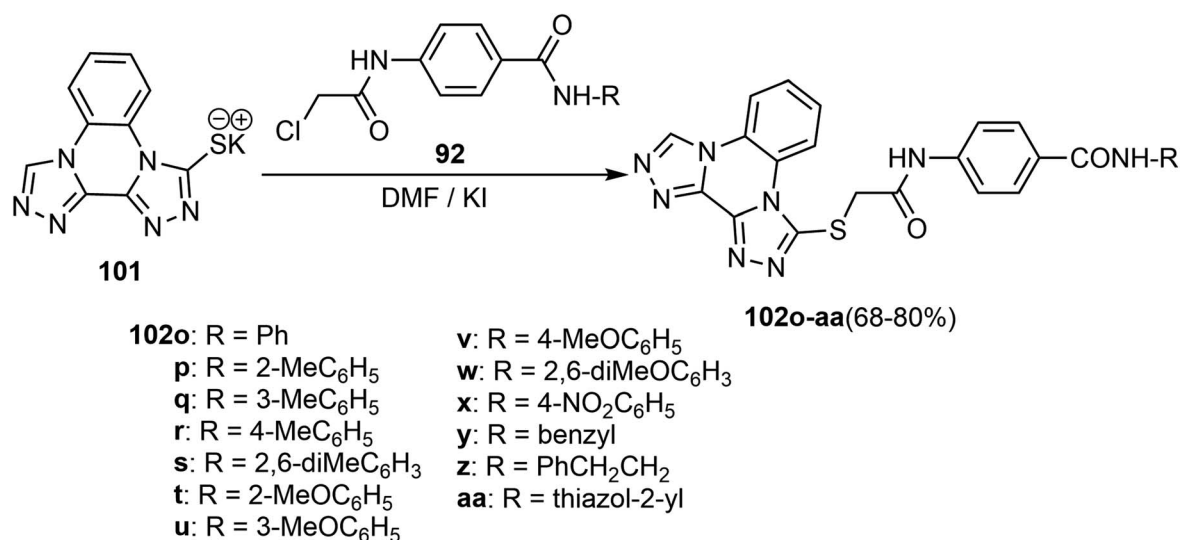
KOH gave the corresponding potassium salt **96**, which, upon treatment with the key intermediates **92** resulted in the production of the 2-oxoquinoxaline **108a–j** in 70–76% (Scheme 30).⁷⁸

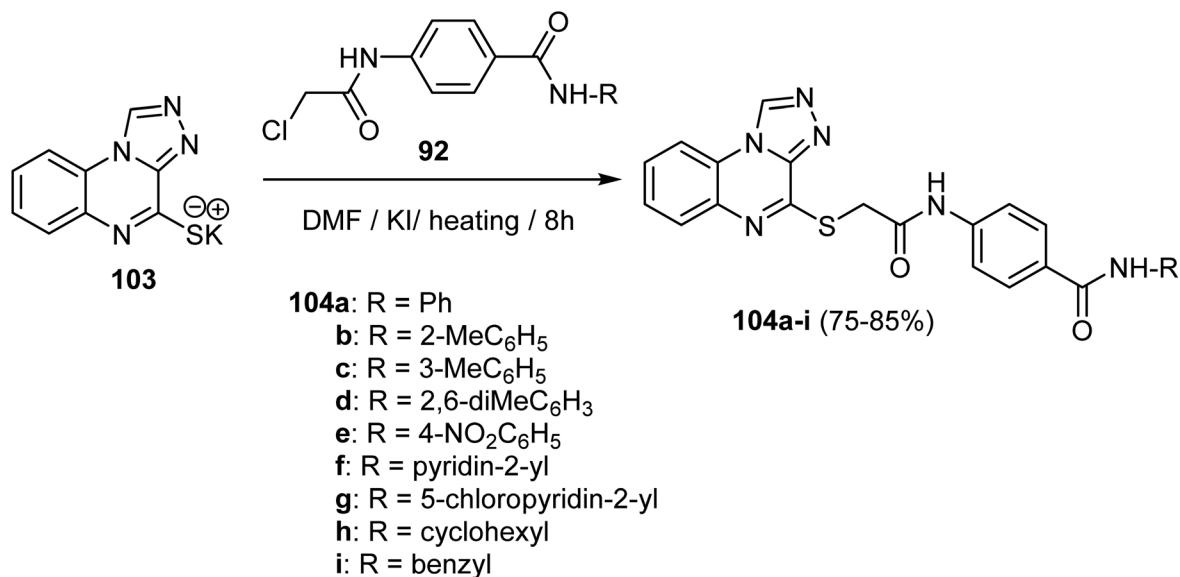
Under eco-friendly reaction conditions, synthesis of the benzoxazolyl quinoxalines **111a, b** was accomplished as shown in Scheme 31. Thus, a mixture of substituted 2-aminophenol **109a, b** and quinoxaline-2-carbaldehyde (**110**) was added to silica chloride (1 eq.), then the mixture was heated on a sand bath at 120 °C for 4 h to furnish the target (1,3-benzoxazol-2-yl) quinoxaline scaffolds **111a, b** in 74–80% yields (Scheme 31).⁷⁹

Kumar *et al.* reported the synthesis of a library of the imidazo[1,2-*a*]quinoxaline derivatives as inhibitors of epidermal growth factor receptor (EGFR).⁸⁰ As per Scheme 32, panel of imidazo

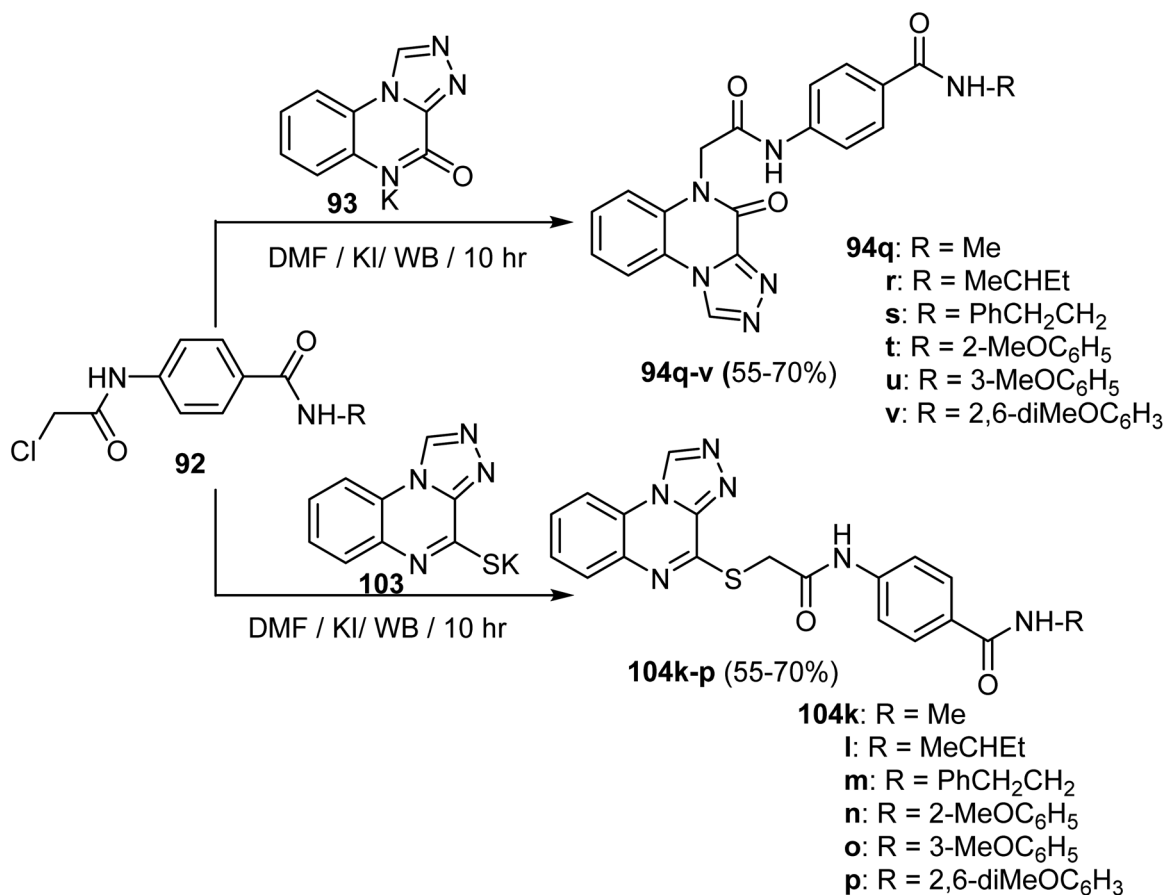
[1,2-*a*]quinoxalines **113–115** were prepared *via* microwave-assisted ring-cyclization of 5-amino-1-(2-amino-phenyl)-1*H*-imidazole-4-carbonitrile (**112**) with variety of aromatic aldehydes in methanolic solution containing *p*-TSA (*p*-toluene sulphonic acid). The reaction resulted in the formation of the imidazo[1,2-*a*]quinoxaline-2-carbonitriles **113a–d** in 70–93% yield and 4,5-dihydroimidazo[1,2-*a*]quinoxaline-2-carbonitriles **114a–k** in 70–92%, respectively. Analogously, the reaction of compound **112** with aryl ketones furnished the dihydroimidazo[1,2-*a*]quinoxaline scaffolds **115a, c** in 88–89% yields.⁸⁰

Alswah *et al.* reported the synthesis of a series of triazoloquinoxaline-chalcone hybrids **119a–k** as described in Scheme 33. Therefore, the fused chlorotriazoloquinoxaline **117** was produced in good yield by cyclizing hydrazinylquinoxaline **116**

Scheme 26 Synthesis of bis([1,2,4]triazolo)[4,3-*a*:3',4'-*c*]quinoxaline derivatives 102o–aa.



Scheme 27 Synthesis of [1,2,4]triazolo[4,3-a]quinoxalin-4-ylthioacetamides 104a–i.

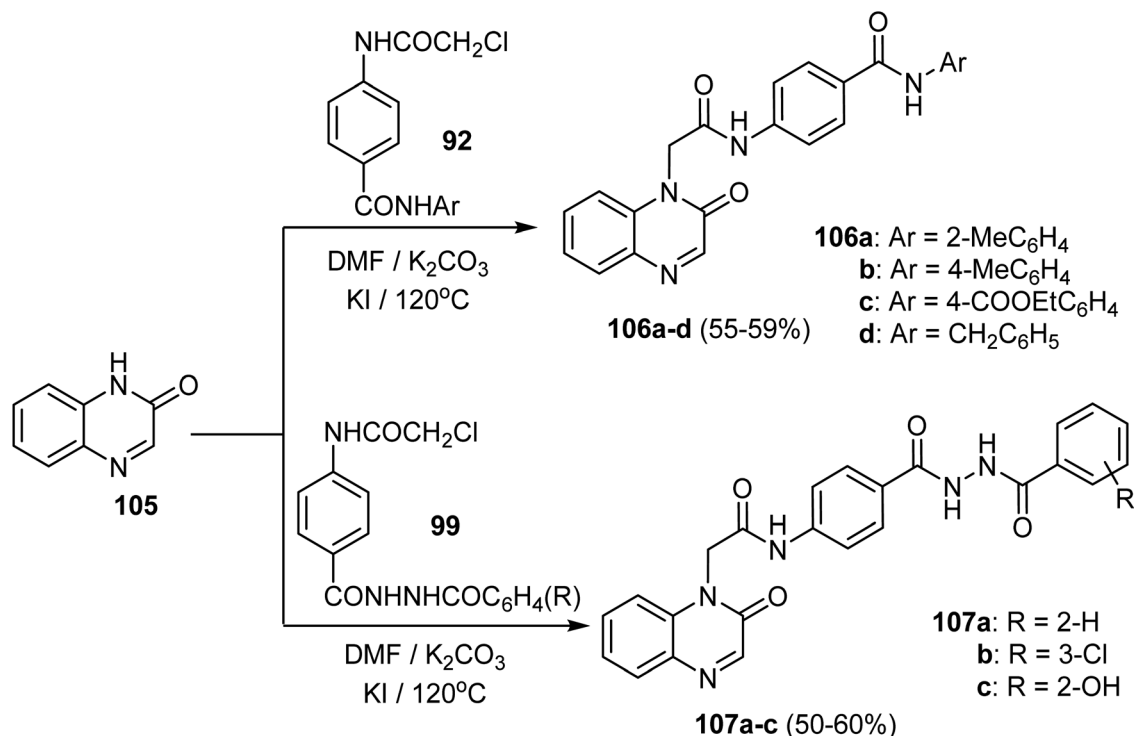


Scheme 28 Synthesis of triazolo[4,3-a]quinoxaline 94q–v and 104k–p.

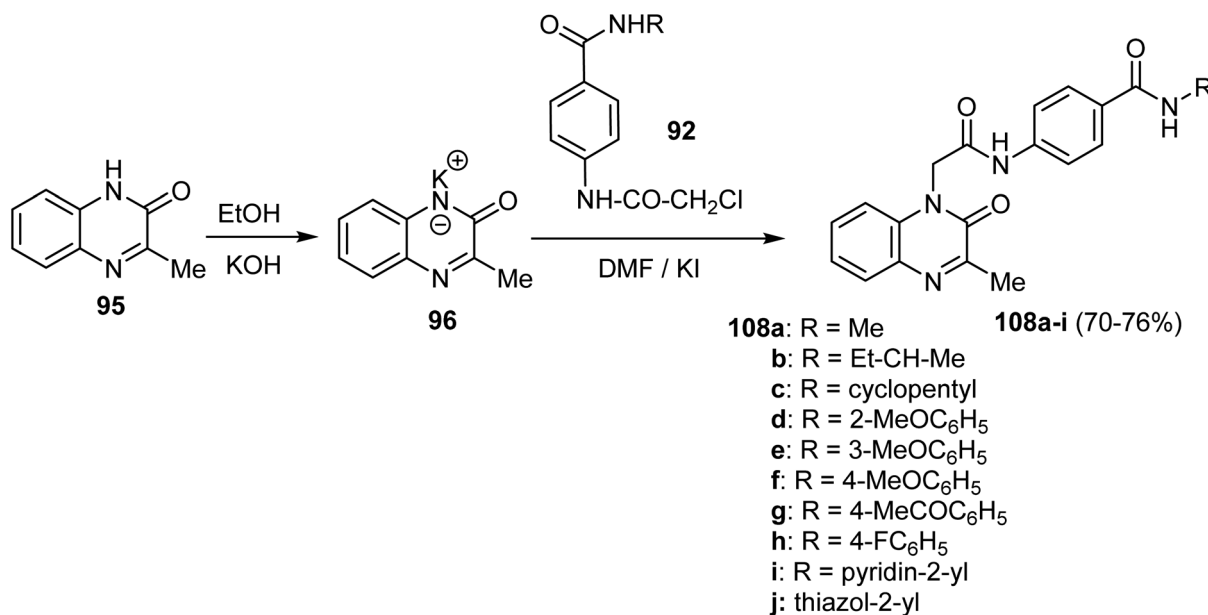
with excess triethylorthopropionate under heating. Next, the preparation of compound **118** involved dissolving **117** in acetonitrile, followed by heating with 4-aminoacetophenone under reflux using a catalytic quantity of TEA to produce the

triazoloquinoxaline **118**. Finally, condensation of compound **118** with aromatic aldehydes led to the construction of the substituted triazoloquinoxaline chalcone derivatives **119a–k** in 11–86% yields.⁸¹





Scheme 29 Synthesis of quinoxaline derivatives 106–107.

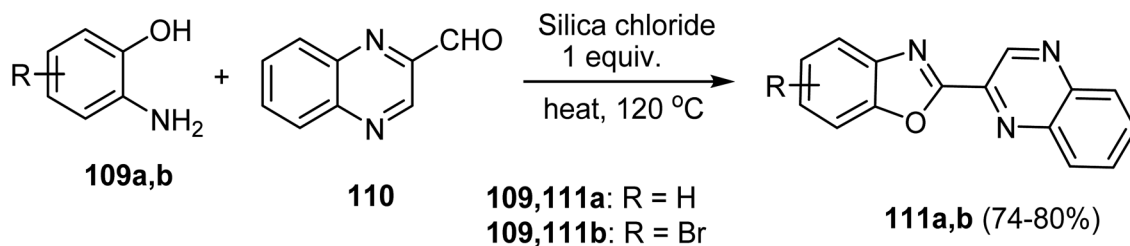


Scheme 30 Synthesis of the 3-methylquinoxaline derivatives 108a–j.

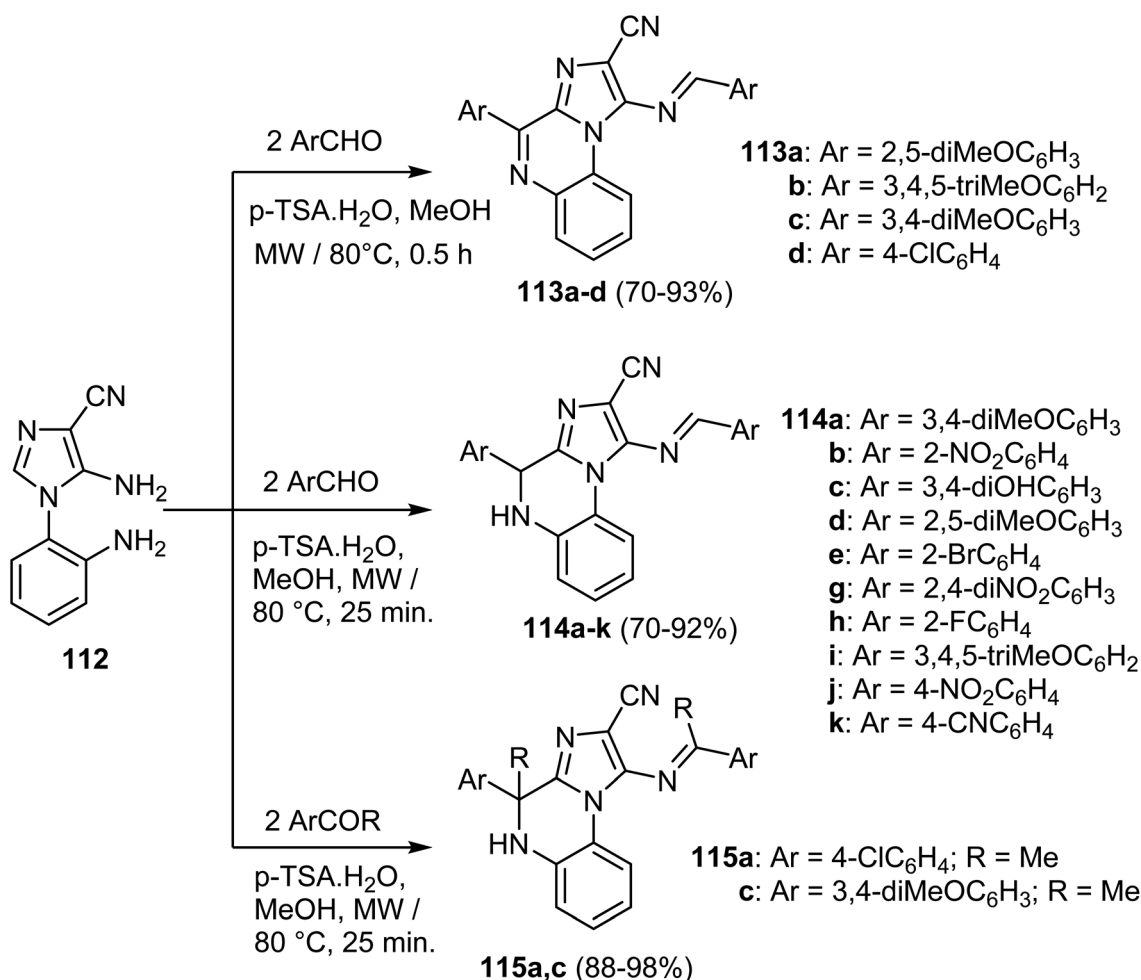
Conjugated polymer nanoparticles (CPNs) consisting of fluorinated thiophene-quinoxaline type conjugated polymers were reported by Koralli *et al.* The conjugated polymers were used to create nano-precipitated and encapsulated aqueous CPNs. As shown in Scheme 34, the thiophene-quinoxaline based polymers with fluorine atoms were constructed by reaction of one equiv. of 3,4-difluorothiophene-2,5-diyl)

bis(trimethylstannane) (**124**) with one equiv. of either 5,8-dibromo-6-fluoro-2,3-bis(3-(octyloxy)phenyl)quinoxaline (**125a**) or 5,8-dibromo-6,7-difluoro-2,3-bis(3-(octyloxy)phenyl)quinoxaline (**125b**) in dry toluene in the presence of tris(dibenzylideneacetone)dipalladium(0) [Pd₂(dba)₃] (0.02 equiv.) and tri(*o*-tolyl)phosphine [P(*o*-tol)₃] to produce the polymeric material **126a**, **b** (**T2fQf** and **T2fQ2f**).⁸²





Scheme 31 Synthesis of (1,3-benzoxazol-2-yl)quinoxalines scaffolds 111a, b.



Scheme 32 Synthesis of the imidazo[1,2-a]quinoxaline scaffolds 113–115.

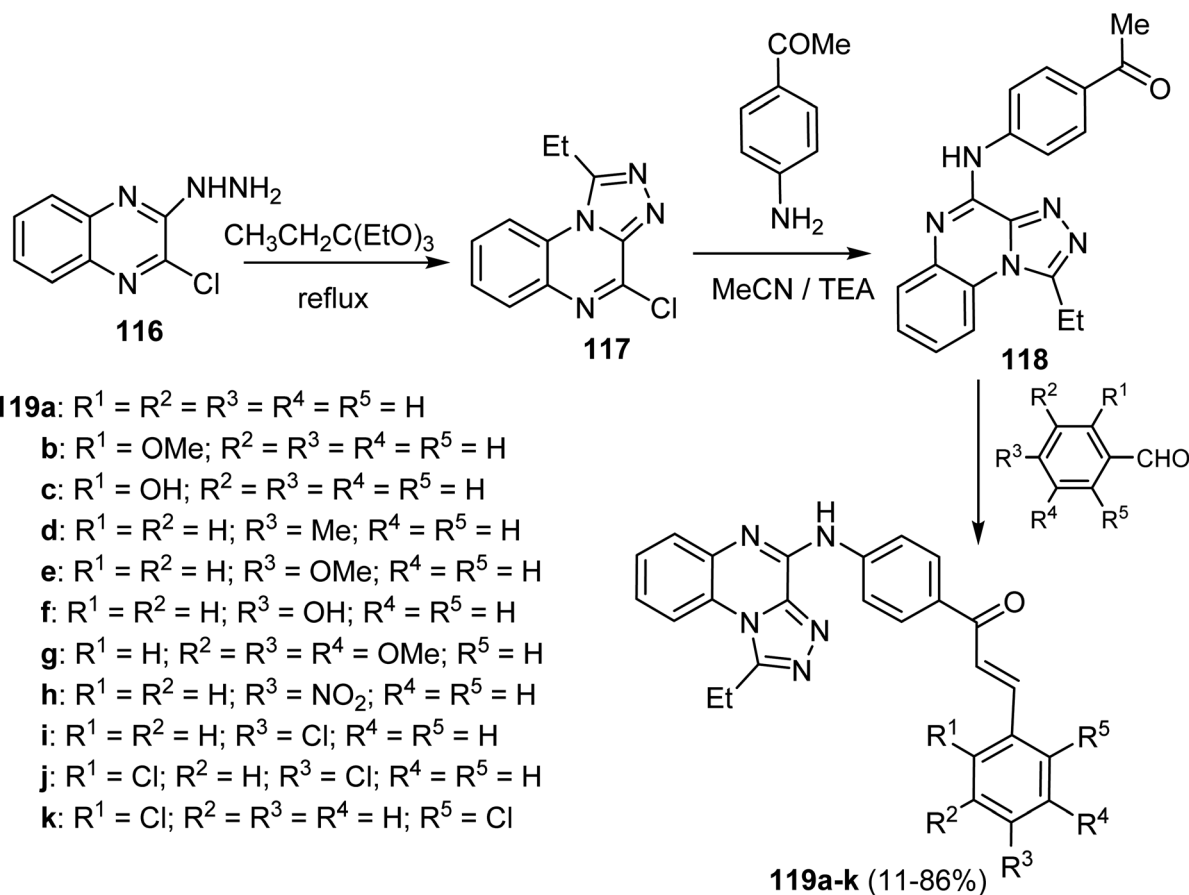
4.1 Anticancer activity of quinoxaline-based derivatives

The synthesized series of [1,2,4]triazolo[4,3-*a*]quinoxalin-4(5*H*)-one and [1,2,4]triazolo[4,3-*a*]quinoxaline derivatives were also examined for their anticancer activity against two cancer cell lines MCF-7 and HepG-2 using Sorafenib and MTT bioassay method was employed. Compound **94d** showed the most potent activity against tested cancer cell lines MCF-7 and HepG2 with IC₅₀ values of 7.2 and 4.1 μM, respectively. The ability of this derivative **94d** to inhibit VEGFR-2 was evaluated *in vitro* and showed a significant IC₅₀ value of 3.4 nM when compared to

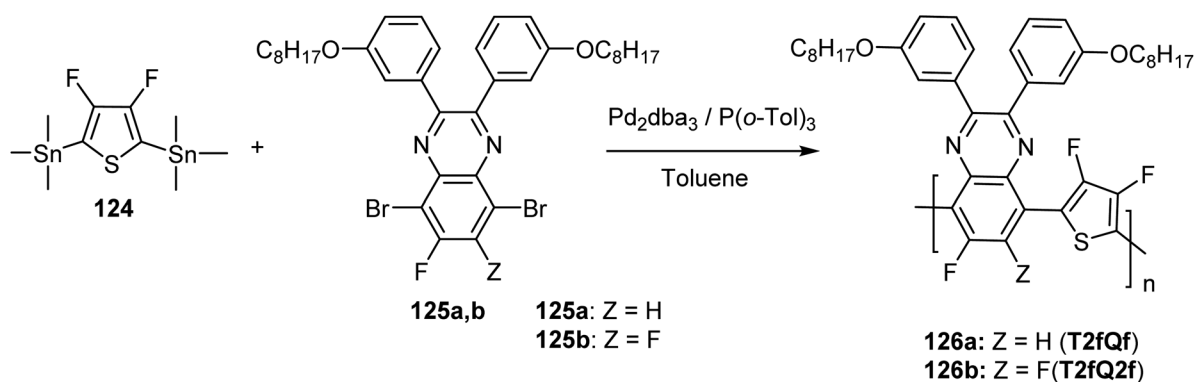
Sorafenib, with an IC₅₀ of 3.2 nM. Molecular docking studies showed that compound (**24**) had binding modes and interactions against VEGFR-2 like Sorafenib.⁷⁰

The antiproliferative activity of another series of quinoxaline-2(1*H*)-one derivatives **98** and **100b** was evaluated against three human cancer cell lines HepG-2 (hepatocellular carcinoma), MCF-7 (breast cancer) and HCT-116 (colorectal carcinoma) compared with Doxorubicin and Sorafenib as reference drugs. The two derivatives, **98** and **100b** demonstrated, exhibited notable activity against HepG-2, HCT-116, and MCF-7, with





Scheme 33 Synthesis of the triazoloquinoxaline-chalcone derivatives 119a–k.



Scheme 34 Synthesis of thiophene-quinoxaline type conjugated polymers T2fQf and T2fQ2f.

IC_{50} values (5.30 μM , 2.20 μM , and 5.50 μM for **98**) and IC_{50} values (6.60 μM , 4.70 μM , and 6.90 μM for **100b**) respectively. It showed significant anticancer activities against the tested cancer cell lines compared to reference drugs. The ability of **98** and **100b** to inhibit VEGFR-2 was evaluated *in vitro*, and these two compounds showed significant activity with IC_{50} values 1.09 and 1.19 μM , respectively, compared to Sorafenib ($IC_{50} = 1.27 \mu M$). Docking studies supported the obtained results and

demonstrated the ability of these derivatives to interact with VEGFR-2 active sites.⁷²

Next, a series of bis([1,2,4]triazolo[4,3-*a*:3',4'-*c*]quinoxaline) derivatives were evaluated for their cytotoxicity against MCF-7 and HepG2 cancer cell lines using MTT assay and Sorafenib as reference drug. Compound **102j** showed an interesting anticancer activity against the tested cancer cell lines MCF-7 and HepG2 with IC_{50} values of 10.3 μM and 6.4 μM ,





Table 3 Cytotoxicity of quinoxaline-based derivatives with kinase inhibition

Entry	Structure	Kinase inhibition activity	Anticancer activity	Ref.
21		Enzymes VEGFR-2 IC ₅₀ [nM] (94d) 3.4 ± 0.3	Sorafenib 3.2 ± 0.1 Cell lines MCF-7 HepG-2 IC ₅₀ [μM] (94d) 7.2 ± 0.6 4.1 ± 0.4	Sorafenib 3.51 ± 0.21 2.17 ± 0.13 70
22		Enzymes VEGFR-2 IC ₅₀ [μM] (98) 1.09	Sorafenib 1.27 Cell lines HepG-2 HCT-116 MCF-7 VERO IC ₅₀ [μM] (98) 5.30 ± 0.21 2.20 ± 0.08 5.50 ± 0.22 11.82 ± 0.14	Doxorubicin 8.28 ± 0.33 9.63 ± 0.39 7.67 ± 0.31 — 72
23		Enzymes VEGFR-2 IC ₅₀ [μM] (100b) 1.19	Sorafenib 1.27 Cell lines HepG-2 HCT-116 MCF-7 VERO IC ₅₀ [μM] (100b) 6.60 ± 0.26 4.70 ± 1.88 6.90 ± 0.28 22.12 ± 0.24	Doxorubicin 8.28 ± 0.33 9.63 ± 0.39 7.67 ± 0.31 — 72
24		Enzymes VEGFR-2 IC ₅₀ [μM] (102j) 3.7	Sorafenib 3.12 Cell lines MCF-7 HepG-2 IC ₅₀ [μM] (102j) 10.3 ± 0.8 6.4 ± 0.5	Sorafenib 3.51 ± 0.22 2.17 ± 0.14 73



Table 3 (Contd.)

Entry	Structure	Kinase inhibition activity	Anticancer activity	Ref.
25		Enzymes VEGFR-2 IC ₅₀ [nM] (94k) 3.9	Sorafenib 3.13 Cell lines MCF-7 HepG-2 IC ₅₀ [μM] (94k) 6.2 4.9	71
26		Enzymes VEGFR-2 IC ₅₀ [μM] (102v) 3.2	Sorafenib 3.1 Cell lines HepG-2 MCF-7 IC ₅₀ [μM] (102h) 3.3 4.4	74
27		Enzymes VEGFR-2 IC ₅₀ [nM] (104a) 3.4	Sorafenib 3.12 Cell lines MCF-7 HepG-2 Normal hepatocytes IC ₅₀ [μM] (104a) 8.2 5.4 31.34	75
28		Enzymes VEGFR-2 IC ₅₀ [nM] (94q) 3.2 ± 0.4	Sorafenib 3.12 ± 0.3 Cell lines MCF-7 HepG-2 IC ₅₀ [μM] (94q) 5.8 ± 0.7 4.3 ± 0.5	76

Table 3 (Contd.)

Entry	Structure	Kinase inhibition activity	Anticancer activity	Ref.
29		Enzymes VEGFR2 IC ₅₀ [μM] (107b) 0.493	Sorafenib 0.589 Cell lines HepG-2 HCT-116 MCF-7 IC ₅₀ [μM] (107b) 7.31 ± 0.29 7.45 ± 0.30 3.04 ± 0.12 7.85 ± 0.31	77
30		Enzymes VEGFR-2 IC ₅₀ [nM] (108e) 2.6	Sorafenib 3.1 Cell line MCF-7 HepG-2 IC ₅₀ [μM] (108e) 2.7 2.1	78
31		Enzymes Tyrosine kinase IC ₅₀ [μM] (111b) 0.10 ± 0.16 is it correct	Sorafenib Cell lines MDA-MB-231 MCF-7 A549 KB HEK293 IC ₅₀ [μM] (111b) 0.53 ± 0.02 0.50 ± 0.08 0.82 ± 0.20 0.90 ± 0.05 14.39 ± 0.28	79
32		Enzymes EGFR IC ₅₀ [nM] (113b) 211.22 ± 0.027 is it correct	Erlotinib Cell lines A549 HCT-116 MDA-MB-231 H1975 IC ₅₀ [μM] (113b) 2.7 ± 0.032 5.1 ± 0.029 4.1 ± 0.031 3.65	80
33		Enzymes EGFR IC ₅₀ [μM] (119g) 0.039 ± 0.16	Staurosporine 0.054 ± 0.10 Cell lines HCT-116 MCF-7 HepG-2 IC ₅₀ [μM] (119g) 3.61 ± 0.18 1.65 ± 0.13 8.58 ± 0.06	81





Table 3 (Contd.)

Entry	Structure	Kinase inhibition activity	Anticancer activity	Ref.
34	<p>Thiophene-quinoxaline-based conjugated polymer nanoparticles (CPNs)</p> <p>126a: Z = H (T2fQf) 126b: Z = F (T2fQ2f)</p>	—	Nanoparticles of T2fQf (1.59 mg mL ⁻¹) significantly showed the growth of MDA-MB-231 cells and increased late apoptosis tenfold after four days	82

respectively. The ability of this derivative **102j** to inhibit VEGFR-2 was evaluated (*in vitro*) and showed a significant IC₅₀ value of 3.7 nM, compared to Sorafenib (IC₅₀ = 3.12 nM). The docking studies supported these results and demonstrated the ability of the **102j** to interact with VEGFR-2 active sites.⁷³

The triazoloquinoxaline-based molecular hybrid **94k** was screened for its antiproliferative activity (*in vitro*) against two human cancer cell lines MCF-7 and HepG-2, using Sorafenib as a reference drug. The bioassay results disclosed that compound **94k** had a promising cytotoxic activity with IC₅₀ values of 6.2 μM and 4.9 μM against MCF-7 and HepG2, respectively, compared to Sorafenib with IC₅₀ values of 3.53 and 2.18 μM, respectively. The ability of **94k** to inhibit VEGFR-2 was evaluated (*in vitro*) and showed a significant IC₅₀ value of 3.9 nM, compared to Sorafenib (IC₅₀ = 3.13 nM). Docking studies supported the obtained results and demonstrated the ability to interact with VEGFR-2 active sites.⁷¹

The antiproliferative activity of **102h** was evaluated (*in vitro*) against two human cancer cell lines HepG-2 and MCF-7, and Sorafenib was used as a reference drug. Compound **102h** displayed significant cytotoxicity against the two cell lines, HepG-2 and MCF-7, with IC₅₀ values of 3.3 μM and 4.4 μM, respectively. Compound **102h** also showed good *in vitro* inhibition potency of VEGFR-2 with IC₅₀ value 3.2 μM, with almost similar potency as the reference drug Sorafenib (IC₅₀ = 3.1 μM). The ability of these novel derivatives to interact with VEGFR-2 active sites and to inhibit its activity was also confirmed by docking studies.⁷⁴

Compound **104a** showed an interesting anticancer activity with IC₅₀ values 8.2 and 5.4 μM, respectively, against MCF-7 and HepG2. The ability of these derivatives to inhibit VEGFR-2 was evaluated (*in vitro*), and **104a** showed a significant IC₅₀ value of 3.4 nM compared to Sorafenib (IC₅₀ = 3.12 nM). Molecular docking studies showed the binding mode and interaction of compound **30** against VEGFR-2.⁷⁵

Compound **94q** was synthesized and tested *in vitro* for its anticancer activity against two human cancer cell lines (MCF-7 and HepG2), and the results were compared to Sorafenib. **94q** showed significant cytotoxic activity against both MCF-7 and HepG2 with IC₅₀ values 5.8 μM and 4.3 μM, respectively, that were very close to Sorafenib drug (IC₅₀ = 3.51 and 2.17 μM, respectively). The *in vitro* inhibitory activity of **94q** against VEGFR-2 was evaluated and showed significant IC₅₀ = 3.2 nM, compared to the reference Sorafenib (IC₅₀ = 3.12 nM). Molecular docking studies also showed binding mode and interaction against VEGFR-2.⁷⁶

Compound **107b** was designed, synthesized, and screened *in vitro* for its anticancer activity against three cancer cell lines "HepG2, HCT-116, and MCF-7". Compound **107b** exhibited good cytotoxicity with (IC₅₀ 7.45, 3.04, and 7.85 μM) against HepG2, HCT-116, and MCF-7, respectively. The inhibitory effect of compound **32** against VEGFR-2 (*in vitro*) showed significant inhibitory activity against VEGFR-2 with an IC₅₀ value of 0.493 μM, compared to Sorafenib (IC₅₀ = 0.589 μM).⁷⁷

Synthesis of **108e** was achieved, and its antiproliferative activity was evaluated by MTT assay against two cancer cell lines, MCF-7 and HepG2, using Sorafenib as a reference drug. The bioassay results showed that **108e** exhibited a high potent

cytotoxicity with IC_{50} values of 2.7 and 2.1 μM against MCF-7 and HepG2, respectively. The *in vitro* inhibition activity of compound **108e** against VEGFR-2 showed significant activities with an IC_{50} value of 2.6 nM, compared with Sorafenib (IC_{50} = 3.1 nM).⁷⁸

Some benzoxazole-based quinoxaline heterocyclic hybrids were synthesized, and their cytotoxicity was evaluated using MTT bioassay against five cancer cell lines (MDA-MB-231, MCF-7, A549, KB, and HEK293). Compound **111b** was the most potent cytotoxic compound against all the tested cancer cell lines MDA-MB-231, MCF-7, A549, KB, and HEK293 with IC_{50} values of 0.53, 0.50, 0.82, 0.90 and 14.39 μM , respectively. In addition, the inhibitory effect of **111b** against tyrosine kinase exhibited potent activity with IC_{50} = 0.10 μM .⁷⁹

Compound **113b** was tested for anticancer activity *in vitro* against A549 “non-small cell lung cancer”, HCT-116 “colorectal carcinoma”, MDA-MB-231 “breast cancer” and H1975 “Gefitinib-resistant non-small cell lung cancer”. Compound **113b** showed significant anticancer activity against the tested cancer cell lines A549, HCT-116, MDA-MB-231, and H1975 with IC_{50} values of 2.7, 5.1, 4.1 and 3.65 μM , respectively. The inhibitory effects of **113b** against EGFR were determined and exhibited promising inhibitory activity. Docking studies also supported the results and demonstrated the ability to interact with EGFR active sites.⁸⁰

Some triazoloquinoxaline-chalcone molecular hybrids were synthesized and screened *in vitro* for their anticancer activity against three human cancer cell lines: MCF-7, HCT-116, and HEPG-2, and compared with Doxorubicin. As an example, **119g** showed the most potent cytotoxic activity with IC_{50} values of 1.65, 3.61, 8.58 μM , against MCF-7, HCT-116, and HEPG-2, respectively. The inhibitory effects of compound **119g** against EGFR TK were significant, with an IC_{50} value of 0.039 μM , compared to the reference drug Staurosporine (IC_{50} = 0.054 μM). The molecular docking studies showed binding modes with the EGFR TK.⁸¹

The study of Koralli *et al.* assessed the biological activity of thiophene-quinoxaline-based conjugated polymer nanoparticles (CPNs) in breast cancer cells (T-47D, MDA-MB-231) and healthy

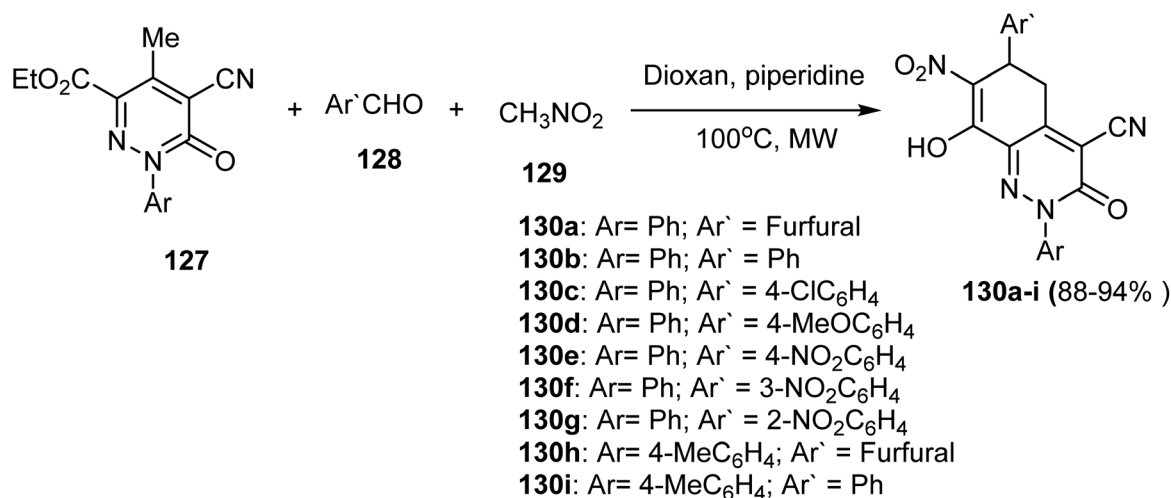
epithelial cells (MCF10A). Nanoprecipitated T2fqf CPNs labeled 80% of MDA-MB-231 cells and 30% of T-47D cells but showed low uptake in MCF10A (<0.15%). Nanoparticles of T2fqf (1.59 mg mL^{-1}) significantly showed the growth of MDA-MB-231 cells and increased late apoptosis tenfold after four days. The encapsulated T2fqf and T2fqf CPNs, on the other hand, didn't kill cancer cells very much. However, at doses as high as 4 mg mL^{-1} , the encapsulated T2fqf caused MCF10A cells to die. Healthy cells tolerated nanoprecipitated T2fqf well at low dosages, while it preferentially induced apoptosis in cancer cells. Nanoparticle of T2fqf may be able to work as a selective theragnostic agent, especially in the treatment of triple-negative breast cancer (Table 3).⁸²

5. Cinnoline derivatives

As illustrated in Scheme 35, Nazmy *et al.* reported an effective one-pot multicomponent reaction for synthesizing the functionalized cinnolines. The anticipated tetrahydrocinnoline-4-carbonitrile derivatives **130** were thus produced in 88–94% yields by reacting cyano-pyridazinone-carboxylates **127** with aromatic aldehydes **128** and nitromethane **129** in dioxane/piperidine under controlled microwave heating at 100 °C for 7–20 min.³⁶

Tian *et al.* have screened a series of cinnoline derivatives for anticancer activity, targeting PI3K, a key pathway that dominates cancer cell proliferation and survival. Several of these cinnoline-derived compounds were strongly inhibitory against PI3K enzymes, several in the nanomolar range of inhibition. Among the synthesized compounds, **134q** exhibited the most potent antiproliferative activity with an IC_{50} of 0.264, 2.04, and 1.14 μM against U87MG, HeLa, and HL60 cells, respectively. This compound exhibited a potent inhibitory activity of PI3K/Akt pathway based on decreased phosphorylation levels and could represent a lead compound for further development as PI3K inhibitor for cancer therapy (Scheme 36).⁸³

El-Dhaibi *et al.* described access to products of the cinnoline-4-carbonitrile derivative **138–139**, employing very simple substrates. Thus, 2-(2-nitrophenyl)-2-(3-oxoisindolin-1-yl) acetonitrile **137** was first synthesized from the reaction



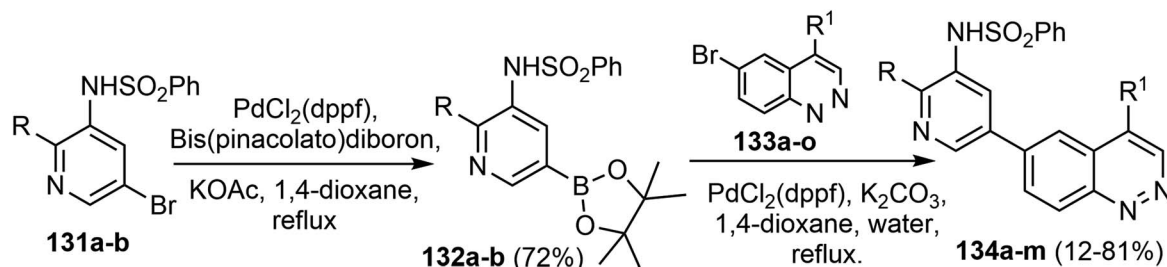
Scheme 35 Synthesis of densely functionalized cinnoline **130a–i** derivatives.



between 2-cyanobenzaldehyde **135** and 2-(2-nitrophenyl)acetonitrile **136**, followed by cyclization and subsequent rearrangement through a one-pot process mechanism in methanolic solution containing TEA as outlined in Scheme 37. Then, the isoindolin-1-one derivative **137** was treated with a solution of 5% KOH in MeOH under reflux for 30 minutes to furnish the anticipated products methyl 2-(4-cyanocinnolin-3-yl)benzoate (**138**) along with its corresponding acid **139** in 60% and 34% yields, respectively.⁸⁴

An efficient approach towards synthesizing 6-aryl-4-azidocinnolines **142** was developed by Danilkina *et al.*,

starting from 3-phenyltriazene derivatives **140**. Thus, Richter cyclization of the triazenes **140a–g** using HBr (20 equiv.) in acetone gave the corresponding 4-bromo-3-pentyl-6-arylcinnoline **141a–g** in a good yield. Subsequent nucleophilic substitution of bromine atom by an azido group using sodium azide for the 4-bromo-cinnoline derivatives **141a–g** proceeded smoothly, to provide the 6-aryl(heteroaryl)-4-azidocinnoline derivatives **142a–g** in high yields 69–91% (Scheme 38). Finally, using copper(II) sulfate/sodium ascorbate catalytic system, the reaction of azidocinnolines **142a–g** both with terminal aromatic alkynes bearing EWG, EDG, and aliphatic alkynes **143a–g** in the



131,132a: R = Cl

131,132b: R = methoxyl

133a: R¹ = morpholin-4-yl

b: R¹ = anilin-N-yl

c: R¹ = 4-acetylaminoanilin-N-yl

d: R¹ = 4-methoxybenzylamine-N-yl

e: R¹ = (R)-1-phenylethylamine-N-yl

f: R¹ = (S)-1-phenylethylamine-N-yl

g: R¹ = pyrrolidin-1-yl

h: R¹ = piperidin-1-yl

i: R¹ = 4-methylpiperidin-1-yl

134a: R = Cl, R¹ = morpholin-4-yl

b: R = methoxyl, R¹ = morpholin-4-yl

c: R = Cl, R¹ = anilin-N-yl

d: R = methoxyl, R¹ = anilin-N-yl

e: R = Cl, R¹ = 4-acetylaminoanilin-N-yl

f: R = methoxyl, R¹ = 4-acetylaminoanilin-N-yl

g: R = Cl, R¹ = Cl

h: R = methoxyl, R¹ = Cl

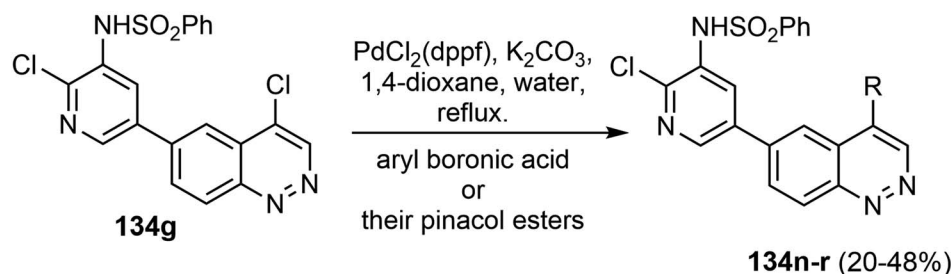
i: R = Cl, R¹ = H

j: R = Cl, R¹ = 4-methoxybenzylamine-N-yl

k: R = Cl, R¹ = (R)-1-phenylethylamine-N-yl

l: R = Cl, R¹ = (S)-1-phenylethylamine-N-yl

m: R = Cl, R¹ = pyrrolidin-1-yl



134n: R = pyridin-4-yl

o: R = phenyl

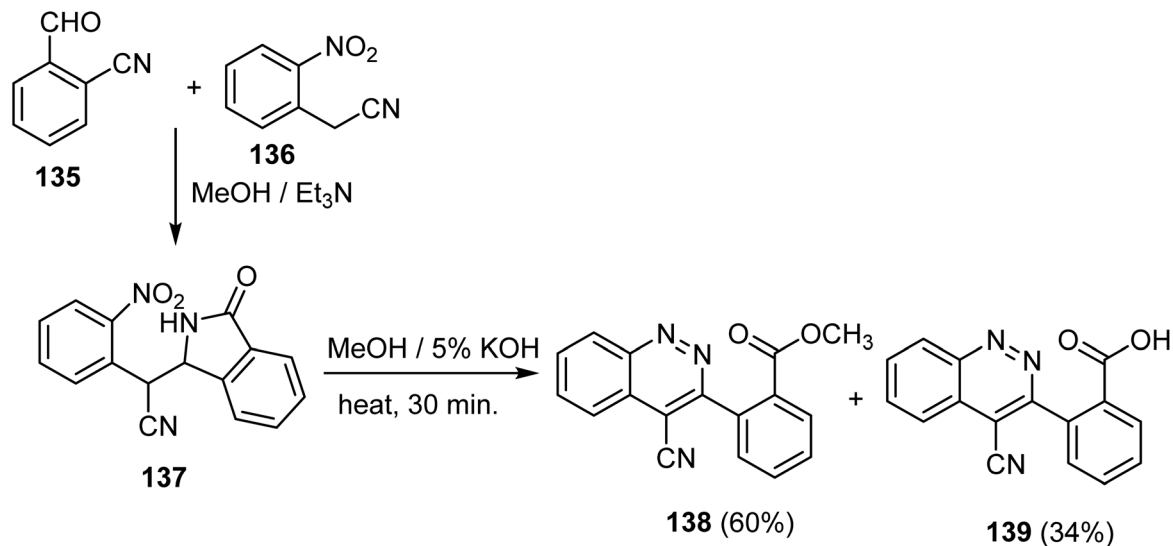
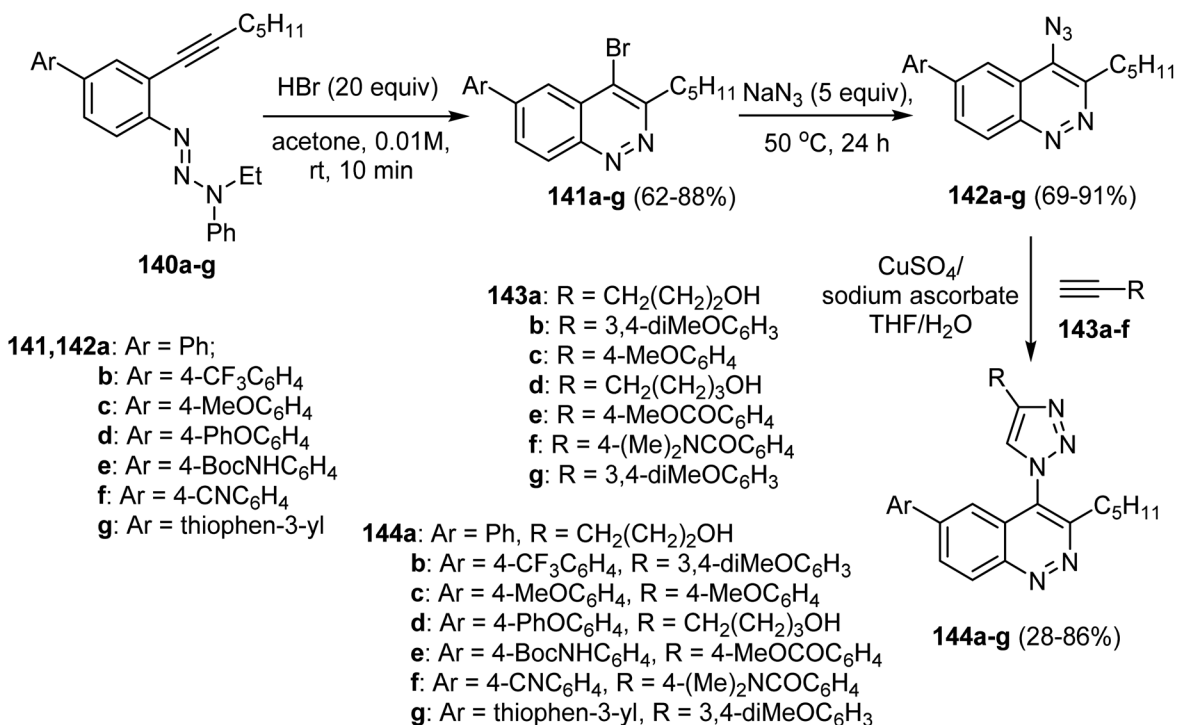
p: R = 4-(morpholin-4-yl)-phenyl

q: R = 2-(4-(morpholin-4-yl))-pyrimidin-5-yl

r: R = 2-(4-(morpholin-4-yl))-pyridin-5-yl

Scheme 36 Synthesis of the cinnoline derivatives **134a–r**.



Scheme 37 Synthesis of the cinnoline derivatives **14** and **15**.Scheme 38 Synthesis of the 6-aryl-4-triazolylcinnolines **144a-g**.

mixture of THF/H₂O resulted in the corresponding 4-triazolylcinnolines **144a-g** mostly in good outcome (28–86%).⁸⁵

5.1 Anticancer activity of cinnoline-based derivatives

Evaluation of the cytotoxic activity of compound **130b** against two human cancer cell lines (RPMI-8226 and LOX IM VI) and WI-38 (normal cell line) was reported. Compound **130b** exhibited notable cytotoxicity against tested cell line "RPMI-8226 and LOX IM VI" with IC₅₀ values of 17.12 μg mL⁻¹ and 12.32 μg

mL⁻¹, respectively, and the IC₅₀ value for the WI-38 cell line was 23.62 μg mL⁻¹. The values of IC₅₀ for **130b** against the normal and malignant cell lines confirmed its specificity and selectivity.³⁶

Tian *et al.*, in their study, explored cinnoline derivatives as potential anticancer agents by targeting the PI3K pathway, which is essential in cancer cell proliferation and survival. Various cinnoline-based compounds exhibited potent inhibitory effects on PI3K enzymes, with many achieving nanomolar



Table 4 Cytotoxicity of cinnoline-based derivatives with kinase inhibition⁷¹

Entry	Structure	Kinase inhibition activity	Anticancer activity			Ref.	
36		—	Cell lines	IC ₅₀ [$\mu\text{g mL}^{-1}$]		36	
			RPMI-8226	17.12 \pm 1.31	Staurosporine		24.97 \pm 1.47
			LOX IM VI	12.32 \pm 0.75			8.45 \pm 0.42
			WI38	23.62 \pm 8.57			14.21 \pm 0.34
37		Enzymes PI3K	IC ₅₀ [nM]	Cell lines	IC ₅₀ [μM]	83	
			0.65 nM	U87MG	0.264		
				HeLa	2.04		
				HepG2	16.6		
				MCF-7	31.1		
				HL60	1.14		

potencies. Compound **134q** showed the highest anti-proliferative activity across multiple cancer cell lines, with notable efficacy against U87MG, HeLa, and HL60 cells (IC₅₀ values of 0.264 μM , 2.04 μM , and 1.14 μM , respectively). This compound effectively inhibited the PI3K/Akt pathway by reducing phosphorylation levels, thus demonstrating potential as a leading structure for further development as a PI3K inhibitor in cancer therapy (Table 4).⁸³

6. Conclusion

In conclusion, phthalazine, quinazoline, quinoxaline, and cinnoline derivatives have been shown to have considerable anticancer activity. Their unique structural properties, together with their ability to interact with a variety of oncogenic targets, propel these compounds to the forefront of new chemotherapeutic development. These compounds not only inhibit important proteins kinases, but they also have multi-targeted effects, which may lead to more effective and long-lasting cancer treatments. Regarding the physio-chemical properties, compounds were investigated for their ADME pharmacokinetics and drug-likeness properties. As illustrated in the citing references whenever it applied, most active compounds exhibited obeyable values following Lipinski's rule of five of "molecular weight, number of rotatable bonds, H-bond donor, and acceptors along with a number of violations". The knowledge gained from biological findings and synthetic development provides intriguing avenues for future research. The increasing need for specific and effective anticancer therapeutics ensures a wide field of study for these heterocycles with promising potential to address the limitations of presently existing cancer therapies. This will be important to guide the development of next-generation anticancer drugs. Increasing

understanding of their molecular mechanisms will be critical for the development of next-generation anticancer drugs.

Data availability

All data associated with this manuscript will be available upon reasonable request from the corresponding authors.

Conflicts of interest

The authors declare that they have no financial or personal interests.

Acknowledgements

Dr Mohamed S. Nafie appreciates to the Seed Research Project No. (24021440154) funded by the Research and Graduate Studies at the University of Sharjah, United Arab Emirates. Also, he acknowledges the electronic library sources at the University of Sharjah, providing full access to published papers and searching on Chemistry databases. Dr Sherif Ashraf Fahmy acknowledges the financial support and sponsorship from the Alexander von Humboldt Foundation, Germany.

References

- R. J. Klement, *Global Transitions*, 2024, **6**, 45–65.
- D. C. Joshi, A. Sharma, S. Prasad, K. Singh, M. Kumar, K. Sherawat, H. S. Tuli and M. Gupta, *Discover Oncol.*, 2024, **15**, 342.
- K. Taruneshwar Jha, A. Shome, Chahat and P. A. Chawla, *Bioorg. Chem.*, 2023, **138**, 106680.
- J. Bariwal, V. Kumar, Y. Dong and R. I. Mahato, *Med. Res. Rev.*, 2019, **39**, 1137–1204.



- 5 A. M. Fahim, E. H. I. Ismael and H. E. M. Tolan, *Polycyclic Aromat. Compd.*, 2023, 1–42.
- 6 R. Pal, G. S. P. Matada, G. Teli, M. Saha and R. Patel, *Bioorg. Chem.*, 2024, **152**, 107696.
- 7 R. J. Obaid, N. Naeem, E. U. Mughal, M. M. Al-Rooqi, A. Sadiq, R. S. Jassas, Z. Moussa and S. A. Ahmed, *RSC Adv.*, 2022, **12**, 19764–19855.
- 8 A. Mushtaq, P. Wu and M. M. Naseer, *Pharmacol. Ther.*, 2024, **254**, 108579.
- 9 P. Taslimi, F. Türkan, K. Turhan, H. S. Karaman, Z. Turgut and İ. Gulcin, *J. Heterocycl. Chem.*, 2020, **57**, 3116–3125.
- 10 O. Mammoliti, K. Jansen, S. El Bkassiny, A. Palisse, N. Triballeau, D. Bucher, B. Allart, A. Jaunet, G. Tricarico, M. De Wachter, C. Menet, J. Blanc, V. Letfus, R. Rupčić, M. Šmehil, T. Poljak, B. Coornaert, K. Sonck, I. Duys, L. Waeckel, L. Lecru, F. Marsais, C. Jagerschmidt, M. Auberval, P. Pujuguet, L. Oste, M. Borgonovi, E. Wakselman, T. Christophe, N. Houvenaghel, M. Jans, B. Heckmann, L. Sanrière and R. Brys, *J. Med. Chem.*, 2021, **64**, 14557–14586.
- 11 R. Samala, S. K. Nukala, N. S. Thirukovela, G. Dasari and S. Bandari, *Polycyclic Aromat. Compd.*, 2023, **43**, 9175–9192.
- 12 J. Sangshetti, S. K. Pathan, R. Patil, S. Akber Ansari, S. Chhahjed, R. Arote and D. B. Shinde, *Bioorg. Med. Chem.*, 2019, **27**, 3979–3997.
- 13 M. M. Khalifa, A. A. Al-Karmalawy, E. B. Elkaeed, M. S. Nafie, M. A. Tantawy, I. H. Eissa and H. A. Mahdy, *J. Enzyme Inhib. Med. Chem.*, 2022, **37**, 299–314.
- 14 K. Budipramana and F. Sangande, *Chem. Biol. Drug Des.*, 2024, **103**, e14534.
- 15 S. Zaib and I. Khan, *Bioorg. Chem.*, 2020, **105**, 104425.
- 16 S. Zare, L. Emami, Z. Faghih, F. Zargari, Z. Faghih and S. Khabnadideh, *Sci. Rep.*, 2023, **13**, 14461.
- 17 S. N. Murthy Boddapati, H. Babu Bollikolla, K. Geetha Bhavani, H. Singh Saini, N. Ramesh and S. Babu Jonnalagadda, *Arabian J. Chem.*, 2023, **16**, 105190.
- 18 I. A. Bala, A. M. Asiri and R. M. El-Shishtawy, *Med. Chem. Res.*, 2024, **33**(12), 2372–2419.
- 19 W. M. Ghorab and M. M. Ghorab, *J. Mol. Struct.*, 2024, **1317**, 139060.
- 20 M. M. Ghorab, A. M. Soliman, K. El-Adl and N. S. Hanafy, *Bioorg. Chem.*, 2023, **140**, 106791.
- 21 S. Hu, C. Jiang, M. Gao, D. Zhang, N. Yao, J. Zhang and Q. Jin, *J. Mol. Struct.*, 2024, **1299**, 137224.
- 22 F. H. Al-Ostoot, S. Salah and S. A. Khanum, *Cancer Invest.*, 2024, **42**, 559–604.
- 23 J. Dhuguru and O. A. Ghoneim, *Molecules*, 2022, **27**, 2294.
- 24 S. K. Suthar, N. S. Chundawat, G. P. Singh, J. M. Padrón and Y. K. Jhala, *Eur. J. Med. Chem. Rep.*, 2022, **5**, 100040.
- 25 G. Yashwantrao and S. Saha, *Org. Chem. Front.*, 2021, **8**, 2820–2862.
- 26 M. G. Salem, S. A. Abu El-ata, E. H. Elsayed, S. N. Mali, H. A. Alshwyeh, G. Almainani, R. A. Almainani, H. A. Almasmoum, N. Altwaijry, E. Al-Olayan, E. M. Saied and M. F. Youssef, *RSC Adv.*, 2023, **13**, 33080–33095.
- 27 V. Montero, M. Montana, M. Carré and P. Vanelle, *Eur. J. Med. Chem.*, 2024, **271**, 116360.
- 28 N. Bhusare and M. Kumar, *Oncol. Res.*, 2024, **32**, 849–875.
- 29 M. A. Ismail, M. S. Abusaif, M. S. A. El-Gaby, Y. A. Ammar and A. Ragab, *RSC Adv.*, 2023, **13**, 12589–12608.
- 30 D. Zeleke and T. Damena, *Results Chem.*, 2024, **7**, 101283.
- 31 S. K. Suthar, N. S. Chundawat, G. P. Singh, J. M. Padrón and Y. K. Jhala, *Eur. J. Med. Chem. Rep.*, 2022, **5**, 100040.
- 32 P. Saini, K. Kumar, S. Meena, D. K. Mahawar, A. Dandia, K. L. Ameta and V. Parewa, in *N-Heterocycles*, ed. K. L. Ameta, R. Kant, A. Penoni, A. Maspero and L. Scapinello, Springer Nature Singapore, Singapore, 2022, pp. 331–354.
- 33 J. R. Yerrabelly, M. B. Bommagani, H. Yerrabelly, S. C. Mullaguri and R. K. Kancha, *J. Heterocycl. Chem.*, 2024, **61**, 958–970.
- 34 H. M. Al-Matar, K. M. Dawood and W. M. Tohamy, *RSC Adv.*, 2018, **8**, 34459–34467.
- 35 B. Kumaraswamy, K. Hemalatha, R. Pal, G. S. P. Matada, K. R. Hosamani, I. Aayishamma and N. V. S. S. Aishwarya, *Eur. J. Med. Chem.*, 2024, **275**, 116561.
- 36 M. H. Nazmy, R. A. Mekheimer, M. E. Shoman, M. Abo-Elsebaa, M. Abd-Elmonem and K. U. Sadek, *Bioorg. Chem.*, 2020, **101**, 103932.
- 37 L. Zhang, C. Cheng, J. Li, L. Wang, A. A. Chumanovich, D. C. Porter, A. Mindich, S. Gorbunova, I. B. Roninson, M. Chen and C. McInnes, *J. Med. Chem.*, 2022, **65**, 3420–3433.
- 38 M. Zabihi, R. Lotfi, A.-M. Yousefi and D. Bashash, *J. Cancer Res. Clin. Oncol.*, 2023, **149**, 1585–1606.
- 39 M. Szumilak and A. Stanczak, *Molecules*, 2019, **24**, 2271.
- 40 R. K. Tonk, S. Bawa and D. Kumar, *Mini-Rev. Org. Chem.*, 2025, **22**(2), 162–176.
- 41 M. M. Kandeel, A. M. Kamal, B. H. Naguib and M. S. A. Hassan, *Anticancer Agents Med. Chem.*, 2018, **18**(8), 1208–1217.
- 42 R. Pal, G. Teli, G. S. P. Matada and P. S. Dhiwar, *J. Mol. Struct.*, 2023, **1291**, 136021.
- 43 F. Sangande, E. Julianti and D. H. Tjahjono, *Int. J. Mol. Sci.*, 2020, **21**, 7779.
- 44 A. Doostmohammadi, H. Jooya, K. Ghorbanian, S. Gohari and M. Dadashpour, *Cell Commun. Signaling*, 2024, **22**, 228.
- 45 A. A. Abbas, T. A. Farghaly and K. M. Dawood, *RSC Adv.*, 2024, **14**, 19752–19779.
- 46 K. M. Dawood, M. A. Raslan, A. A. Abbas, B. E. Mohamed and M. S. Nafie, *Anticancer Agents Med. Chem.*, 2023, **23**(3), 328–345.
- 47 D. M. Mohamed, N. A. Kheder, M. Sharaky, M. S. Nafie, K. M. Dawood and A. A. Abbas, *RSC Adv.*, 2024, **14**, 24992–25006.
- 48 M. E. Salem, E. M. Mahrous, E. A. Ragab, M. S. Nafie and K. M. Dawood, *ACS Omega*, 2023, **8**, 35359–35369.
- 49 F. M. Thabet, K. M. Dawood, E. A. Ragab, M. S. Nafie and A. A. Abbas, *RSC Adv.*, 2022, **12**, 23644–23660.
- 50 K. El-Adl, M. K. Ibrahim, F. Khedr, H. S. Abulkhair and I. H. Eissa, *Arch. Pharm.*, 2022, **355**, 2100278.
- 51 F. Khedr, M. Ibrahim, I. H. Eissa, H. S. Abulkhair and K. El-Adl, *Arch. Pharm.*, 2021, **354**, 2100201.
- 52 H. H. Bayoumi, M. K. Ibrahim, M. A. Dahab, F. Khedr and K. El-Adl, *RSC Adv.*, 2024, **14**, 21668–21681.



- 53 S. M. Emam, S. M. E. Rayes, I. A. I. Ali, H. A. Soliman and M. S. Nafie, *BMC Chem.*, 2023, **17**, 90.
- 54 U. Boda, V. Guguloth, S. Mood and H. Guguloth, *Russ. J. Org. Chem.*, 2023, **59**, 1064–1070.
- 55 C. A. Lipinski, *Drug Discovery Today: Technol.*, 2004, **1**, 337–341.
- 56 R. Patil, S. Das, A. Stanley, L. Yadav, A. Sudhakar and A. K. Varma, *PLoS One*, 2010, **5**, e12029.
- 57 Y. Xu, W. Zhao, X. Zhang, X. Yu, Y. Chen, Z. Wang, Y. Chu, X. Zhu and P. Zhang, *Bioorg. Med. Chem.*, 2024, **99**, 117608.
- 58 Y. Liu, Q. Ma, X. Kong, X. Huo, Z. Dong, Y. Ma, K. Yang, W. Niu and K. Zhang, *Bioorg. Chem.*, 2024, **143**, 107087.
- 59 A. Hassan, A. M. Mosallam, A. O. A. Ibrahim, M. Badr and A. H. Abdelmonsef, *Sci. Rep.*, 2023, **13**, 18567.
- 60 M. Mortazavi, M. Eskandari, F. Moosavi, T. Damghani, M. Khoshneviszadeh, S. Pirhadi, L. Saso, N. Edraki and O. Firuzi, *Sci. Rep.*, 2023, **13**, 14685.
- 61 N. F. M. El Hamaky, A. Hamdi, W. A. Bayoumi, A. A. Elgazar and M. N. A. Nasr, *Bioorg. Chem.*, 2024, **148**, 107437.
- 62 W. Han, Y. Yang, F. Yu, Q. Li, A. Liu, W. Xu, J. Li and X. Xue, *Bioorg. Med. Chem.*, 2023, **95**, 117501.
- 63 H. Shi, H. Tang, Y. Li, D. Chen, T. Liu, Y. Chen, X. Wang, L. Chen, Y. Wang, H. Xie and B. Xiong, *Eur. J. Med. Chem.*, 2023, **248**, 115064.
- 64 M. F. Ahmed, A. S. Khalifa and E. M. Eed, *Russ. J. Bioorg. Chem.*, 2022, **48**, 739–748.
- 65 M. F. Ahmed, E. Y. Santali and R. I. Alsantali, *Russ. J. Gen. Chem.*, 2022, **92**, 2047–2057.
- 66 M. Li, D. Wang, Q. Li, F. Luo, T. Zhong, H. Wu, L. Xiong, M. Yuan, M. Su and Y. Fan, *Int. J. Mol. Sci.*, 2023, **24**, 6851.
- 67 H. A. Allam, E. E. Aly, A. K. B. A. W. Farouk, A. M. El Kerdawy, E. Rashwan and S. E. S. Abbass, *Bioorg. Chem.*, 2020, **98**, 103726.
- 68 A. S. Altamimi, A. S. El-Azab, S. G. Abdelhamid, M. A. Alamri, A. H. Bayoumi, S. M. Alqahtani, A. B. Alabbas, A. I. Altharawi, M. A. Alossaimi and M. A. Mohamed, *Molecules*, 2021, **26**, 2992.
- 69 R. M. Borik and M. A. Hussein, *Curr. Pharm. Biotechnol.*, 2022, **23**, 1179–1203.
- 70 N. A. Alsaif, M. A. Dahab, M. M. Alanazi, A. J. Obaidullah, A. A. Al-Mehizia, M. M. Alanazi, S. Aldawas, H. A. Mahdy and H. Elkady, *Bioorg. Chem.*, 2021, **110**, 104807.
- 71 N. A. Alsaif, A. Elwan, M. M. Alanazi, A. J. Obaidullah, W. A. Alanazi, A. F. Alasmari, H. Albassam, H. A. Mahdy and M. S. Taghour, *Mol. Diversity*, 2022, **26**, 1915–1932.
- 72 K. El-Adl, H. M. Sakr, R. G. Yousef, A. B. M. Mehany, A. M. Metwaly, M. A. Elhendawy, M. M. Radwan, M. A. ElSohly, H. S. Abulkhair and I. H. Eissa, *Bioorg. Chem.*, 2021, **114**, 105105.
- 73 N. A. Alsaif, M. S. Taghour, M. M. Alanazi, A. J. Obaidullah, A. A. Al-Mehizia, M. M. Alanazi, S. Aldawas, A. Elwan and H. Elkady, *J. Enzyme Inhib. Med. Chem.*, 2021, **36**, 1093–1114.
- 74 M. M. Alanazi, H. A. Mahdy, N. A. Alsaif, A. J. Obaidullah, H. M. Alkahtani, A. A. Al-Mehizia, S. M. Alsubaie, M. A. Dahab and I. H. Eissa, *Bioorg. Chem.*, 2021, **112**, 104949.
- 75 N. A. Alsaif, M. S. Taghour, M. M. Alanazi, A. J. Obaidullah, W. A. Alanazi, A. Alasmari, H. Albassam, M. A. Dahab and H. A. Mahdy, *Bioorg. Med. Chem.*, 2021, **46**, 116384.
- 76 N. A. Alsaif, H. A. Mahdy, M. M. Alanazi, A. J. Obaidullah, H. M. Alkahtani, A. M. Al-Hossaini, A. A. Al-Mehizi, A. Elwan and M. S. Taghour, *Arch. Pharm.*, 2022, **355**, 2100359.
- 77 K. El-Adl, H. M. Sakr, R. G. Yousef, A. B. M. Mehany, H. S. Abulkhair and I. H. Eissa, *Arch. Pharm.*, 2022, **355**, 2200048.
- 78 M. M. Alanazi, A. Elwan, N. A. Alsaif, A. J. Obaidullah, H. M. Alkahtani, A. A. Al-Mehizia, S. M. Alsubaie, M. S. Taghour and I. H. Eissa, *J. Enzyme Inhib. Med. Chem.*, 2021, **36**, 1732–1750.
- 79 S. Desai, V. Desai and S. Shingade, *Bioorg. Chem.*, 2020, **94**, 103382.
- 80 M. Kumar, G. Joshi, S. Arora, T. Singh, S. Biswas, N. Sharma, Z. R. Bhat, K. Tikoo, S. Singh and R. Kumar, *Molecules*, 2021, **26**, 1490.
- 81 M. Alswah, A. Bayoumi, K. Elgamal, A. Elmorsy, S. Ihmaid and H. Ahmed, *Molecules*, 2017, **23**, 48.
- 82 P. Koralli, S. Tsikalakis, M. Goulielmaki, S. Arelaki, J. Müller, A. D. Nega, F. Herbst, C. R. Ball, V. G. Gregoriou, A. Dimitrakopoulou-Strauss, S. Wiemann and C. L. Chochos, *Mater. Chem. Front.*, 2021, **5**, 4950–4962.
- 83 C. Tian, C. Yang, T. Wu, M. Lu, Y. Chen, Y. Yang, X. Liu, Y. Ling, M. Deng, Y. Jia and Y. Zhou, *Bioorg. Med. Chem. Lett.*, 2021, **48**, 128271.
- 84 F. B. El Dhaibi, A. Youssef, J. C. Fettinger, M. J. Kurth and M. J. Haddadin, *ACS Omega*, 2022, **7**, 26871–26880.
- 85 N. A. Danilkina, N. S. Bukhtiarova, A. I. Govdi, A. A. Vasileva, A. M. Romyantsev, A. A. Volkov, N. I. Sharaev, A. V. Povolotskiy, I. A. Boyarskaya, I. V. Korniyakov, P. V. Tokareva and I. A. Balova, *Molecules*, 2019, **24**, 2386.

